AD 402 823

(18) (19)
ASD-TDR-62-8

(17) AP
(8) GL
(9) [illegible] pp.
(12) 13 p.
(13)-(14) N/A
(20) U.

6333

(6) DEVELOPMENT OF ULTRASONIC TECHNIQUES FOR DEFECT EVALUATION

TECHNICAL DOCUMENTARY REPORT NO. ASD-TDR-62-8

(11) Feb[illegible]63

Directorate of Materials and Processes
Aeronautical Systems Division
Air Force Systems Command
Wright-Patterson Air Force Base, Ohio

(16) Project No. 7381, (17) Task No. 73812

(15) (Prepared under Contract No. AF 33(616)-6793
by Automation Industries, Inc., Torrance, California)
(10) J. B. Ramsey and W. M. Rowe, Authors)

17

NOTICES

When Government drawings, specifications, or other data are used for any purpose other than in connection with a definitely related Government procurement operation, the United States Government thereby incurs no responsibility nor any obligation whatsoever; and the fact that the Government may have formulated, furnished, or in any way supplied the said drawings, specifications, or other data, is not to be regarded by implication or otherwise as in any manner licensing the holder or any other person or corporation, or conveying any rights or permission to manufacture, use, or sell any patented invention that may in any way be related thereto.

Qualified requesters may obtain copies of this report from the Armed Services Technical Information Agency, (ASTIA), Arlington Hall Station, Arlington 12, Virginia.

This report has been released to the Office of Technical Services, U.S. Department of Commerce, Washington 25, D.C., in stock quantities for sale to the general public.

Copies of this report should not be returned to the Aeronautical Systems Division unless return is required by security considerations, contractual obligations, or notice on a specific document.

25-583C, 700, 4-22-63

Aeronautical Systems Division, Dir/Materials and Processes, Metals and Ceramics Lab, Wright-Patterson AFB, Ohio.
Rpt Nr ASD-TDR-62-8. DEVELOPMENT OF ULTRASONIC TECHNIQUES FOR DEFECT EVALUATION. Final report, Feb 63, 136p. incl illus., tables, 14 refs.

Unclassified Report

The results of investigations to determine the effects of several metallurgical and acoustical variables on the ultrasonic signal strength using commercially available ultrasonic flaw detection equipment are reported. Applied to various metals used in aerospace structures and components, these investigations resulted in the separation and determination of important acoustical properties that were expected to indicate the cause for differencies in the transmission of ultrasonic energy in the various materials. A method was developed for applying correction factors to test blocks of one metal in order to estimate the size of defects in other metals. Beam collimation techniques were studied to determine optimum conditions for detecting defects and displaying them on both cathode ray image and C-Scan (plan view) facsimile paper recordings. Some investigations were also performed to separate and identify shear and surface (Rayleigh) waves.

(over)

1. Method of forming and heat treatment of alloys
2. Ultrasonic energy
3. Flaw detection
I. AFSC Project 7381, Task 73812
II. Contract AF 33 (616)-6793
III. Automation Industries, Inc., Torrance, Calif.
IV. J. B. Ramsey, W. M. Rowe
V. Aval fr OTS
VI. In ASTIA collection

Aeronautical Systems Division, Dir/Materials and Processes, Metals and Ceramics Lab, Wright-Patterson AFB, Ohio.
Rpt Nr ASD-TDR-62-8. DEVELOPMENT OF ULTRASONIC TECHNIQUES FOR DEFECT EVALUATION. Final report, Feb 63, 136p. incl illus., tables, 14 refs.

Unclassified Report

The results of investigations to determine the effects of several metallurgical and acoustical variables on the ultrasonic signal strength using commercially available ultrasonic flaw detection equipment are reported. Applied to various metals used in aerospace structures and components, these investigations resulted in the separation and determination of important acoustical properties that were expected to indicate the cause for differencies in the transmission of ultrasonic energy in the various materials. A method was developed for applying correction factors to test blocks of one metal in order to estimate the size of defects in other metals. Beam collimation techniques were studied to determine optimum conditions for detecting defects and displaying them on both cathode ray image and C-Scan (plan view) facsimile paper recordings. Some investigations were also performed to separate and identify shear and surface (Rayleigh) waves.

(over)

1. Method of forming and heat treatment of alloys
2. Ultrasonic energy
3. Flaw detection
I. AFSC Project 7381, Task 73812
II. Contract AF 33 (616)-6793
III. Automation Industries, Inc., Torrance, Calif.
IV. J. B. Ramsey, W. M. Rowe
V. Aval fr OTS
VI. In ASTIA collection

FOREWORD

This report was prepared by the Ultrasonics Division of Automation Industries, Inc., under USAF Contract No. AF 33(616)-6793. This contract was initiated under Project No. 7381, "Materials Application", Task No. 73812, "Data Collection and Correlation". The work was administered under the direction of the Directorate of Materials and Processes, Deputy Commander/Technology, Aeronautical Systems Division, with Mr. R. R. Rowand acting as project engineer.

Final rept., 1

This contract is a continuation of the work carried out under Contract No. AF 33(616)-3363 and Contract No. AF 33(616)-5877, and covers work conducted during the period December 1959 to October 1961.

The authors wish to thank all persons, institutions and firms who assisted in this research project. Acknowledgement is given here for the assistance and cooperation rendered by the following persons in the preparation of this report:

Dr. Rohn Truell	R. D. McKown
H. E. Babb	C. M. Johnson
G. L. Cross	R. E. Kleint
W. C. Hitt	B. L. Winters

ABSTRACT

The results of investigations to determine the effects of several metallurgical and acoustical variables on the ultrasonic signal strength using commercially available ultrasonic flaw detection equipment are reported. Applied to various metals used in aerospace structures and components, these investigations resulted in the separation and determination of important acoustical properties that were expected to indicate the cause for differences in the transmission of ultrasonic energy in the various materials. A method was developed for applying correction factors to test blocks of one metal in order to estimate the size of defects in other metals. Beam collimation techniques were studied to determine optimum conditions for detecting defects and displaying them on both cathode ray image and C-Scan (plan view) facsimile paper recordings. Some investigations were also performed to separate and identify shear and surface (Rayleigh) waves.

This report has been reviewed and is approved.

W. J. TRAPP
Chief, Strength and Dynamics Branch
Metals and Ceramics Laboratory
Directorate of Materials and Processes

SUMMARY

The effects of forming method and heat treatment upon the ultrasonic signal response of several of the newer alloys were investigated. Generally, rolled material displayed consistently higher response characteristics than the forged materials. For most of the materials, heat treatment tended to improve the transmission of ultrasound. These effects appeared to be more significant as test frequencies were increased.

Specific acoustic impedance and other acoustical properties were determined. Using immersed testing, it was found that the impedance mismatch at the water/metal interfaces was the most important factor when comparing one material to another due to the large energy loss at the interface. The attenuation losses in most materials was considerably smaller.

The attenuation values obtained included all losses of acoustical energy within the material including those due to sound-beam geometry which would be encountered in normal testing. The apparent attenuation generally was less than one decibel per inch of metal travel.

A method was developed for applying correction factors to compensate for different acoustical properties of materials. It was found that by correcting for the difference in impedance, attenuation and defect size (in terms of decibels) between a reference set of test blocks of one material and the material being inspected, a good approximation of discontinuity size could be obtained.

The use of beam collimators for flaw evaluation was investigated. Particular emphasis was placed on the use of collimators for C-Scan recording. The minimum useful collimator size was found to be about 2-1/2 wavelengths measured in the material being tested. Metal depth ranges for best definition were determined. The results were compared with those using focused transducers.

The propagation of shear and surface (Rayleigh) waves was investigated. It was found that shear waves generated over a wide range of incident angles had nearly the same reflected amplitude. This amplitude was greater than that using longitudinal waves, indicating closer impedance match with the coupling medium. The signal losses due to attenuation became significant at higher frequencies, however.

The use of surface (Rayleigh) waves in the higher frequency range was apparently limited due to the low signal strength obtainable. Using a single transducer technique it was found, however, that a compound wave motion could be propagated in thin plates by either immersed or contact methods. The characteristics were those of Lamb waves.

TABLE OF CONTENTS

LIST OF APPENDIXES

LIST OF ILLUSTRATIONS

LIST OF ILLUSTRATIONS (Continued)

LIST OF ILLUSTRATIONS (Continued)

LIST OF ILLUSTRATIONS (Continued)

LIST OF ILLUSTRATIONS (Continued)

LIST OF TABLES

LIST OF TABLES (Continued)

SECTION I

INTRODUCTION

With the continued development of new materials for the aerospace industry, ultrasonic standards for inspecting these materials must be developed. Present techniques employ at least one set of reference test blocks for each alloy that is being evaluated. It is readily seen that such an operation would entail a large capital investment with the higher costs of some of the newer super alloys. The special machining techniques which are required in some cases would further increase the cost. If one set of blocks could be used to evaluate several materials the number of test blocks, and consequently the cost, would be considerably reduced.

It was believed that by isolating and measuring the more significant variables which affect the transmission of ultrasonic energy through a material, compensations or correction factors might be applied for simplifying flaw size evaluation techniques. Means could then be established whereby one set of test blocks would be used to evaluate several materials. In order to establish correction factors the effects of material variables such as differences in alloys, method of forming and heat treatment must be determined. In addition, there are variations in results which arise due to the nature of the ultrasonic energy employed and the conditions under which the energy enters and leaves the part. The latter factors are primarily functions of the transducer type, the coupling medium, and the geometrical relationship between the transducer and the surface of the part.

The investigations of all these factors performed for this report were designed to supplement the knowledge obtained under two previous research and development contracts. The results of those contracts are available as WADC Technical Reports 57-268 and 59-466, both entitled "Research and Development Leading to the Establishment of Ultrasonic Test Standards for Aircraft Materials". Those reports present information pertaining to several alloys of aluminum, steel, magnesium and titanium. The principle variables considered were grain direction, heat treatment, degree of working, frequency of the energy employed and transducer type. All variables were analyzed with respect to their effect upon the amplitude of the ultrasonic energy reflected from internal defects. On some alloys, tests were performed to determine the effects of variations in flaw size, surface roughness, surface curvature, flaw orientation, internal porosity and ultrasonic beam diameter. Where internal porosity was examined, the results were correlated in terms of energy reflected from the porosity, loss of back reflections from the samples, and variations in tensile and fatigue properties.

Supplementary data was obtained employing ultrasonic shear and surface waves to test thin sheet materials. The effect of beam collimation on flaw detection and evaluation was also investigated.

For this investigation, several new alloys were added and evaluated. This data was then related to the alloys and variables previously studied. The investigations were grouped into several phases. First, the effects of material variables

---

Manuscript released by the authors 15 November, 1961 for publication as an ASD Technical Data Report.

on signal response of the new alloys were evaluated. Second, observations were made to determine the acoustical properties of most of the alloys used in this and previous investigations. Attenuation and impedance losses were then calculated. Third, shear and surface (Rayleigh) wave methods as applied to thin sheets were investigated. Additional tests were performed to evaluate the distinguishing characteristics of shear and surface (Rayleigh) waves. Fourth, collimation techniques were studied more thoroughly to permit flaw size evaluation on the basis of plan view scanning. Accordingly this report has been divided into four sections, each containing the test procedures, results, discussion and conclusions for that particular phase.

SECTION II

MATERIAL VARIABLES

In previous investigations the material variables evaluated were those due to differences in alloy composition, direction of grain, method of forming, and heat treatment. The alloys were classified into three basic groups of materials: aluminum, steel, and titanium. For each of these groups, one alloy was selected as a control for the entire group and the results of all tests in the group were referenced to the set of test blocks made from the control alloy.

In order to correlate the results of this investigation to those obtained from the previous investigations, the same basic group classifications were retained and the same sets of test blocks were used as the control alloys.

EQUIPMENT

The basic test apparatus used for this study is illustrated in Figure 1. A list of these apparatus is as follows:

1. Curtiss-Wright Immerscope, Model 424A. Frequency range - 2.25 mc to 25.0 mc.
2. Sola Constant Voltage Transformer. Capacity - 500 VA, 110 volts, 4.24 amps, 60 cycles.
3. Ultrasonic Testing and Research Laboratory designed research test tank.
4. Ultrasonics Division, Automation Industries, Inc. Adjustable Transducer Mount, Model 1026.
5. Ultrasonic Transducers as listed in Table 1.

MATERIALS AND TEST SAMPLES

The basic type of test samples used for this investigation is shown in Figure 2. Unless otherwise specified, a set of test blocks will refer to nineteen (19) blocks each having a 5/64 inch diameter flat bottom hole at a different metal distance (L_1). These test blocks conform to the dimensional requirements of ASTM E127-58T Recommended Practice. The test blocks were machined from the materials shown in Table 2.

TEST PROCEDURES

For this investigation the measurement of ultrasonic energy was accomplished by observing the amplitude of the reflected signal from a 5/64 inch diameter flat bottom hole drilled in the bottom of each block. This amplitude, expressed in inches of

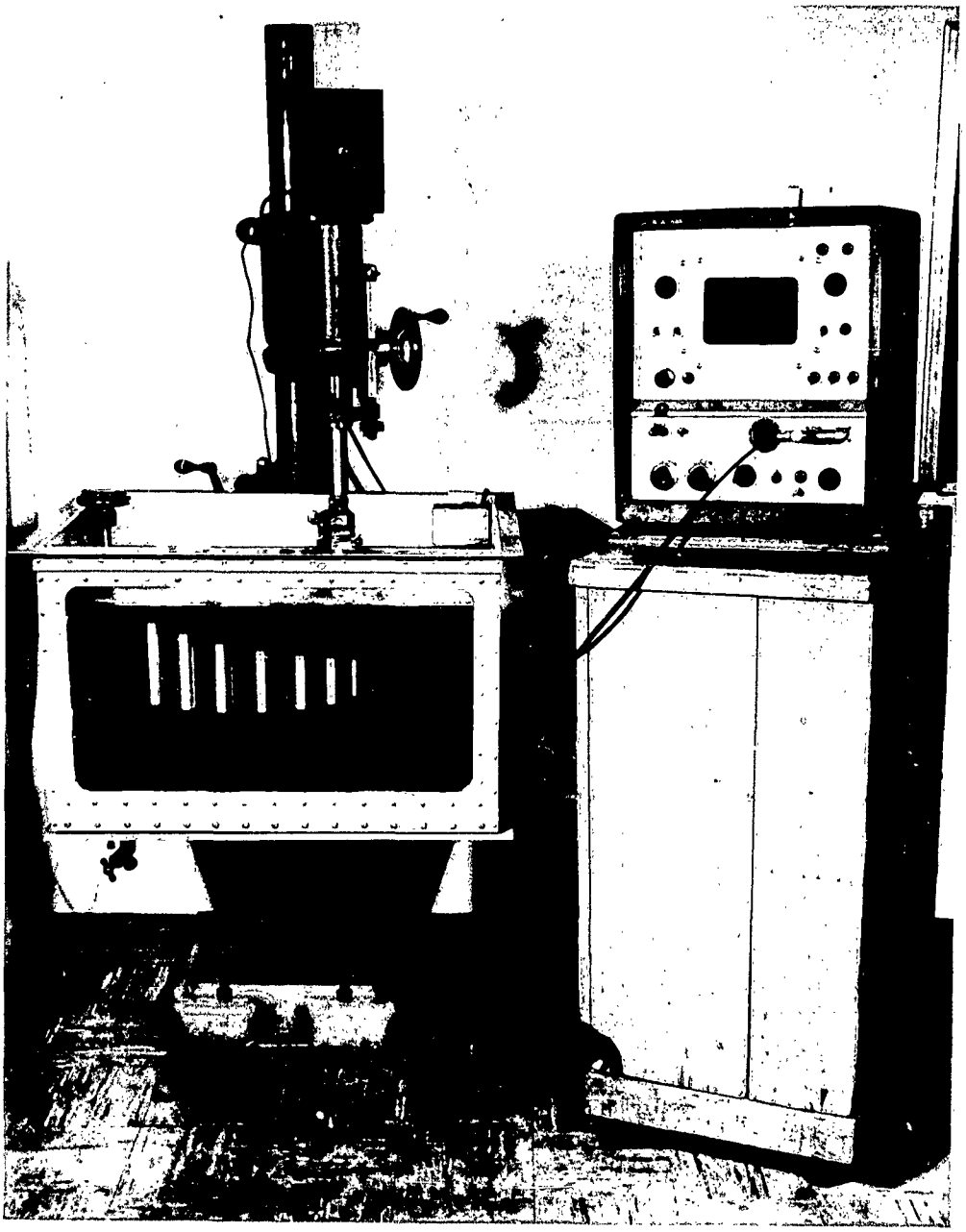

Figure 1. Test Configuration Using Research Test Tank.

TABLE 1

TRANSDUCERS USED TO MEASURE MATERIAL VARIABLES			
MANUFACTURER	TYPE	FREQUENCY Megacycles	DIAMETER
Immersion Style			
Automation Industries	Lithium Sulphate	2.25	0.75
Automation Industries	Lithium Sulphate	5.0	0.75
Automation Industries	Lithium Sulphate	10.0	0.75
Automation Industries	Lithium Sulphate	10.0	0.375
Automation Industries	Quartz	25.0	0.375
Contact Style			
Sperry Products	Quartz	2.25	0.75
Sperry Products	Quartz	5.0	0.75
Sperry Products	Quartz	10.0	0.75

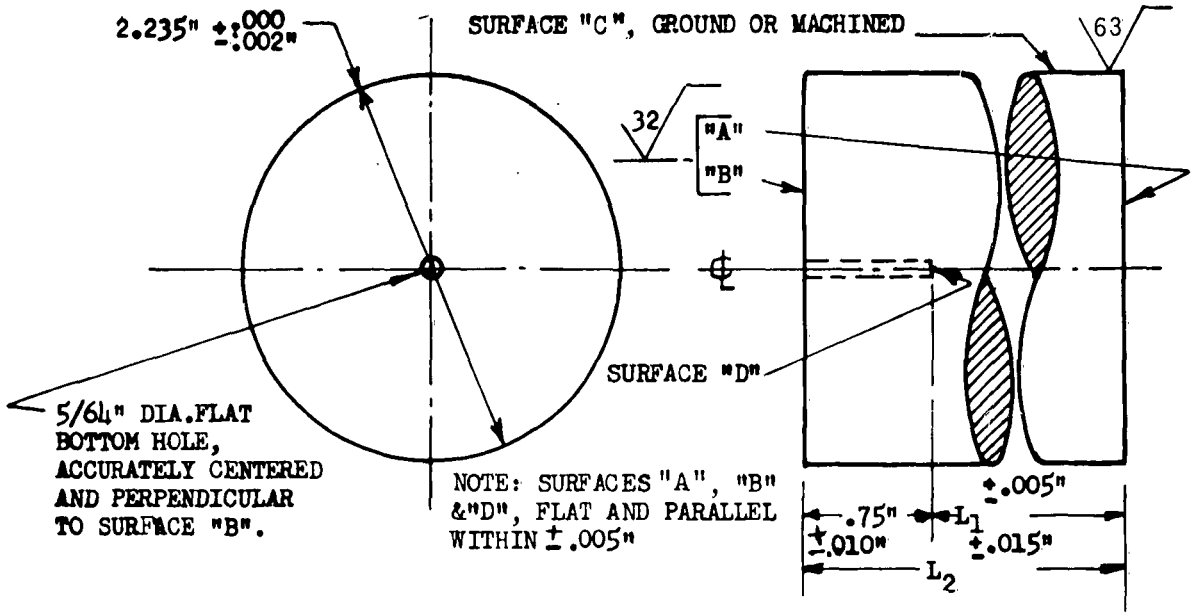

No.	L_1"	L_2"	No.	L_1"	L_2"	No.	L_1"	L_2"	No.	L_1"	L_2"
1	.0625	.8125	5	.500	1.250	10	1.250	2.000	15	3.750	4.500
2	.125	.875	6	.625	1.375	11	1.750	2.500	16	4.250	5.000
3	.250	1.000	7	.750	1.500	12	2.250	3.000	17	4.750	5.500
4	.375	1.125	8	.875	1.625	13	2.750	3.500	18	5.250	6.000
			9	1.000	1.750	14	3.250	4.000	19	5.750	6.500

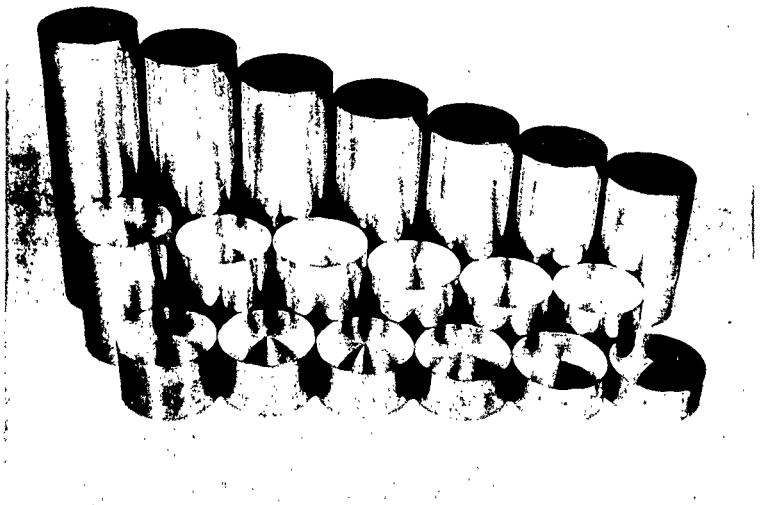

Figure 2. Test Blocks Used to Measure Material Variables.

TABLE 2

MATERIAL AND TEST SAMPLES FOR MEASURING MATERIAL VARIABLES

GROUP	MASTER CONTROL BLOCKS	MATERIAL	GRAIN DIRECTION	TEST HOLE DIAMETER Inches	HEAT TREAT CONDITIONS EVALUATED		ORIGINAL MATERIAL FORM
					Condition I	Condition II	
I	X	4130 Steel	L	5/64	Normalized	No H.T.	2-1/4" dia RB
		Inconel X	L	5/64	Annealed	H.T. & Aged	2-1/4" dia RB
Steel		Inconel X	L.T.	5/64	Annealed	H.T. & Aged	2-1/4" x 7" FB
		Commercially Pure Molybdenum	L	5/64	Annealed	-----	2-1/4" dia RB
		Vascojet 1000	L	5/64	Annealed	H.T. & Tempered	2-1/4" dia RB
		Vascojet 1000	L.T.	5/64	Annealed	H.T. & Tempered	2-1/4" x 7" FB
II	X	Ti-100A Titanium Alloy	L	5/64	Annealed	No H.T.	2-1/4" dia RB
		B120 VCA Titanium Alloy	L	5/64	Annealed	H.T. & Aged	2-1/4" dia RB
Titanium		B120 VCA Titanium Alloy	L.T.	5/64	Annealed	H.T. & Aged	2-1/4" x 7" FB
III	X	7075 Aluminum	L	5/64	T-6	-----	2-1/4" dia RB
		*7075 Aluminum	L	5/64	T-6	-----	2-1/4" dia RB
Aluminum		*7075 Aluminum	L	5/64	T-6	-----	2-1/4" dia RB
		*7075 Aluminum	L.T.	5/64	T-6	-----	2-1/4" x 7" FB
		*7075 Aluminum	L.T.	5/64	T-6	-----	2-1/4" x 7" FB

L - longitudinal
L.T.- long transverse

RB - rolled bar
FB - forged bar
HT - heat treated

*all four sets from different heats

signal height, was measured on the cathode ray tube of the Immerscope.

All ultrasonic immersion tests were performed in the special research tank shown in Figure 1. The path of the ultrasound was normalized with relation to the test block face by means of a double-angle adjustable transducer mount and the water distance between transducer and test block faces was maintained constant at 1.75 inches.

To obtain data using the contact transducers, the test blocks were wiped clean and arranged on a wooden work table. A few drops of glycerin were placed on the top of each test block and readings were taken by placing the contact probe on the lubricated surface and applying hand pressure until the height of the reflected flaw signal reached a stable peak. The signal heights observed were then recorded.

Two types of data were used to present the information obtained. First, test block calibration curves were made which indicated reflected signal height as a function of metal distance to the test hole for each material evaluated. The instrument gain was maintained at a constant level for each set of test blocks. This data was referred to as "Amplitude vs. Distance Curves". The second type of data consisted of a series of plots of the variables investigated with respect to a set of control blocks, where a reference signal height was maintained. This data is referred to as "Datum Line Curves".

A. AMPLITUDE VS. DISTANCE DATA

The purpose of the "Amplitude vs. Distance" data is twofold: (1) it provides a means of quality control on test block manufacturing techniques by the relative smoothness of the curve; and (2) it illustrates the response pattern for the particular material and transducer. Since deviations due to material variables must be interpreted over a range of different signal heights, these curves were used only for quality control measures rather than to show differences between material variables. Each nineteen block set was checked at 2.25, 5.0 and 10.0 mc by this method before testing for material variables. Amplitude vs. Distance curves for the control blocks of the three groups evaluated are shown in Appendix I. The curve obtained at 5.0 mc for each control set is shown. The curves obtained at 2.25 mc were identical to those shown in WADC Technical Report 59-466 entitled "Research and Development Leading to the Establishment of Ultrasonic Test Standards for Aircraft Materials".

B. DATUM LINE CURVES

The "Datum Line Curves" were utilized to present the effects of different variables on the response characteristics of several materials. A reference signal height of 1.5 inches was maintained on each of the control blocks in each group. This was accomplished by allowing the instrument sensitivity to be adjusted for each metal distance of the nineteen (19) control blocks. A horizontal line of 1.5 inches signal height vs. metal distance was obtained as the reference curve. At each one of the nineteen settings, the reflected signals were observed from the other test blocks of the same length in the particular group being evaluated. These signal heights were plotted in relation to the 1.5 inch reference signal.

Datum Line Curves were obtained on all materials in heat treat Condition 1 as listed in Table 2. The transducers indicated in Table 1 were used. The test blocks in the Steel and Titanium Group were then heat treated to Condition 2 and the tests repeated using the same transducers. The control blocks were not heat treated. The procedures which were followed for heat treating the various test blocks are contained in Appendix II.

C. ADDITIONAL TESTING

In order to assure that aircraft quality material was obtained for fabrication of the test samples used in this investigation, all raw materials were subject to preliminary ultrasonic, tensile, and Rockwell hardness tests. Ultrasonic inspection of the materials was performed in accordance with current technical society specifications. However, no attempt was made to select materials of superior ultrasonic quality, since it was desired to maintain the quality as typical of that used by industry.

Three tensile bars were machined from each set of test blocks for each heat treatment. These tensile bars were heat treated concurrently with the ultrasonic test blocks. Representative photomicrographs were obtained for each alloy and heat treat condition. Rockwell hardness tests were performed on all test blocks and tensile bars in each heat treat condition. At least three readings were taken on each sample. The results of the tensile and hardness tests are shown in Appendix II along with the photomicrographs.

In addition, two 7075-T6 aluminum test blocks from the control set were metallographically examined in an effort to determine causes for the high reflected signal level observed. Photomicrographs of these blocks are also shown in Appendix II.

RESULTS AND DISCUSSION

The tests performed on the three groups of materials are discussed in this section. For all investigations, immersed as well as contact methods were used to obtain data. The variations in the results using the two methods were so slight that only the data obtained with immersed tests is presented.

A. GROUP I - STEEL

Three materials were compared with 4130 normalized steel. Different forming methods and heat treatments of two of these alloys, Vascojet 1000 and Inconel X, are shown in relation to each other and as compared with the control alloy, 4130 N. Annealed C.P. Molybdenum was also compared with these alloys. Datum line curves for this group of materials are shown in Figures 3 through 6.

1. Vascojet 1000

Test blocks made from hand forged and rolled bar Vascojet 1000, a 5 per cent Cr-Mo-V steel alloy, were evaluated. Datum line curves were obtained from both the annealed and heat treated conditions.

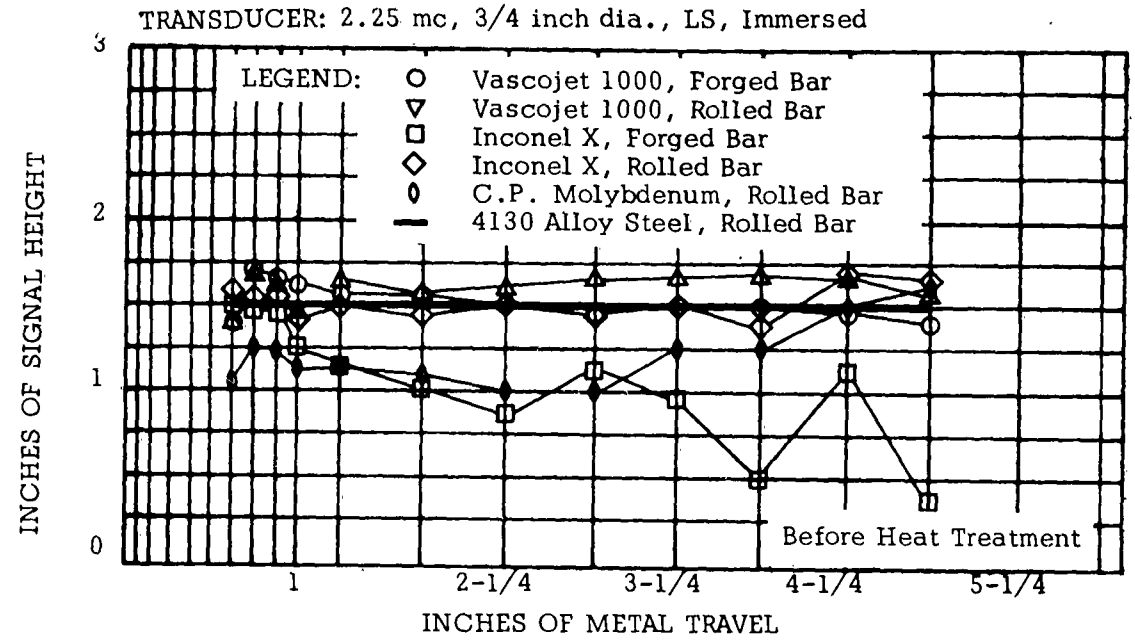

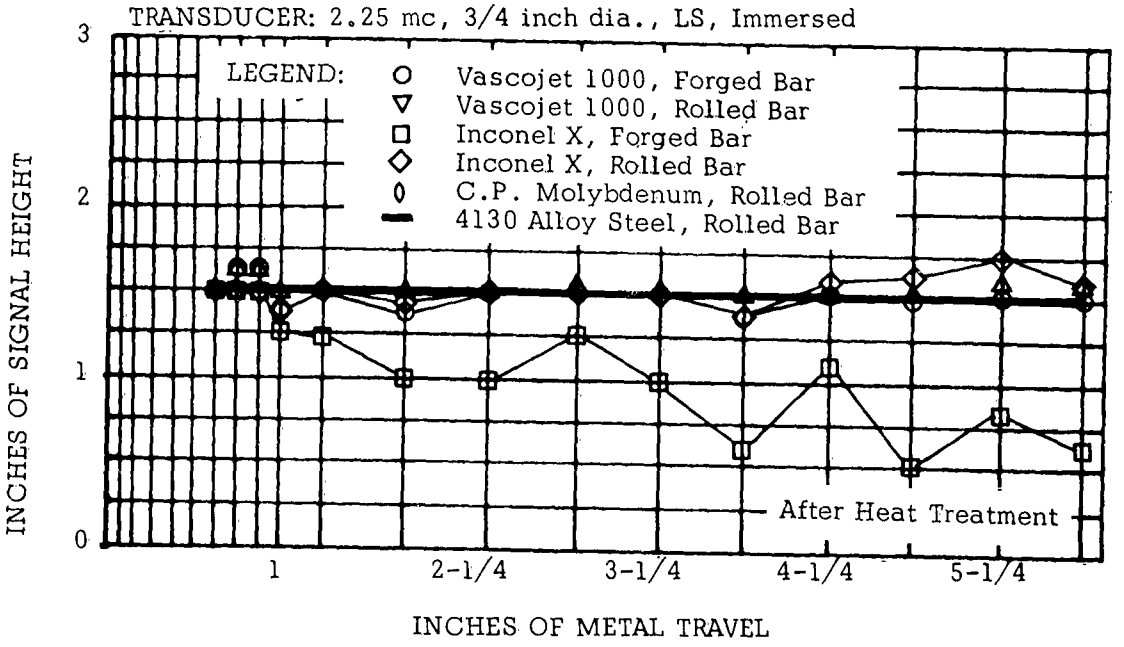

Figure 3. Datum Line Curves, Group I Materials Before and After Heat Treatment at 2.25 mc.

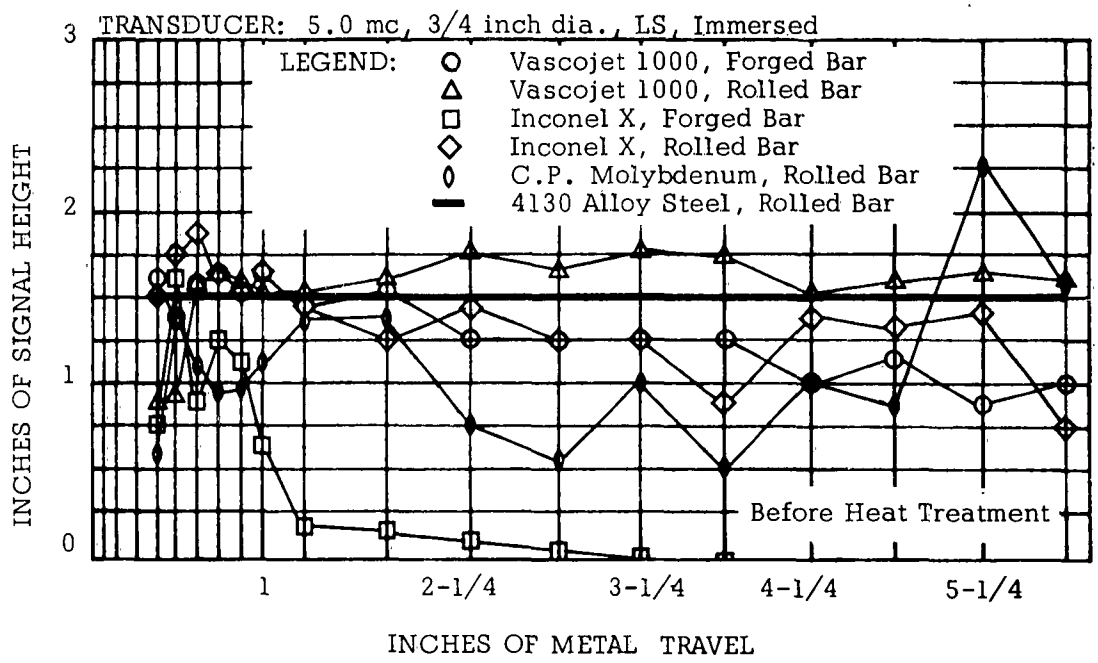

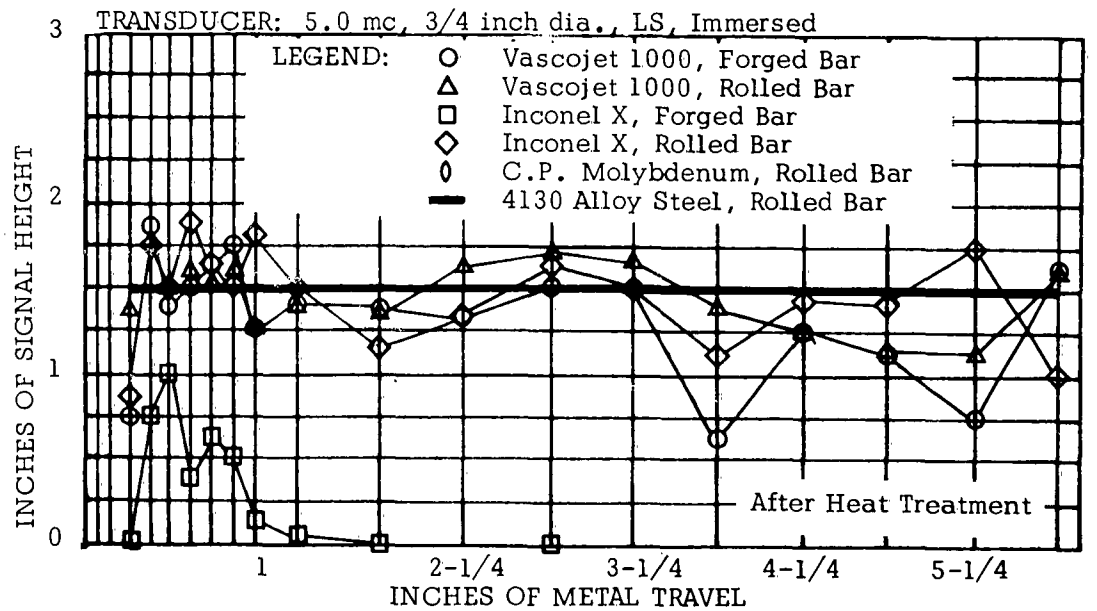

Figure 4. Datum Line Curves, Group I Materials Before and After Heat Treatment at 5.0 mc.

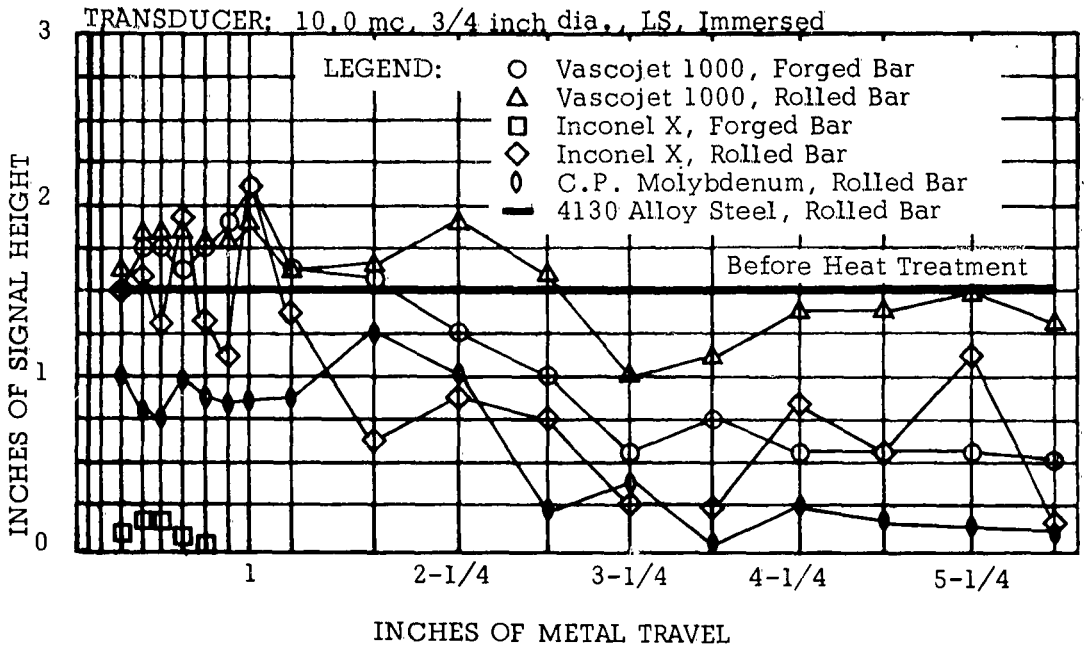

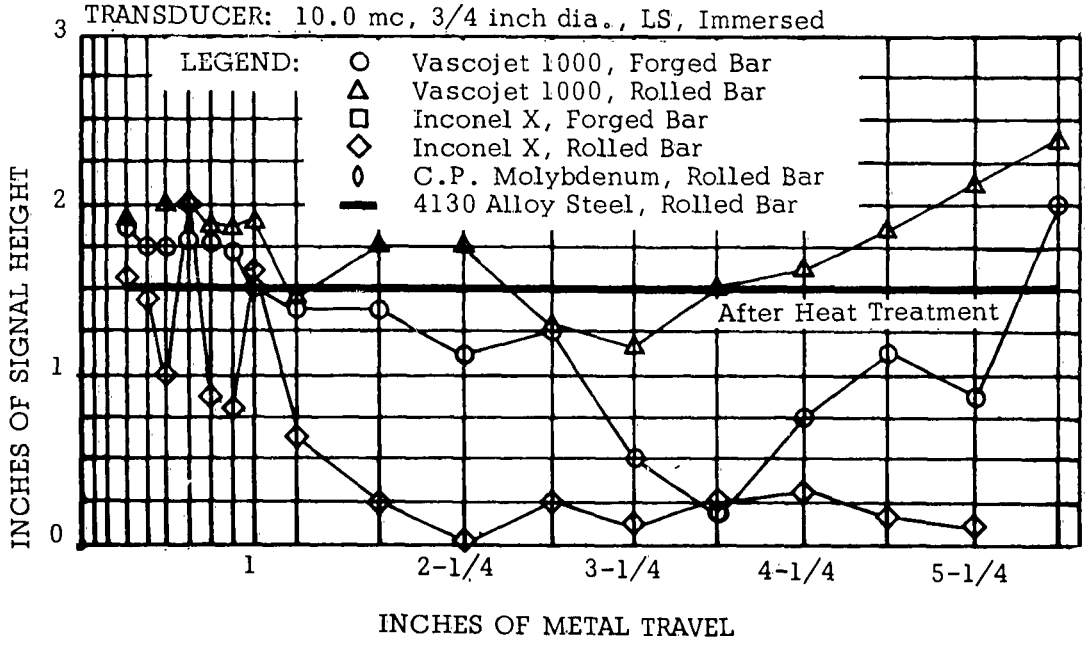

Figure 5. Datum Line Curves, Group I Materials Before and After Heat Treatment at 10.0 mc.

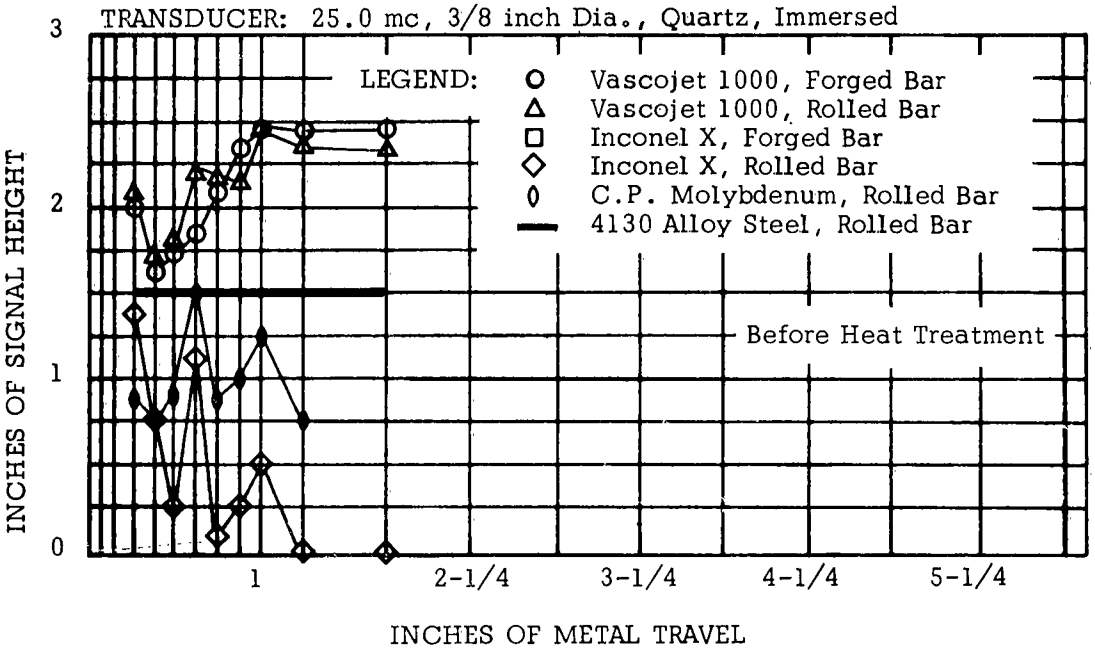

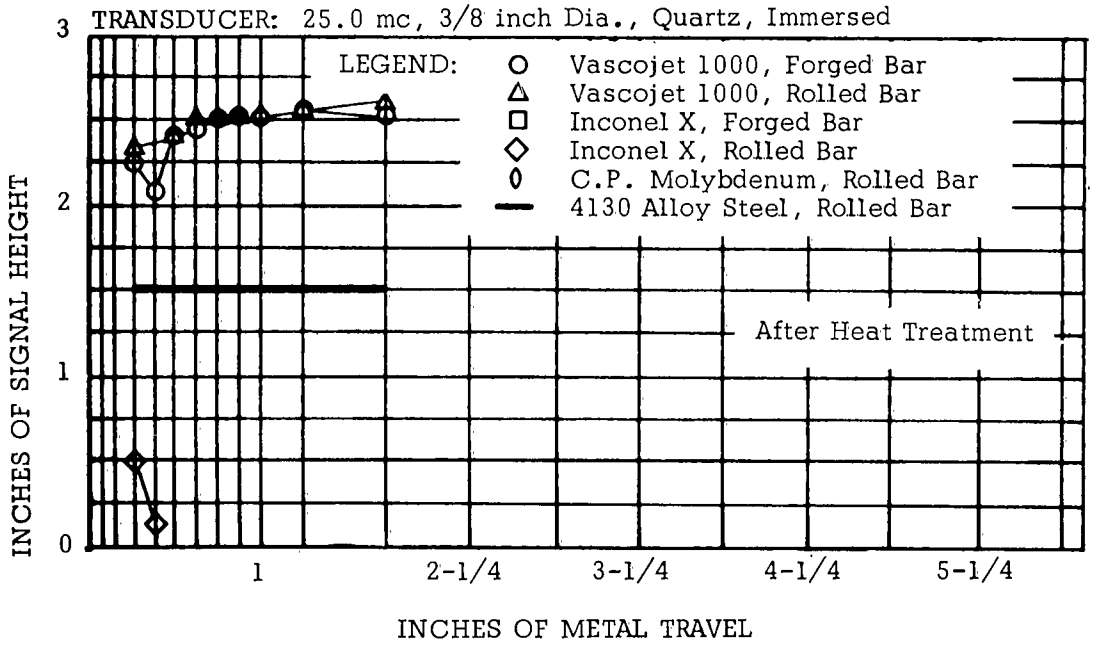

Figure 6. Datum Line Curves, Group I Materials Before and After Heat Treatment at 25.0 mc.

a. Forming Method

At 2.25 mc no appreciable difference between forged and rolled bar was noted. When tested at 5.0 and 10.0 mc, the rolled bar had slightly higher response than the hand forged material in both the annealed and heat treated conditions. However, at 25.0 mc there is no significant difference between the two. At 25.0 mc the response for both forming methods was higher than the 4130 N material but no significant difference was observed at 2.25 mc.

b. Heat Treatment

There was no difference noted between annealed and heat treated conditions at 2.25 mc. When tested at 5.0 mc the rolled bar exhibited slightly lower response after heat treatment. This was also true of the forged blocks up to 3-3/4 inches metal distance where the response after heat treatment became somewhat scattered. At 10.0 and 25.0 mc the response increased slightly following heat treatment in both rolled and forged test blocks. This increase was more noticeable beyond 3-3/4 inches metal distance at 10.0 mc.

2. Inconel X

Hand forged and rolled bar Inconel X test blocks were evaluated in the annealed and heat treated condition.

a. Forming Method

At all test frequencies, the hand forged blocks had lower signal response than the rolled bar. Using test frequencies of 2.25 and 5.0 mc the response from the rolled bar compared favorably to that from the 4130 N. At 10.0 mc the reflected signal from the forged blocks practically disappeared and the response from the rolled bar decreased considerably. When tested at 25.0 mc only a slight signal response was observed from the rolled bar and none could be detected from the forged test blocks.

b. Heat Treatment

The effects of heat treatment on the signal response were negligible at 2.25 mc. It was interesting to note that at 5.0 mc the response from the forged blocks decreased while the reflected signal from the rolled bar increased slightly beyond 2-1/4 inches metal distance after heat treating. However, at 25.0 mc slightly better response was observed from the rolled blocks prior to heat treatment, i.e., in the annealed condition.

3. C. P. Molybdenum

Commercially pure (C.P.) molybdenum rolled bar was evaluated in the annealed condition only. Comparisons are shown between this material and the other two alloys evaluated in this group. The signal response varied with the test frequency employed. As the frequency was increased from 2.25 to 10.0 mc the signal response

generally decreased with reference to the 4130 N control blocks. At 25.0 mc the signal response was about the same as at 10.0 mc. The signal amplitude was consistently lower than that observed from the control blocks. In order to evaluate C.P. molybdenum using 4130 N test blocks some correction would be required.

The signal response from C.P. molybdenum was most nearly like Inconel X rolled bar where both materials were in the annealed condition. It would not be advisable to evaluate flaws compared to Inconel X, however, since there was sufficient variation in response to cause misinterpretation. These variations in signal response from C. P. molybdenum may have been caused by anisotropic properties of this material.

B. GROUP II - TITANIUM

For this part of the investigation the test blocks were fabricated from an all beta titanium alloy, B120 VCA. The test blocks were evaluated in the annealed and heat treated condition using Ti-100A alloy as the control alloy. Figures 7 through 10 show the datum line curves obtained from the titanium test blocks both before and after heat treatment.

1. B120 VCA Titanium

Both rolled bar and hand forged materials were tested.

a. Forming Method

The method of forming appeared to have very little effect on signal response. The response curves obtained were very similar in appearance and, in fact, nearly the same amplitude throughout. It was found that both the forged and rolled bar had large, irregular shaped grains probably accounting for the similarity in response. See Appendix II.

b. Heat Treatment

Age hardening of this alloy resulted in greatly improved signal response. This higher response after aging probably was caused by the decomposition of some of the unstable phases which was initiated in the alloy by the heat treatment. Prior to heat treating the 5/64 inch test hole could be observed only up to 2-1/4 inches metal distance, and then only at frequencies of 10.0 mc or lower. After heat treating a reflected signal was observed throughout the entire range of metal distance tested.

Except at 25.0 mc the response from the B120 VCA blocks was lower than that from the Ti-100A reference set. In the annealed condition the B120 VCA exhibited greater response than Ti-100A at 25.0 mc. However, reflected signals were observed up to only 1/2 inch metal distance.

It appears that a test frequency of 2.25 mc would produce the most consistent results with respect to flaw evaluation. Higher frequencies such as 5.0, 10 or 25.0 mc should be used, however, for material with flaw

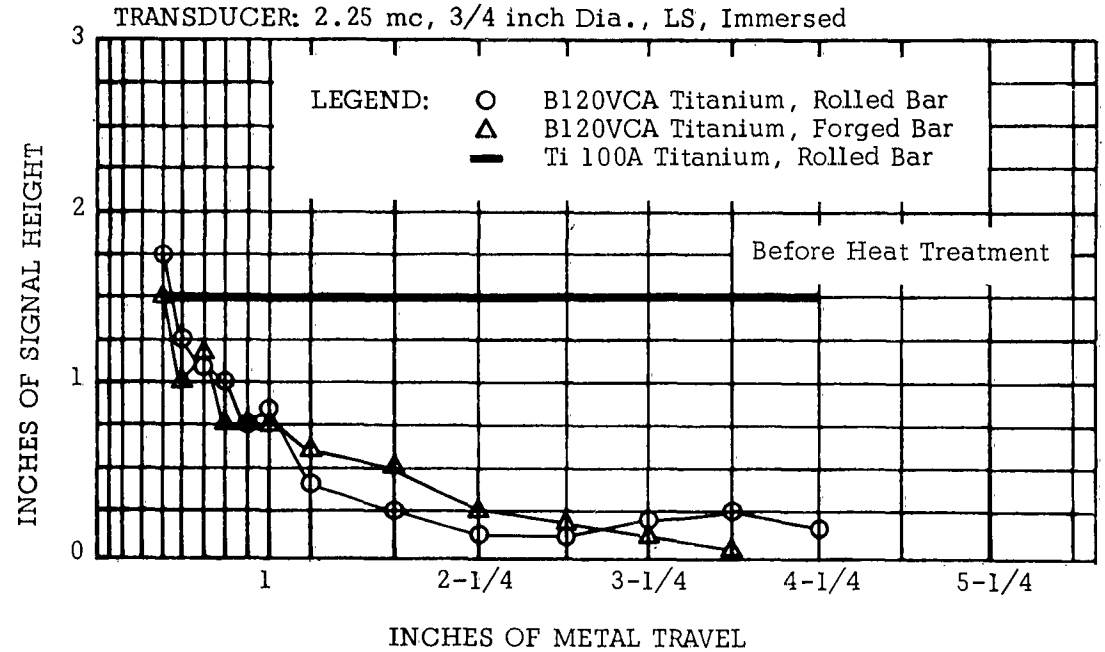

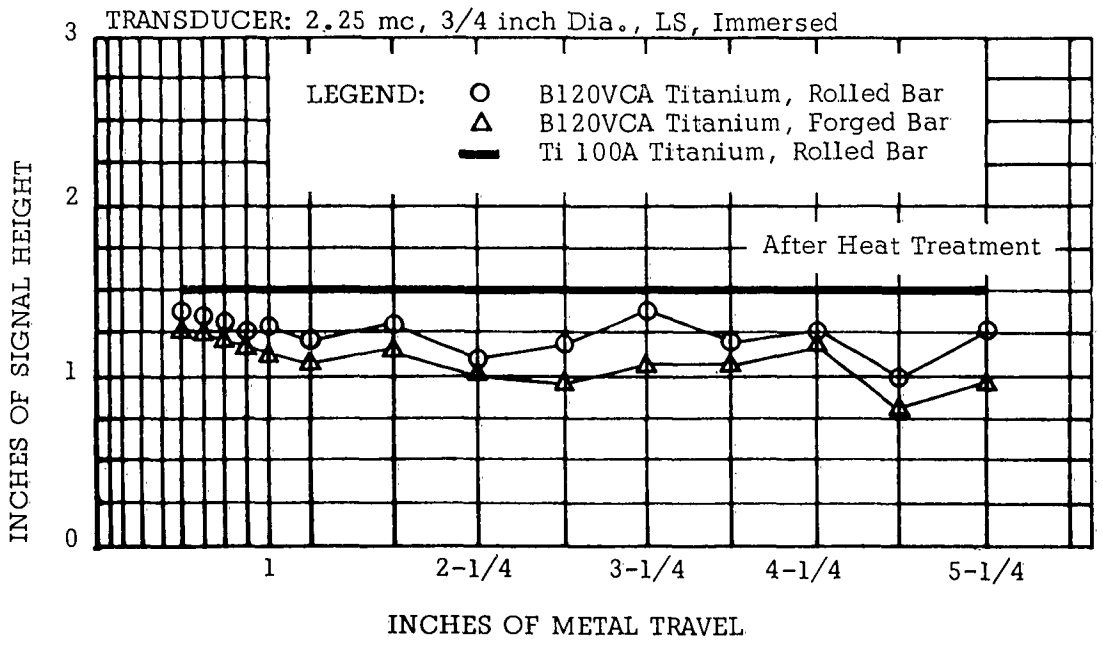

Figure 7. Datum Line Curves, Group II Materials Before and After Heat Treatment at 2.25 mc.

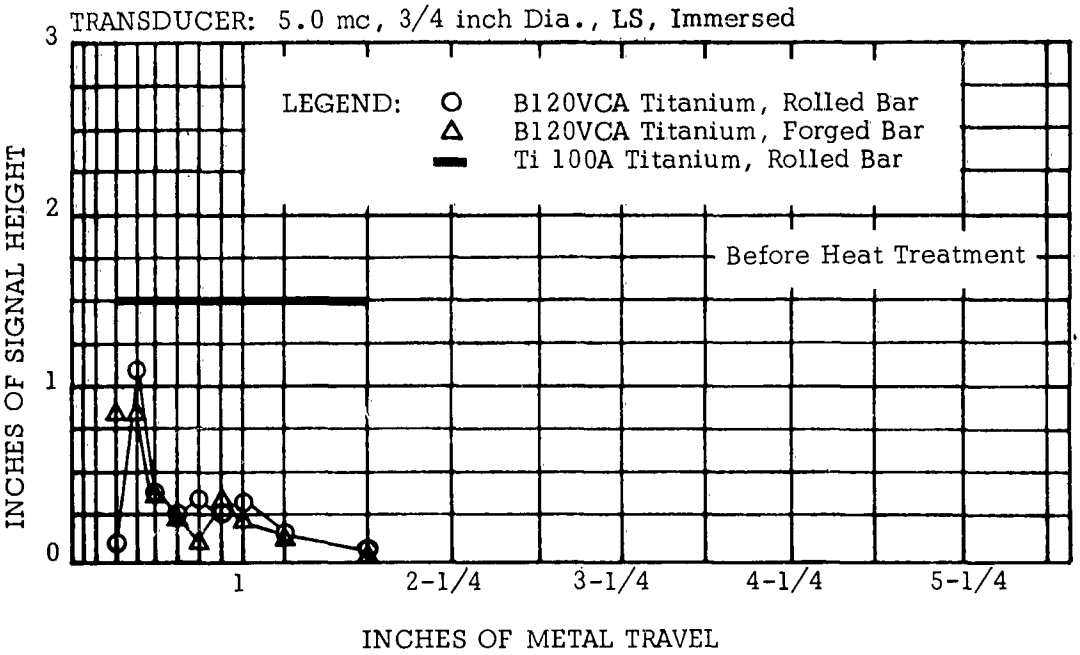

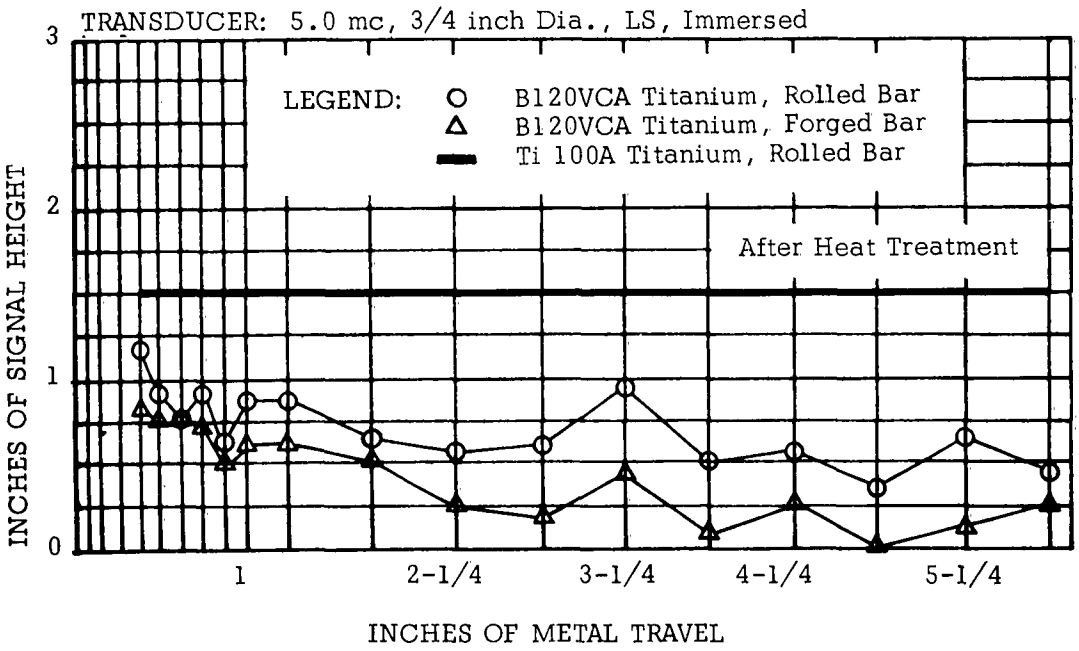

Figure 8. Datum Line Curves, Group II Materials Before and After Heat Treatment at 5.0 mc.

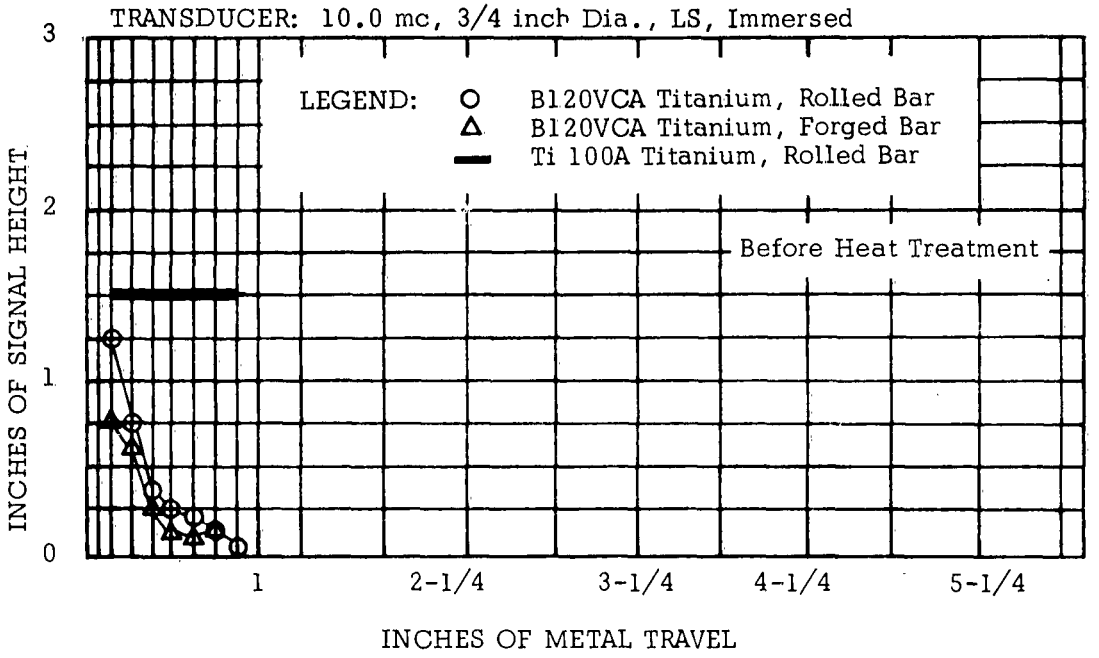

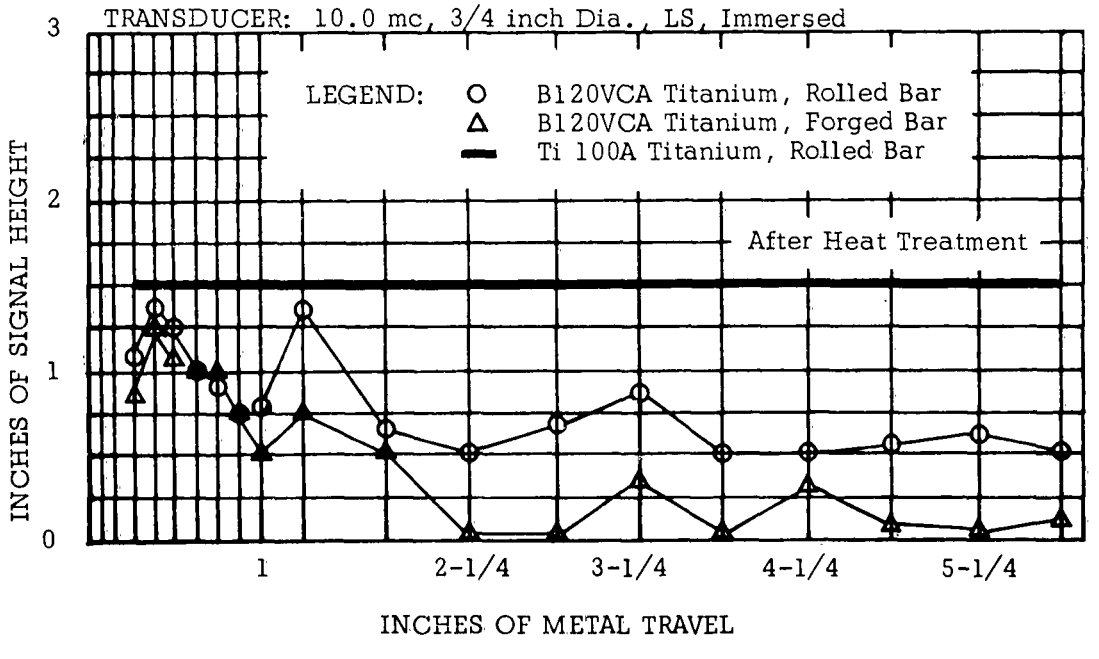

Figure 9. Datum Line Curves, Group II Materials Before and After Heat Treatment at 10.0 mc.

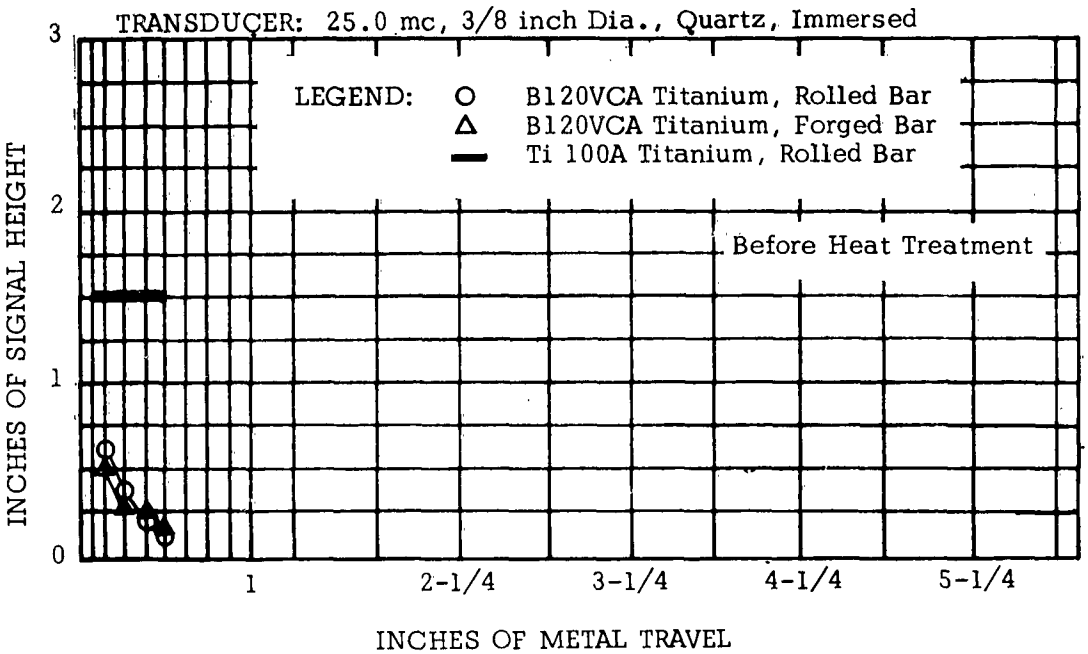

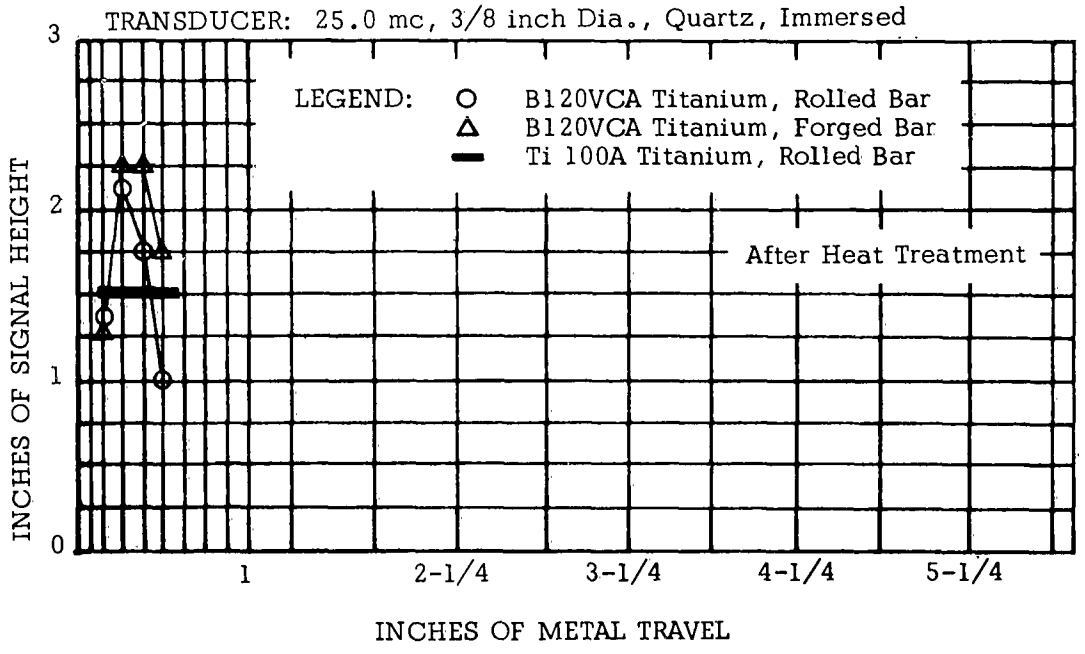

Figure 10. Datum Line Curves, Group II Materials Before and After Heat Treatment at 25.0 mc.

depths of one inch or less. The test frequencies recommended in WADC Technical Report 59-466 concerning the use of Ti-100A test blocks as standards appear to be applicable to the hardened condition of the B120 VCA.

C. GROUP III - ALUMINUM

The last group of materials investigated included four sets of 7075-T6 aluminum test blocks. Each set was fabricated from a different heat of material. The various heats were obtained from different manufacturers. The only variable tested was method of forming. Two sets were made from rolled bar and two from forged bar stock fabricated in the longitudinal and long transverse grain directions. This part of the investigation was performed to determine the acoustical variations, if any, between heats and the significance of any deviations on the reliability of ultrasonic flaw evaluation.

The test blocks from the four heats were compared to a set of blocks made from 7075-T6 rolled bar used for a previous contract (Contract No. AF 33(616)-5877). This set was used as the control set. All test blocks had 5/64 inch diameter, flat bottom holes.

The datum line curves obtained are shown in Figures 11 through 14. It was observed that at the test frequencies of 2.25, 5.0 and 10.0 mc. all four test sets responded similarly. In most cases, however, the control set displayed a stronger signal response where the metal travel was greater than one inch. The only exception to this was at 10.0 mc where the response of the four heats was observed to increase after a metal distance of 4 inches was reached.

These indications suggested that the test block set employed as the control alloy was not typical. The control set of test blocks was fabricated from rolled bar stock.

It was found that Rolled Bar #2 generally had the lowest of the four heats investigated. The two sets of blocks made from forged bar had almost identical response. Thus, although variations in ultrasonic response characteristics existed between different heats of the rolled bar, no significant variations were apparent in forged material.

When the mechanical properties of the four heats were examined it was found that the two forged heats had similar mechanical properties while the two rolled bar heats were not similar to each other in tensile strength and percent elongation. The ultimate tensile strength for Rolled Bar #1 was 80,900 psi and elongation was 16.2 percent while for Rolled Bar #2 these values were 93,330 psi and 10.0 percent respectively. This possibly would explain the variations in signal response observed between the two heats of rolled bar. The rolled bar with the higher signal response had the lower mechanical properties. Thus, flaw evaluation techniques appear to be affected by variations in the microstructure and the resulting mechanical properties of a given alloy.

Differences in the grain structure of these two test block sets, Rolled Bar #1 and Rolled Bar #2, apparently caused the difference in ultrasonic response. In examining

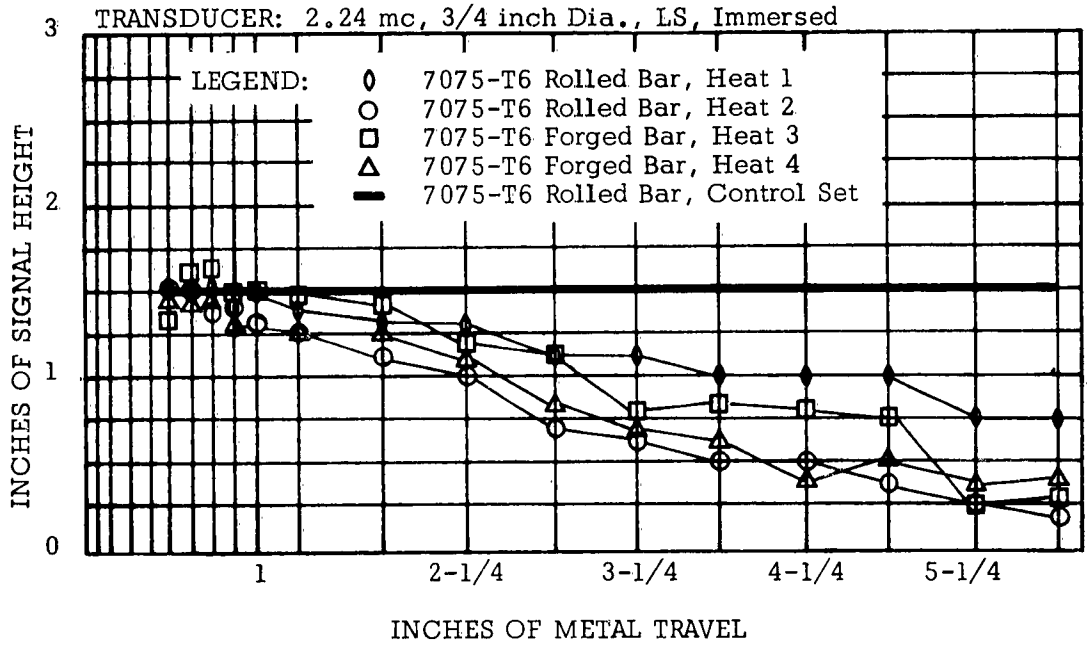

Figure 11. Datum Line Curve, Group III Material, Four Different Heats at 2.25 mc.

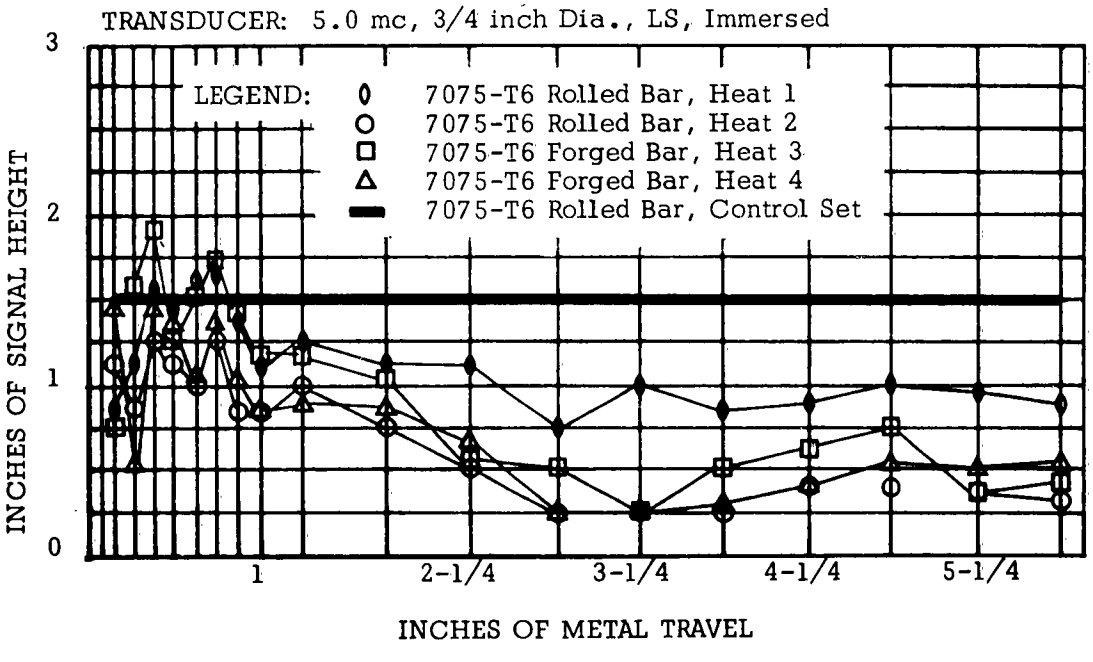

Figure 12. Datum Line Curves, Group III Materials, Four Different Heats at 5.0 mc.

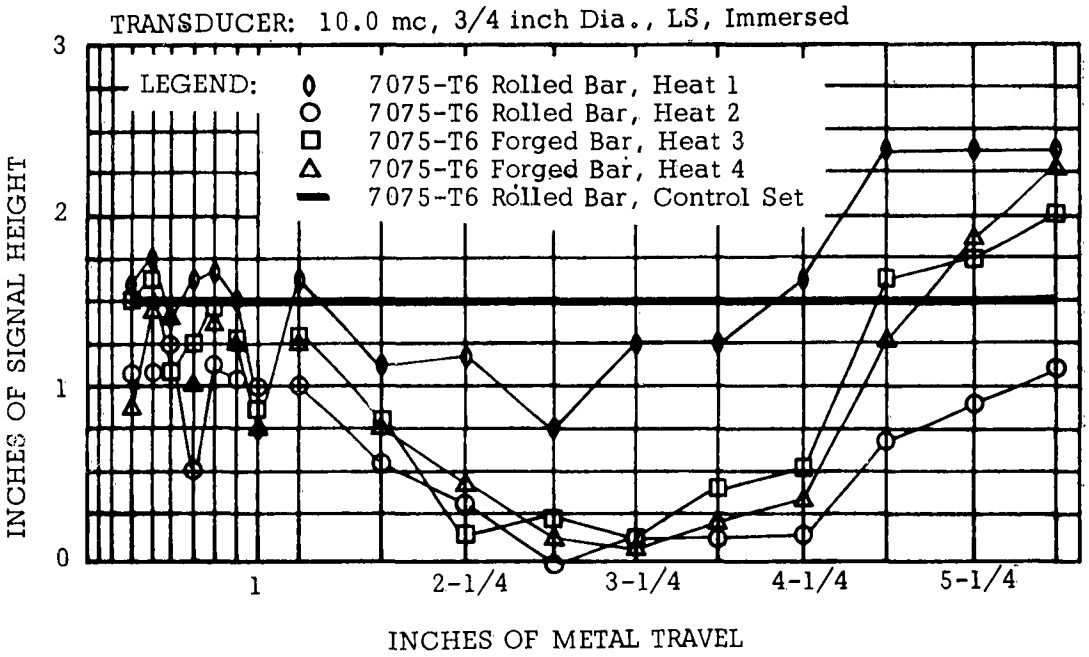

Figure 13. Datum Line Curve, Group III Materials Four Different Heats at 10.0 mc.

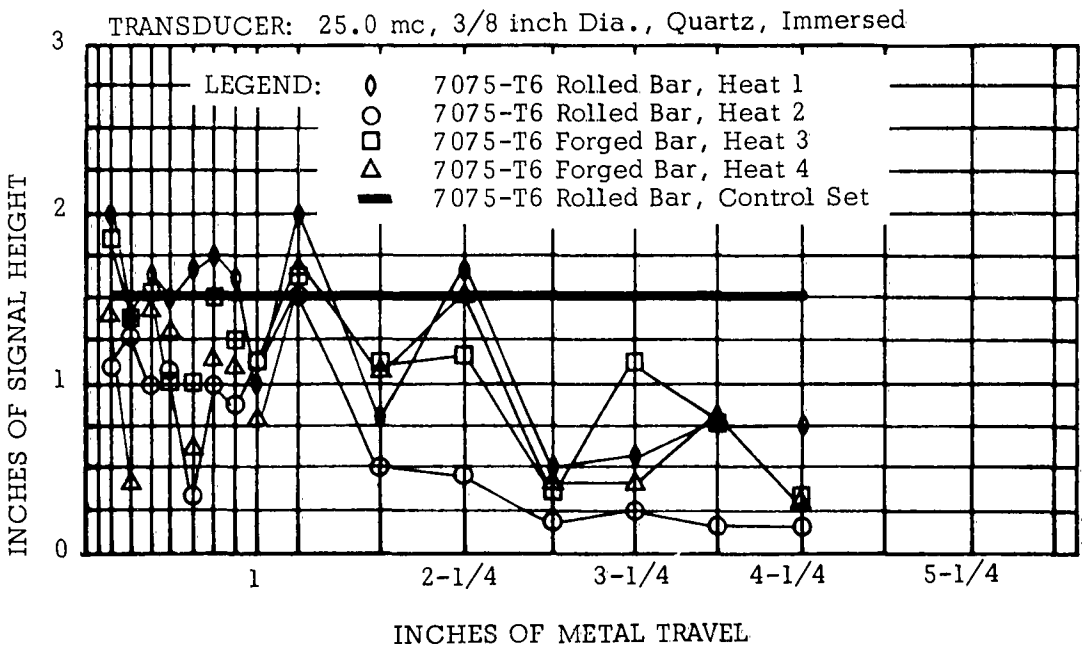

Figure 14. Datum Line Curve, Group III Materials Four Different Heats at 25.0 mc.

photomicrographs of these heats, it appears that Rolled Bar #2 was more fully aged than Rolled Bar #1. The finer grain structure occurred in Rolled Bar #1. Rolled Bar #2 showed more directionality of grain and was apparently rolled at a lower temperature.

The control set, which displayed the highest response of the three rolled bar heats, had the largest grain structure. The degree of working seemed to be less than that in the other heats.

It seems that the microstructure does have some effect on ultrasonic signal response. The extent of this effect seems to be limited, so that, no serious problem is apparent. Further exploration in this area seems advisable.

CONCLUSIONS

A. GROUP I - STEEL

The results of evaluations performed on the three materials in this group indicated that the effects of changes in variables such as alloy, method of forming and heat treatment were slight at the lower test frequencies. As the test frequency was increased, the difference in signal response due to method of forming became more apparent. The rolled materials consistently displayed higher response characteristics than the forged materials.

Heat treatment also appeared to be significant at higher frequencies. An overall increase in scatter of results was observed at 10.0 and 25.0 mc which emphasized this variable. At 2.25 and 5.0 mc, however, the curves indicated less scatter after heat treatment. At 10.0 and 25.0 mc, the signal response of the materials increased. However, the differences appeared at metal travel distances that normally result in inconsistent flaw evaluation using the 10.0 mc transducer. The 25.0 mc range appeared to be useful for evaluating most of this group of materials at metal travel distances up to one inch.

The 4130 reference blocks appear to be a useful reference for the Vascojet 1000 alloy and the Inconel X rolled bar. However, in order to evaluate the forged Inconel X using 4130, a correction factor would have to be applied. The same is true for the C.P. Molybdenum. A tentative method for accomplishing these corrections is presented later in this report.

B. GROUP II - TITANIUM

The results of datum line curves before and after heat treatment of the all beta titanium alloy, B120 VCA, indicate that aging substantially increases the ultrasonic response characteristics of this alloy. At every test frequency there was generally an increase in reflected signal heights. The forged bar had a slightly lower response than the rolled bar at all test frequencies.

In comparison to the Ti-100A control blocks, the B120 VCA had lower response at 2.25, 5.0 and 10.0 mc, but at 25.0 mc slightly higher response was observed from the heat treated blocks. The depth penetrated at 25.0 mc was only 1/2 inch, however.

At 2.25 mc the annealed Ti-100A blocks could be used to evaluate heat treated B120 VCA titanium if metal distances greater than 1 inch were tested. This limits the technique considerably, hence, evaluation in this manner is not recommended unless corrections are applied.

C. GROUP III - ALUMINUM

The results obtained from investigating four different heats of 7075-T6 aluminum alloy indicated that the variations due to the difference in method of forming and different heats of the alloy could normally be disregarded. However, variations in reflected signal heights due to differences in grain structure or mechanical properties such as yield strength and percent elongation should be considered especially where 10.0 or 25.0 mc test frequencies are employed. The range over which mechanical properties could be allowed to vary was not established in this report. It was apparent, however, that rolled bar test blocks can be satisfactorily used to evaluate defects in forged structures without compensation.

Conditions such as grain size, hot working temperature, heat treat response and alloy segragation can affect the ultrasonic response. The effects appear to be limited, however, some investigation should be conducted to establish these limits.

SECTION III

EFFECTS OF ACOUSTICAL PROPERTIES

It was apparent that material variables, as described in Section II, were not the only factors to be considered in flaw evaluation. Acoustical properties, such as acoustic impedance and attenuation, were known to result in differences in signal response from various materials. Only a few of these measurements were available in published data.

These measurements were necessary to determine the extent to which theoretical or empirical results could be applied as correction factors for simplifying flaw size evaluation techniques. Therefore, it was essential that the acoustical properties which caused amplitude response differences between various materials be found.

The following section describes the tests and results of the investigations used to determine these acoustical properties. Correction factors were then derived from the acoustical property relationships. Appendix III presents a method for expressing the relationships that affect the transmission of ultrasound from one medium into a second in terms of decibels.

EQUIPMENT

The test apparatus used was as follows:

1. Curtiss-Wright Immerscope, Model 424A. Frequency range - 2.25 mc to 25.0 mc.

2. Branson Instruments Sonoray. Frequency range - 0.4 mc to 10.0 mc.

3. Sperry Ultrasonic Attenuation Comparator. Frequency range - 5.0 mc to 200 mc. See Figure 15.

4. Sola Constant Voltage Transformer. Capacity 500 VA, 100 volts, 4.24 Amps, 60 cycles.

5. Ultrasonic Testing and Research Laboratory designed research buffer tank. See Figure 16.

6. Ultrasonic Testing and Research Laboratory designed research test tank. See Figure 1 in Section II, Material Variables.

7. Ultrasonic Division, Automation Industries, Inc. Adjustable Transducer Mount, Model 1026.

8. Kay Electric Co. Attenuator, Model 32-0. See Figure 17.

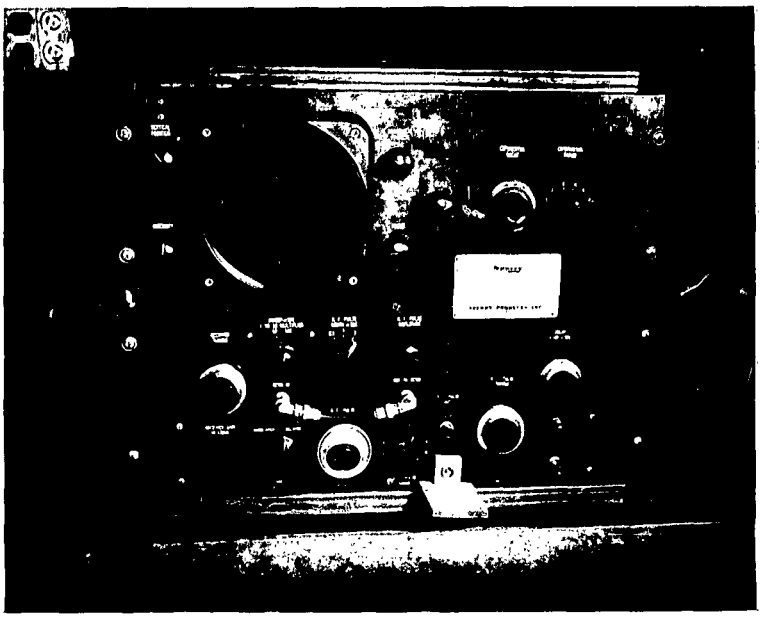

Figure 15. Sperry Instruments Ultrasonic Attenuation Comparator.

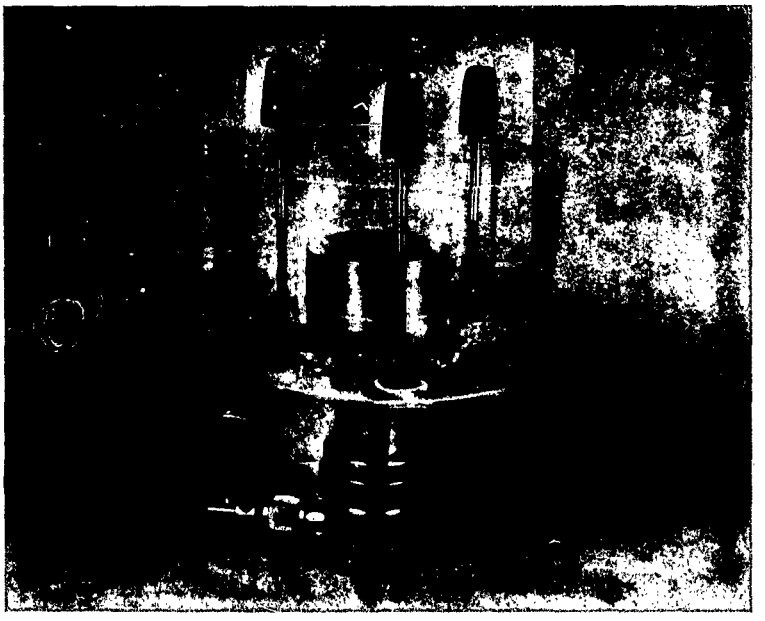

Figure 16. Research Buffer Tank.

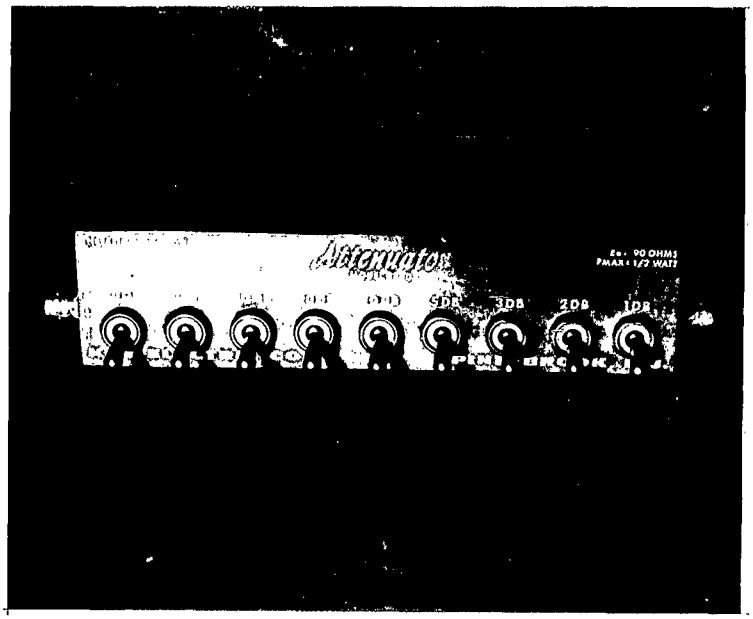

Figure 17. Kay Electric Company Attenuator.

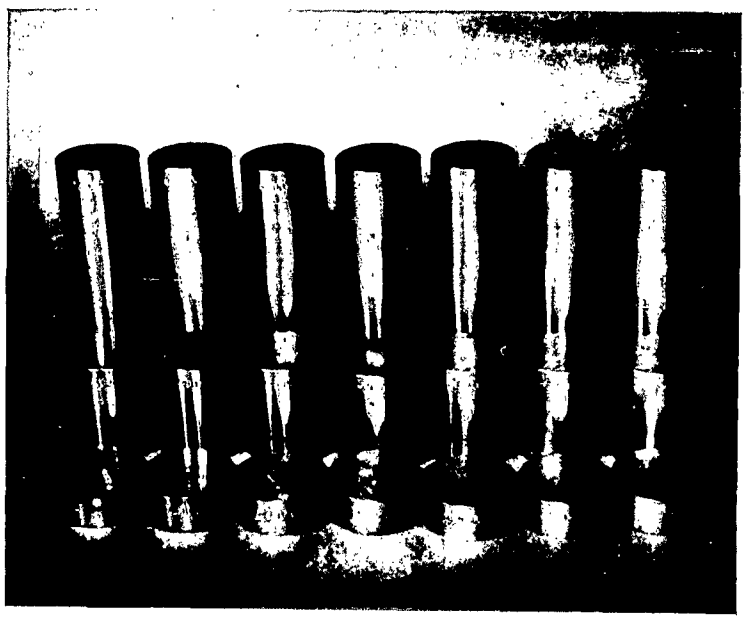

Figure 18. Twenty-One Block Test Set.

9. Wayne Kerr Wide-Band Attenuator, Model Q251.

10. Ultrasonic Transducers as listed in Table 3.

MATERIAL AND TEST SAMPLES

The samples which were tested to determine acoustical properties are listed in Table 4. These twenty-one (21) block sets contained test blocks of three different lengths and seven (7) different hole sizes as shown in the above referenced table. Except for the 0.875 inch blocks where the test hole depth was 0.375 inches, the block diameter, surface finish, and all tolerances for the twenty-one (21) block sets are the same as those given in Figure 2, Section II. A twenty-one (21) block test set is shown in Figure 18.

In addition, specially machined samples were fabricated from the eight materials listed above and nine materials from previous contracts. Parallelism of the sample surfaces was maintained within 0.0001 inches per inch. Two samples 0.500 inches and two samples 0.250 inches were made from each material. These samples were used to establish sonic velocity and attenuation values using the Attenuation Comparator. Table 5 lists the materials used from previous contracts.

TEST PROCEDURES

A. VELOCITY AND IMPEDANCE

The acoustic impedance of a material determines the amount of sonic energy transmitted and reflected at interfaces between the material and some other given medium, e.g., water. It is a function of the sonic velocity and density of the material.

Velocity was measured using the Attenuation Comparator method described in Appendix III. The measurements were made on several samples of each material using a 10.0 mc lithium sulphate transducer and the densities of the various materials were obtained from the manufacturers specifications. The specific acoustic impedance was then calculated using the following relationship:

$$Z = \rho V$$

where

ρ = density, lb/in^3

V = velocity, in/sec

Z = specific acoustic impedance, $lb/in^2 sec$

The results of these measurements are tabulated in Table 6.

The energy loss between front and back reflections due to impedance mismatch was calculated for each material from the following relationships:

TABLE 3

TRANSDUCERS USED TO MEASURE ACOUSTICAL PROPERTIES			
MANUFACTURER	TYPE	FREQUENCY Megacycles	DIAMETER Inches
Immersed Style			
Automation Industries	Lithium Sulphate	2.25	0.75
Automation Industries	Lithium Sulphate	5.0	0.375
Automation Industries	Lithium Sulphate	5.0	0.75
Automation Industries	Lithium Sulphate	10.0	0.375
Automation Industries	Lithium Sulphate	10.0	0.75
Automation Industries	Lithium Sulphate	15.0	0.375
Automation Industries	Quartz	25.0	0.375
Contact Style*			
Sperry Products	X-Cut Quartz	3.0	0.50
Sperry Products	X-Cut Quartz	5.0	0.50
Sperry Products	X-Cut Quartz	7.0	0.50
Sperry Products	X-Cut Quartz	9.0	0.50

*These crystals were used with the Sperry Attenuation Comparator.

TABLE 4

MATERIAL AND TEST SAMPLES FOR ACOUSTICAL PROPERTY MEASUREMENTS					
Material	Grain Direction	Original Material Form	Heat Treat Condition	Hole Sizes in 64ths of an Inch	Test Block Length* Inches
Inconel X	L	2-1/4" dia RB	Annealed	2 through 8	0.875, 2.50, 6.5
Commercially Pure Molybdenum	L	2-1/4" dia RB	Annealed	2 through 8	0.875, 2.50, 6.5
Vascojet 1000	L	2-1/4" dia RB	Annealed	2 through 8	0.875, 2.50, 6.5
7075 Aluminum	L	2-1/4" dia RB	T-6	2 through 8	0.875, 2.50, 6.5
4130 Steel	L	2-1/4" dia RB	Normalized	2 through 8	0.875, 2.50, 6.5
Ti-100A Titanium	L	2-1/4" dia RB	Annealed	2 through 8	0.875, 2.50, 6.5
17-4 PH Stainless	L	2-1/4" dia RB	Annealed	2 through 8	0.875, 2.50, 6.5
ZK-60 Magnesium	L	2-1/4" dia. EB	As Extruded	2 through 8	0.875, 2.50, 6.5

L - longitudinal

RB - rolled bar
EB - extruded bar

*dimension "L_2" in Figure 2

TABLE 5

ATTENUATION SAMPLES - MATERIALS FROM PREVIOUS CONTRACTS		
MATERIAL*	ORIGINAL MATERIAL FORM	HEAT TREAT CONDITION
7075 Aluminum	RB	T-6
7075 Aluminum	EB	T-6
7075 Aluminum	FB	T-6
7075 Aluminum	RP	T-6
4340 Alloy Steel	FB	180,000 psi
403 Stainless Steel	FB	Air Hardened
6 Al-4V Titanium Alloy	FB	Solution Treated and Aged
2014 Aluminum	RB	T-6
2024 Aluminum	RB	T-4
7079 Aluminum	FB	Annealed
J-1 Magnesium	EB	As Extruded
AZ-31B Magnesium	EB	As Extruded

RB - rolled bar
RP - rolled plate
FB - forged bar
EB - extruded bar

*NOTE: The grain direction was longitudinal for all samples. Two samples, one 0.250 and one 0.500 inches thick, were tested for each material and form listed.

$$R = \frac{(Z_2 - Z_1)^2}{(Z_2 + Z_1)^2}$$

$$T = 1 - R$$

$$D = 10 \log_{10} \frac{R}{T^2} \quad \text{(one face of sample submerged)}$$

where

Z_2 = specific acoustic impedance of metal lb/in^2-sec

Z_1 = specific acoustic impedance of water, 0.213×10^4 lb/in^2-sec

R = reflection coefficient (water to metal)

T = transmission coefficient (water to metal)

D = water/metal impedance loss, in decibels.

The results of these calculations are listed in Table 6. The methods used to find this loss experimentally are contained in Appendix III, Measurements of Acoustical Properties.

The energy loss attributed to the reflection coefficient was calculated from:

$$R_d = 10 \log_{10} \frac{1}{R}$$

where

R_d = reflection coefficient loss, decibels

R = reflection coefficient (water/metal)

Direct measurements of R_d were obtained using the Attenuation Comparator method described in Appendix III.

B. ATTENUATION MEASUREMENTS

Two types of test blocks were used for attenuation measurements. First, the twenty-one (21) block sets were tested and second, special blocks which had been machined from materials used on previous contracts were tested. These special blocks were 0.250 and 0.500 of an inch long. The machining tolerance was ±0.0001 of an inch per inch parallelism of the reflecting surfaces.

Three techniques were used to measure attenuation of the twenty-one (21) block sets by the immersion method. These techniques were (1) Front Surface to First Back Echo, (2) Successive Back Echo, and (3) Attenuation Comparator. Detailed procedures for these techniques are described in Appendix III. The test frequencies were 2.25, 5.0 and 10.0 mc.

The special 0.250 and 0.500 of an inch blocks were tested using the Attenuation Comparator technique employing contact transducers. Measurements of these special blocks were also obtained by the immersed method using the Successive Back Echo technique and the Attenuation Comparator technique. Test frequencies for the contact method ranged from 5 to 64 mc. Contact readings at 2.25 mc were obtained using the Branson Sonoray.

The values of apparent attenuation listed in Table 7 are average values of all the readings obtained using immersed techniques for each material. Figure 19 shows a graph of attenuation versus test frequency for data obtained using the contact method.

C. RELATIONSHIP OF FLAW SIZE TO ENERGY LOSSES

When the attenuation measurements had been completed, flat bottom holes were drilled in the twenty-one (21) block test sets. The hole sizes were 2, 3, 4, 5, 6, 7, and 8/64 of an inch diameter for each of the three metal distances as listed in Table 4.

Using the reflected signal from the 5/64 inch diameter flat surface contained within each alloy (set of test blocks), a reference signal height of 1.5 inches was established with a predetermined value of attenuation (decibels) inserted into the input line to the receiver of the instrument. After normalizing the transducer, the attenuation was either increased or decreased so that the reference signal height was maintained when test hole diameters of 2, 3, 4, 6, 7 and 8/64 of an inch were observed. This system provided a means for the differences in signal amplitude to be evaluated in terms of decibels in relation to a reference hole size. Test frequencies were 2.25, 5.0 and 10.0 mc. Tables 9, 10 and 11 show the results obtained.

In order to relate one material to another further tests were performed. In these tests the 5/64 of an inch test hole in 7075-T6 aluminum was used as the reference signal. A predetermined value of attenuation was placed in the receiver line. The 5/64 of an inch test holes were observed at corresponding metal distances in the materials being compared with aluminum. The attenuation was then increased or decreased to obtain a signal amplitude equal to the 1.5 inches reference height using aluminum test blocks. Test frequencies of 2.25, 5.0 and 10.0 mc were used. The results of these measurements are shown in Table 12.

Several tests were made to verify the correction method. The 5/64 of an inch diameter test holes in a set of 7075-T6 aluminum test blocks were used as the reference signal. The 8/64 of an inch test holes in a set of 4130 N steel blocks was compared to the aluminum. Both 3/8 and 3/4 of an inch transducers were used to determine the effects of beam spreading. Several other materials were evaluated using randomly selected test blocks.

To perform these tests the signal from the "unknown" was adjusted to 1.5 inches amplitude on the cathode ray tube with a predetermined value of attenuation in the receiver line (10 db for these tests). Leaving the gain as adjusted, the signal was observed from the aluminum block with comparable metal distance. Attenuation was

then increased or decreased to obtain the 1.5 inch reference height. The measured attenuation difference was recorded and the value compared with the value calculated using the correction factor. The results are shown in Table 13.

Where the defect size is not known as in normal inspection, a slightly different approach can be followed in applying the correction factor. In that case, assume a defect size of 5/64 of an inch (the same as the reference blocks) and obtain a measured attenuation difference as in the tests described above. The calculated correction factor in this evaluation will be C.F. = $(D_x - D_s) + (\alpha_x - \alpha_s)2L$. Subtract the measured value from the calculated value assuring that the sign of this quantity is correct. Depending upon the test frequency, look in Tables 9, 10 or 11 to determine the actual defect size.

All ultrasonic tests for this part of the investigation were performed in the special research tank shown in Figure 1. The water distance was maintained constant at 1.75 inches.

D. LENGTH AND NUMBER OF BACK REFLECTIONS

The probable correlation of information from multiple back surface reflections and acoustical properties prompted some investigation in this area. The number of A-Scan multiples of the back surface echo and the cumulative lengths (heights) of these signals was obtained. The average number of back echos and an average cumulative signal heights were determined using seven test blocks of each material before the flat bottomed holes were drilled.

The sensitivity setting used for all the tests gave one back reflection of 50 percent amplitude using a 2.5 inch Inconel X test block. Although not having the highest attenuation, Inconel X did have the greatest total energy loss from impedance and attenuation combined. The tests were made at 2.25, 5.0 and 10.0 mc. It was not possible to make tests at higher frequencies due to high energy losses in some materials. Limited data was obtained from the 2.50 and 6.50 inch test blocks due to increased losses caused by longer metal travel. The results of these tests are shown in Table 14.

RESULTS AND DISCUSSION

In order to account for variations in energy losses from one material to another, it was necessary to refer to differences between the losses that result from (1) impedance mismatch, (2) attenuation, and (3) the amount of energy returning from a known size defect in the case where standard test blocks of only one hole size were used.

The results of investigations to determine the various losses are discussed below. Once these were found, differences in response from one material to another could be expressed in terms of correction factors. Thus, a relationship could be derived enabling the use of test blocks made of one metal to estimate the size of defects in another.

Known variables which could be measured and compensated for were then incorporated into the following expression:

$$C.F. = (D_x - D_s) + (\alpha_x - \alpha_s)2L + (H_s - H_x)$$

where $C.F.$ = correction factor, decibels

D_x = impedance mismatch loss (Material x), decibels

D_s = impedance mismatch loss (Standard block), decibels

α_x = attenuation coefficient (Material x), decibels/inch

α_s = attenuation coefficient (Standard block), decibels/inch

L = metal travel, inches

$H_s - H_x$ = difference in unknown flaw size and 5/64 of an inch test holes in Material x, decibels.

The correction factor, C.F., indicates the attenuation which must be added (+) to or removed (-) from the receiver line using a test configuration as shown in Figure 77, Appendix III.

Tests to verify the use of the correction factor are discussed in Section III, C, which follows.

Some precaution in using the attenuator is required. Readings should be obtained beginning with some attenuation load in the receiver line, e.g., 10 or 15 db. This must be done so that no readings are obtained without an electrical load in the receiver line. The actual difference in attenuation with and without a load is several decibels greater than indicated. However, the attenuator is quite accurate in comparing differences while the receiver line is loaded. Also, comparisons must be made using the same frequency, transducer diameter and water distance to test both materials.

Many variations of the method outlined above are possible. However, the tables and data in this report present values which can be substituted directly in the formula without any change of sign or other consideration.

The tests used to obtain the various factors are discussed in the following sections.

A. VELOCITY AND IMPEDANCE

For sound velocity measurements the Attenuation Comparator method appeared to be fairly accurate when the material samples were accurately machined. For example, the faces of the sample whose velocity is being measured must be flat and parallel within ±0.0005 inches per inch in order to prevent a 180° phase change in the echo pattern. This phase difference can occur if non-parallelism exists and thus give an erroneous velocity measurement.

It was found that the samples between 3/8 and 5/8 inch in thickness were most suitable for obtaining a maximum number of back echoes to calculate the average time for the sound pulse to make one round trip. More precise velocity measurements were obtained on materials with low attenuation losses. These samples presented longer back echo patterns, thus allowing more readings to be obtained.

Acoustic impedance values were obtained by calculation from the velocity and density values for each material. Any discrepancies in measured velocities affect calculated impedance values directly. The precautions observed to obtain velocity measurements necessarily applied to impedance.

The measured longitudinal wave velocities are shown in Table 6. Those values represent an average of several readings from two samples of each material. Specific acoustic impedance and several other properties calculated from impedance values are also included in Table 6.

B. ATTENUATION

The indicated (or apparent) attenuation coefficients are listed in Tables 7 and 8. For the purposes of this investigation the apparent attenuation included those losses due to true absorption, sound-beam geometry, scattering, and certain diffraction effects. Most of these loss factors remain approximately constant for each material at each frequency, however, the beam geometry losses vary with metal travel and transducer size at each test frequency. Thus, the same transducer diameter and comparable metal distances must be used to make valid comparisons. In normal ultrasonic inspection procedures the effects of all these losses would be observed. The attenuation coefficients in Tables 7 and 8 include these losses.

It was found that the loss at 2.25 mc was usually larger than at 5.0 or 10.0 mc. This was probably the result of beam-geometry losses which were greater at the lower test frequencies resulting in high apparent attenuation.

In some cases the length of the test blocks seemed to influence the apparent attenuation nonlinearly. For instance, it was observed that the signal returning from the front surface of thin specimens (0.250 and 0.500 of an inch) sometimes interfered with the first signal returning from the back surface. Thus, when using the Front Surface to First Back Echo technique, the apparent attenuation loss was greater than that observed using other techniques. On these shorter blocks both the Successive Back Echo method and the Attenuation Comparator methods appeared to be more reliable.

TABLE 6

ACOUSTICAL PROPERTIES							
MATERIAL	DENSITY, lb/in^3	LONGITUDINAL VELOCITY, V $in/sec \times 10^5$	SPECIFIC ACOUSTICAL IMPEDANCE $lbs/in^2\text{-}sec \times 10^4$	REFLECTION COEFFICIENT R (water/metal)	TRANSMISSION COEFFICIENT T (water/metal)	IMPEDANCE MISMATCH LOSS (water/metal) decibels	REFLECTION LOSS decibels
	ρ	V_L	$Z = \rho V_L$	$R = \left(\frac{Z_2 - Z_1}{Z_2 + Z_1}\right)^2$	$T = 1 - R$	$D = 10 \log_{10} \frac{R}{T_2}$	$R_d = 10 \log_{10} \frac{1}{R}$
7075-T6	0.101	2.45	2.46	.707	.293	9.14	1.51
4130	0.283	2.31	6.54	0.878	0.122	17.69	.57
C.P. Mo	0.369	2.52	9.30	0.912	0.088	20.75	.39
Inconel X	0.300	2.35	7.05	0.886	0.114	18.34	.53
V-1000	0.281	2.33	6.55	0.878	0.122	17.71	.57
17-4 SS	0.280	2.32	6.50	0.877	0.123	17.64	.57
Ti-100	0.164	2.36	3.87	0.802	0.198	13.12	.96
ZK-60	0.066	2.28	1.51	0.566	0.434	4.77	2.47
7079	0.101	2.38	2.40	0.702	0.298	8.98	1.52
2014	0.107	2.42	2.59	0.719	0.281	9.60	1.43
2024	0.100	2.42	2.42	0.702	0.298	8.98	1.52
AZ 31	0.064	2.13	1.36	0.532	0.468	3.85	2.74
J1 Mg	0.065	2.09	1.36	0.531	0.469	3.83	2.75
403 SS	0.278	2.31	6.42	0.876	0.124	17.55	0.57
4340	0.283	2.28	6.46	0.876	0.124	17.55	0.57
Ti 6-4	0.160	2.36	3.78	0.798	0.202	12.90	0.98
Water	0.0361	0.586	0.213				

TABLE 7

IMMERSED ATTENUATION DATA - 21 BLOCK SETS

AVERAGE ATTENUATION , DECIBELS/INCH

ALLOY	FRONT TO FIRST BACK				BACK ECHOES			ATTENUATION COMPARATOR		AVERAGE*			
	2.25 mc	5.0 mc	10.0 mc	25.0 mc	2.25 mc	5.0 mc	10.0 mc	5.0 mc	10.0 mc	2.25 mc	5.0 mc	10.0 mc	25.0 mc
7075-T6	.67	.59	.48	1.29	.75	.19	.66	.44	1.09	.70	.36	.63	1.3
4130	.77	.53	.60	2.95	.88	.27	.98	.13	.99	.81	.33	.81	2.9
V-1000	.54	.66	.26	2.16	.55	.19	.45	.13	.54	.55	.46	.39	2.2
17-4	.60	.85	.23	1.67	.58	.11	.29	.10	.26	.59	.43	.26	1.7
Inconel X	.66	.79	1.42	---	.85	.34	1.64	.57	1.66	.74	.57	1.54	---
Ti-100	.80	1.03	2.43	12.4	1.16	1.43	4.11	1.11	3.72	.89	1.12	3.17	12.4
C.P. Mo	.53	.72	1.45	2.96	.29	---	1.13	---	1.01	.45	.72	1.21	3.0
ZK-60	.63	.52	.46	.58	.95	.58	.47	.19	.28	.76	.42	.43	.58

*Average of 3 methods where applicable.

TABLE 8

IMMERSED ATTENUATION DATA - MATERIAL FROM PREVIOUS CONTRACTS

ALLOY	AVERAGE ATTENUATION, DECIBELS/INCH											
	BACK ECHOES				ATTENUATION COMPARATOR				AVERAGE			
	5.0 mc	10.0 mc	15.0 mc	25.0 mc	5.0 mc	10.0 mc	15.0 mc	25.0 mc	5.0 mc	10.0 mc	15.0 mc	25.0 mc
7075-T6 FB	1.7	1.1	1.7	2.7	1.3	1.4	1.8	2.9	1.5	1.3	1.7	2.8
7075-T6 RB	1.5	1.6	2.3	2.7	1.1	1.4	2.5		1.3	1.5	2.4	2.7
7075-T6 EB	2.1	1.7	1.6	1.8	2.0	1.7	1.4	1.9	2.0	1.7	1.5	1.9
7075-T6 RP	2.1	2.1	2.1	2.8	.92	1.7	2.2	3.0	1.5	1.6	2.1	2.9
7079	1.4	1.8	1.4	1.9	1.5	1.0	1.4	2.2	1.5	1.7	1.4	2.1
2014	1.8	1.6	1.8	2.1	1.5		2.1	2.5	1.7	1.6	1.9	2.3
2024	1.4	1.3	1.7		1.6	1.2	1.7	2.4	1.5	1.3	1.7	2.4
AZ-31	1.3	.66	1.1	2.7	1.3	.47	.70	2.5	1.3	0.5	.9	2.6
J1	.9		.5	1.1	1.2	.43	.57	2.2	1.1	0.4	.5	1.7
403	1.4	.63	1.5	2.7	1.3	.56	1.2	2.4	1.3	0.6	1.3	2.1
4340	1.2	.73	1.2	1.1	1.0	.70	.80	.9	1.1	0.7	1.0	1.0
Ti 6-4	2.2	2.3	3.6	6.5	1.9	1.5	2.8	6.8	2.1	1.9	3.2	6.7

FB - forged bar
RB - rolled bar
EB - extruded bar
RP - rolled plate

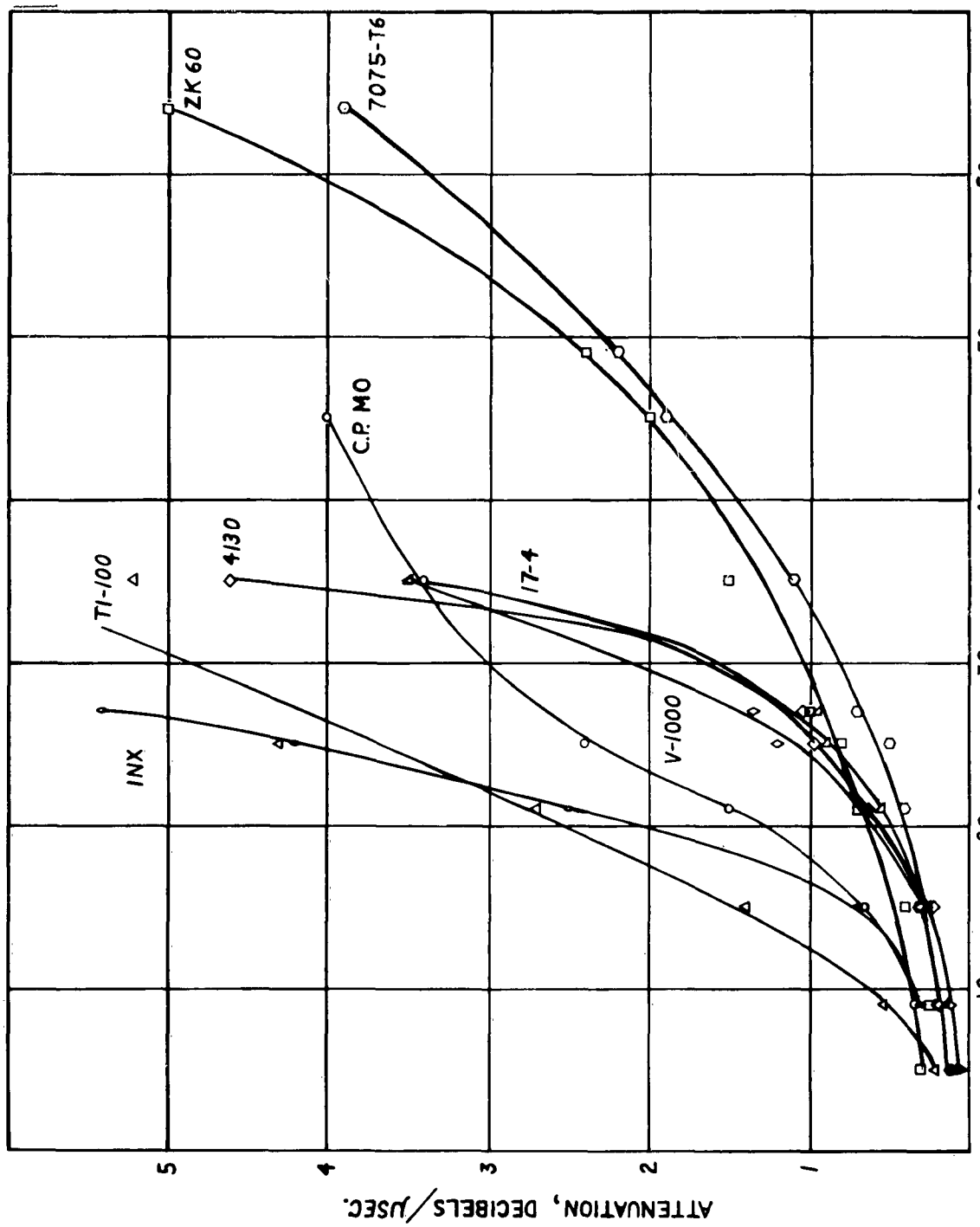

Figure 19. Attenuation vs. Test Frequency, Contact Method.

Another important factor in evaluating one material with another is the impedance loss in comparison to the attenuation loss at normal test frequencies. In most cases the impedance loss was much larger than the attenuation loss. For example, when inspecting 4130 steel the loss due to the impedance mismatch with water was about 17 decibels while the attenuation loss was less than one decibel per inch of metal travel at test frequencies of 2.25, 5.0 and 10.0 mc. It is seen, then, that considerable caution is required for accurate attenuation measurements.

The apparent attenuation measured in the 0.250 and 0.500 of an inch thick blocks was found to be larger than that obtained from the longer (0.875, 1.75 and 5.75 inches) twenty-one block sets at all frequencies. See Tables 7 and 8. This variance in test results was apparently caused by energy losses occurring at the water-metal or metal-air interfaces that were not accounted for by ordinary reflection losses. Thus, on shorter samples where attenuation measurements were averaged from a greater number of back echoes (reflections) the loss resulted in somewhat higher values of apparent attenuation since it was not accounted for by the reflection loss, Rd.

Measurements of attenuation losses were also made using the contact method. It is felt that these results were not as reliable as those obtained by immersed techniques. When using direct coupling of the transducer to specimen through a thin film of glycerin or light oil a consistent thickness of couplant film was difficult to obtain so that a margin of error was introduced. The results obtained are shown in Figure 19 where attenuation versus test frequency is plotted. It was interesting to observe that the attenuation values were nearly the same for all materials at 2.25 mc, and at 5.0 mc the difference was still small. However, above 10.0 mc there was a great difference. In fact, the high attenuation of several of the materials would make inspection quite difficult at the higher frequencies.

C. RELATIONSHIP OF FLAW SIZE TO ENERGY LOSSES

Using the twenty-one (21) block test sets the relationship between the different hole sizes in each set was measured in terms of decibels with reference to the 5/64 of an inch test hole in the test set. Also, the 5/64 of an inch test holes in all other materials were compared to those in the 7075-T6.

The information obtained was used to determine corrections to be applied to a standard reference test block set to account for differences both in material and in hole size at frequencies of 2.25, 5.0 and 10.0 mc.

Tables 9, 10 and 11 show the attenuation required (added or removed from the receiver line) for the signal from a 3, 4, 6, 7 or 8/64 of an inch test hole to equal the 1.5 inch reference signal height obtained from a 5/64 of an inch test hole at three different length blocks of each material.

It was found that, generally, the difference in signal amplitude that existed between the 5/64 hole and any one of the other sizes remained relatively constant for all three test block lengths. The differences were about the same using 2.25, 5.0 or 10.0 mc test frequencies. Although at 10.0 mc the difference between reflected signals from the 5/64 and 8/64 of an inch test holes was slightly less than observed

TABLE 9

SIGNAL AMPLITUDE FROM VARIOUS TEST HOLES COMPARED TO 5/64 INCH TEST HOLES, 2.25 mc.					
	DIFFERENCE IN SIGNAL AMPLITUDE, decibels				
MATERIAL	TEST HOLE DIAMETER, inches				
	3/64	4/64	6/64	7/64	8/64
7075-T6	-9	-2	+3.5	+6.5	+9
4130	---	-3	+3	+5	+8
V-1000	---	-3.5	+3	+5.5	+7
17-4 PH	---	---	+4	+7	+8
Inconel X	-8	-4	+2	+4	+8
Ti-100A	-5	-3	+4	+5.5	+8.5
C.P. Mo	---	-2	+6	+7	+9
ZK 60	-8.5	-4.5	+3	+6	+7.5

TABLE 10

SIGNAL AMPLITUDE FROM VARIOUS TEST HOLES COMPARED TO 5/64 INCH TEST HOLES, 5.0 mc.					
	DIFFERENCE IN SIGNAL AMPLITUDE, decibels				
MATERIAL	TEST HOLE DIAMETER, inches				
	3/64	4/64	6/64	7/64	8/64
7075-T6	-11.5	-3	+3	+5.5	+9
4130	----	-3	+3	+5	+8
V-1000	----	-3.5	+3.5	+6	+8
17-4 PH	-7	-3	+4	+7.5	+10
Inconel X	-8	-3	+3	+6	+7.5
Ti-100A	-11.5	-4.5	+3.5	+5	+7
C.P. Mo	-6	-3	+5	+7.5	+9
ZK 60	-10	-4	+4	+7	+9

TABLE 11

SIGNAL AMPLITUDE FROM VARIOUS TEST HOLES COMPARED TO 5/64 INCH TEST HOLE DIAMETER, 10.0 mc.					
	DIFFERENCE IN SIGNAL AMPLITUDE, decibels				
MATERIAL	TEST HOLE DIAMETER, inches				
	3/64	4/64	6/64	7/64	8/64
7075-T6	-7	-2	+3	+4.5	+7
4130	-8	-3	+3	+5.5	+8
V-1000	-8.5	-4	+3	+6	+7
17-4 PH	-10	-4	+2.5	+4	+5.5
Inconel X	-9	-1.5	+1	+1.5	+3.5
Ti-100A	-8.5	-3	+2	+4.5	+4.5
ZK 60	-9	-4	+3.5	+5	+7.5

at 5.0 or 2.25 mc. The difference was not large enough to be significant for most evaluations. This difference would probably decrease further to some minimum difference if the test frequency were increased. In that event, the reflected patterns would become narrower (less beam spreading) until a frequency was reached where the size of the reflected beams equaled the transducer size. The difference in reflected signals should then remain constant as the frequency was increased further.

In all materials the average difference between a 3/64 and 5/64 of an inch test hole was 8.5 decibels while the average difference between the 5/64 and 8/64 of an inch test holes was 7.5 decibels. Thus, if the reflection losses and attenuation are known corrections can be made to include different hole sizes when comparing different materials.

The signal strength obtained from the majority of the 2/64 inch diameter hole sizes was not great enough to be monitored simultaneously with the other test blocks. Consequently, no data from test blocks with these hole sizes is reported. At test frequencies of 2.25 and 5.0 mc, when evaluating test blocks with the smaller hole sizes insufficient signal strength was obtained from some blocks.

Table 12 shows the difference in signal amplitude (in decibels) of 5/64 of an inch test holes in the other twenty-one (21) block sets compared to the 5/64 of an inch test holes in 7075-T6 aluminum. Both calculated and measured values are shown.

The calculated values were obtained using the correction factor,

$$C.F. = (D_x - D_s) + (\alpha_x - \alpha_s)2L + (H_s - H_x).$$

The third term was zero since the test holes in the materials was 5/64 of an inch diameter. It was found that the measured loss closely approximated the calculated loss using the 1.75 inch test blocks. The responses were somewhat erratic on the 0.500 of an inch test blocks suggesting the possibility of "near" zone effects. On the longer blocks only the 10 mc signals could be monitored using the 7075-T6 as the reference material. Since most of the materials tested have higher impedance losses than the aluminum better results in this frequency range might be obtained using 4130 steel as the reference alloy.

Table 13 shows the results of tests to verify the use of the Correction Factor, C.F., for flaw evaluation. Generally, the measured results agreed quite well with calculated values. Through the range of metal distances tested, the measurements were sufficiently accurate to provide a means for defect evaluation.

Several precautions should be observed in attempting to use this evaluation technique. It was found that the reference blocks should have a smooth Amplitude-Distance curve. A defective test block could result in acceptance of material which might otherwise be rejected.

It was also found that the reflected signal from the defect should be large enough to saturate the A-Scan display. The gain can then be reduced to provide a signal of about 1.5 inches height for evaluation. Weak signals can result in gross inaccuracies.

TABLE 12

COMPARISON OF REFLECTED SIGNAL AMPLITUDE FROM 5/64 TEST HOLES IN SEVEN MATERIALS TO 5/64 TEST HOLE IN 7075 ALUMINUM

MATERIAL	METAL DISTANCE Inches	CALCULATED DIFFERENCE Decibels			MEASURED DIFFERENCE Decibels		
		2.25 mc	5.0 mc	10.0 mc	2.25 mc	5.0 mc	10.0 mc
4130	0.500	8.5	8.5	9	13.5	9.5	7
C.P. Mo	0.500	11.5	12	12	14	12.5	10.5
Inconel X	0.500	9.2	9.5	10.1	11	8.5	6
V-1000	0.500	8.5	8.5	8.5	12	9	7.5
17-4	0.500	8.5	8.5	8	14	9.5	7
Ti-100A	0.500	4.	4.5	6.5	2	3.5	4
ZK-60	0.500	-4.5	-4.5	-4.5	-2.5	-3	-3.5
4130	1.75	9	8.5	9	8	9.5	7.5
C.P. Mo	1.75	10.5	13	13.5	11	11.5	14
Inconel X	1.75	9.5	10	12.5	8	9	10.5
V-1000	1.75	8.0	9	8	7	7	6
17-4	1.75	8	8.5	7	7.5	7.5	6.5
Ti-100A	1.75	4.5	6.5	13	4.5	5.5	11.5
ZK-60	1.75	-4.5	-4	-4	-4	-2.5	-2.5
4130	5.75	----	----	11	----	----	10.5
C.P. Mo	5.75	----	----	17	----	----	11.5
Inconel X	5.75	----	----	19	----	----	14
V-1000	5.75	----	----	6	----	----	1.5
17-4	5.75	----	----	5	----	----	1
Ti-100A	5.75	----	----	34	----	----	could not measure
ZK-60	5.75	----	----	-2	----	----	-1

TABLE 13

VERIFICATION OF CORRECTION FACTOR AT 5.0 MC USING 5/64 - 7075-T6 ALUMINUM REFERENCE BLOCKS AND 8/64 - 4130N STEEL TEST BLOCKS					
Metal Distance	C.F., decibels				
		3/4 Inch Diameter Quartz Transducer		3/8 Inch Diameter Lithium Sulphate Transducer	
Inches	Calculated	Measured	Difference	Measured	Difference
1/2	-0.01	0	+0.01	-0.5	-0.49
5/8	-0.02	-0.5	-0.48	0	+0.02
3/4	-0.02	-1.0	-0.98	-1.0	-0.98
7/8	-0.03	0	+0.03	0	+0.03
1	-0.04	-1.0	-0.96	0	+0.04
1-1/4	-0.05	+1.0	+1.05	-0.5	+0.55
1-3/4	-0.08	0	+0.08	-2.0	-1.92
2-1/4	-0.11	+2.0	+2.11	0	+0.11
2-3/4	-0.14	+0.5	+0.64	0	+0.14
3-1/4	-0.17	+0.5	+0.67	-2.0	-1.83
3-3/4	-0.20	0	+0.20	-0.5	-0.30
4-1/4	-0.23	+1.0	+1.23	+1.0	+1.23
4-3/4	-0.26	+0.5	+0.76	+1.5	+1.76
5-1/4	-0.29	+1.0	+1.29	+1.0	+1.29
5-3/4	-0.32	0	+0.32	-1.5	-1.18

The use of a 3/8 of an inch diameter transducer at 5.0 mc apparently did not affect the results. The equivalent beam diameter at 5.0 mc in aluminum was about 7.5 wavelengths. It is expected that any further decrease in transducer size would affect the test results appreciably since beam spread would be increased.

Additional tests of other materials were made choosing test blocks at random from sets used for this contract. Evaluation was made knowing only the material being tested. The results obtained were acceptable for normal inspection procedure and, in fact, were quite accurate.

It seems that evaluation of defects in most materials could be performed using one set of reference blocks if the attenuation and impedance losses of the material being tested are known.

D. LENGTH AND NUMBER OF BACK REFLECTIONS

The cumulative height in inches and the number of back surface reflections were recorded for the 0.875 inch blocks. Similar data was attempted from the other two test block sizes (2.50 and 6.50 inches). Generally, an insufficient number of back echoes was obtained to make any valid determinations using the longer blocks.

Some correlation seemed to exist between (1) the attenuation loss, (2) the impedance mismatch loss and the decay pattern of the back echos. Materials with the higher reflection coefficients generally, displayed a higher number of back echos. The cumulative signal height was not greater, however. Where attenuation values were comparatively high the number of back reflections and the cumulative heights decreased rapidly as the test frequency was increased. Inconel X and Ti-100A were good examples of this.

The samples of 7075-T6 aluminum and ZK-60 magnesium had the smallest number of back reflections. These materials also had the lowest losses due to impedance mismatch. The attenuation values were also low for these materials. The effects of the low attenuation values were observed in the slight increase in signal height and number of back reflections as the frequency was increased. The probable cause for the increases was less loss due to beam spreading as the frequency increased.

Comparative information is easily available observing the number and height of back reflections, however, accurate measurements of attenuation or impedance losses would require additional study. It is possible that a constant or some factor could be obtained from this data which would yield information regarding the attenuation and impedance losses. Although, attempts to relate the data directly to energy losses were not fruitful.

CONCLUSIONS

It was found that, generally, the energy loss due to impedance mismatch with water was quite high compared to the energy loss due to attenuation within the material. The attenuation losses measured include factors such as beam spreading and diffraction affects.

TABLE 14

BACK REFLECTION - ENERGY LOSS DATA OBTAINED USING 0.875 INCH BLOCKS						
MATERIAL	NUMBER OF BACK REFLECTIONS			TOTAL SIGNAL HEIGHTS, INCHES		
	2.25 mc	5.0 mc	10.0 mc	2.25 mc	5.0 mc	10.0 mc
7075-T6	9	11	11	10.4	8.8	10.6
4130	11	11	12	5.9	4.6	7.4
Vascojet 1000	20	20	24	8.4	8.5	10.8
17-4 PH	22	21	25	10.4	9.7	11.8
Inconel X	13	9	4	6.3	4.4	3.3
C.P. Molybdenum	24	20	10	10.2	9.4	5.4
ZK-60	8	9	11	9.5	9.0	12.6
Ti-100A	14	5	3	8.2	4.8	3.0

In the ZK-60 magnesium specimens the apparent attenuation losses were observed to decrease as the test frequency was increased. It would seem that energy losses due to beam spreading are fairly significant in materials with low attenuation values. This would include most of the materials tested since the apparent energy losses were nearly all less than 3 db/inch even at 10.0 mc.

Above 10.0 mc there was a considerable increase in apparent attenuation in Ti-100A, Ti6-4, Inconel X and C.P. Molybdenum. In this range of frequencies the losses due to beam spreading are lower, thus real attenuation is higher.

Of the immersed techniques employed to measure attenuation and impedance losses the Successive Back Echo and Attenuation Comparator methods appeared to be more reliable. Where the long samples were used the Front Surface to First Back Echo was the only technique which was useful. Attenuation measurements using the contact method were not felt to be as reliable as immersed techniques. However, it was possible to obtain values for attenuation at frequencies above 25 mc using contact techniques, whereas this was not possible with the immersed method.

Using the twenty-one (21) block test sets it was found that a fairly constant difference in signal amplitude was reflected from the different size test holes in each material. The average difference between reflected signals from 3/64 and 5/64 of an inch test holes was 8.5 decibels while the average difference was 7.5 decibels between 5/64 and 8/64 of an inch test holes. The highest test frequency was 10.0 mc. At 10.0 mc the difference between the signals reflected from 5/64 and 8/64 of an inch test holes was slightly less than at 2.25 or 5.0 mc. If the test frequency was increased this difference would probably decrease. Thus, if the figures above are used they should be applied to tests at 10.0 mc or lower.

A correction factor was established to account for impedance, attenuation and defect size. Thus, making possible corrections between different materials for evaluation of defects. The correction factor was:

$$C.F. = (D_X - D_S) + (\alpha_X - \alpha_S)2L + (H_S - H_X)$$

where

D_X = Material x/water impedance loss, decibels

D_S = Reference standard/water impedance loss, decibels

α_X = Attenuation loss in Material x, decibels/inch

α_S = Attenuation loss in reference material, decibels/inch

L = Metal travel, inches

$(H_S - H_X)$ = Difference in signal amplitude between a 5/64 of an inch and selected defect size in Material x, decibels.

The correction factor, C.F., indicates the attenuation which must be added to or removed from the receiver line using a test configuration as shown in Figure 77.

Tests using the correction factor indicated good accuracy throughout the range of metal distances tested. It appears that the technique can be applied to evaluate defects during normal inspection procedures. The economic savings when evaluating exotic materials would more than compensate for the minimal additional equipment (attenuator) and time required.

It is expected that further use and investigation of this evaluation technique will result in more refined measuring techniques and acoustical data. However, the results presented in this report are immediately applicable.

Comparative information about impedance and attenuation can be readily obtained from information of number and cumulative heights of back echos. For example, a low number of back echos combined with a high value of back echo heights indicates that the material has a low impedance value and a low attenuation loss. Direct measurements of these values are more readily obtained using present techniques. However, a method for obtaining quantitative values from the back echo information appears within reason. Further study would probably allow development of these techniques.

SECTION IV

EVALUATION OF BEAM COLLIMATORS FOR C-SCAN RECORDING

Earlier work completed for WADC Technical Report 59-466 discussed the use of beam collimators and reported increased signal amplitude where the collimated beam was the same diameter as the first Fresnel zone.

As a result of that work there appeared to be a possibility of using beam collimators for C-Scan recording. Additional testing was necessary to define the limits of applicability, however. The information required was (1) optimum collimator diameters, and (2) the effect of variation of metal distance on defect presentation. It was also thought that a comparison of test results with those obtained using focused transducers would be useful.

This section describes and evaluates the tests performed.

EQUIPMENT

1. Curtiss-Wright Immerscope, Model 424A, modified (pulse rate variable from 400 pps to 1600 pps)
2. Automation Industries Model 1047 Ultragraph Recorder
3. Automation Industries 4' x 15' Immersion Tank with automatic scanning bridge and facsimile paper recorder. See Figure 20
4. Ultrasonic Transducers as listed in Table 15
5. Automation Industries, Type 110 Beam Collimators, with orifice diameters of 1/16, 1/8, 1/4, 3/8 and 1/2 of an inch. See Figure 21

MATERIAL AND TEST SAMPLES

A. THICK PLATE TESTS

1. One (1) 2024-T4 Aluminum Plate 1-1/2 inches thick. Configuration as shown in Figure 22

B. THIN PLATE TESTS

1. Three (3) 2024-T4 Test Plates, 1/4, 1/8, and 1/16 of an inch in thickness. Configuration as shown in Figure 23.

TABLE 15

TRANSDUCERS USED IN COLLIMATOR TESTS			
MANUFACTURER	TYPE	FREQUENCY Megacycles	DIAMETER Inches
Automation Industries	Lithium Sulphate, Flat	2.25	0.75
Automation Industries	Lithium Sulphate, Flat	5.0	0.75
Automation Industries	Lithium Sulphate, Flat	10.0	0.75
Automation Industries	Lithium Sulphate, Focused	2.25	0.75
Automation Industries	Lithium Sulphate, Focused	5.0	0.75
Automation Industries	Lithium Sulphate, Focused	10.0	0.75

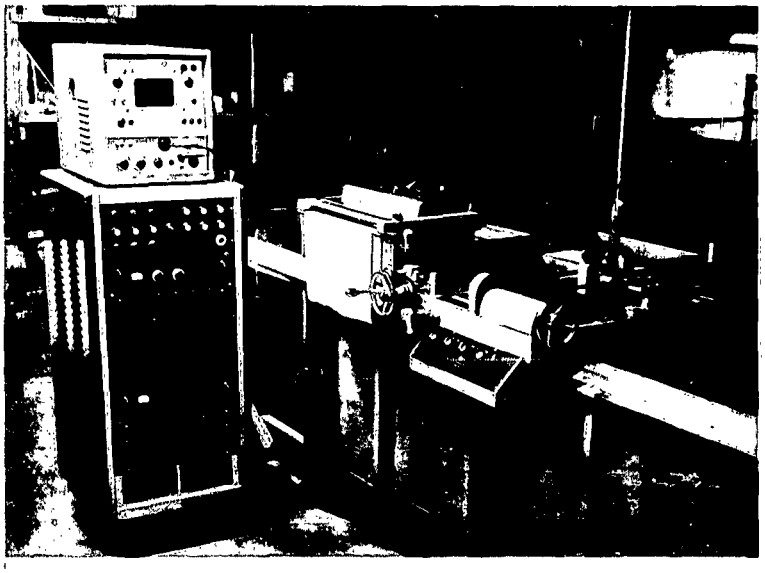

Figure 20. Facsimile Paper Recording Equipment.

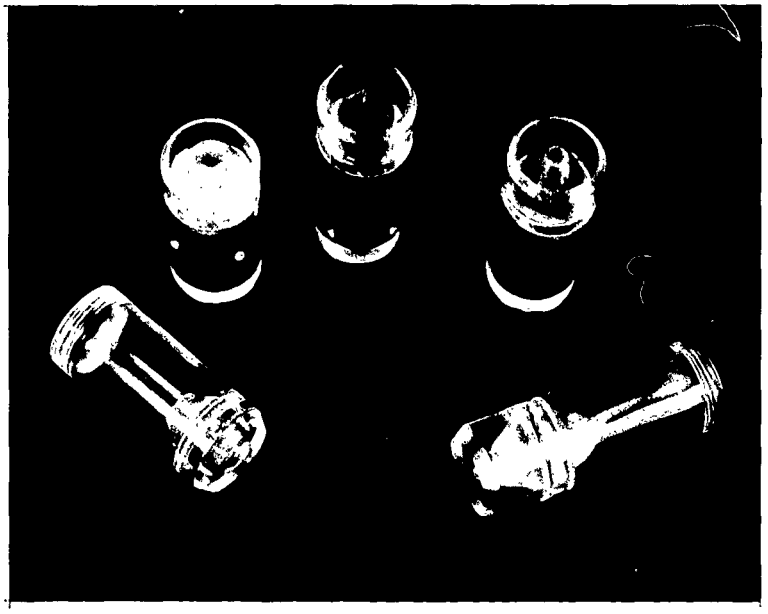

Figure 21. Ultrasonic Beam Collimators.

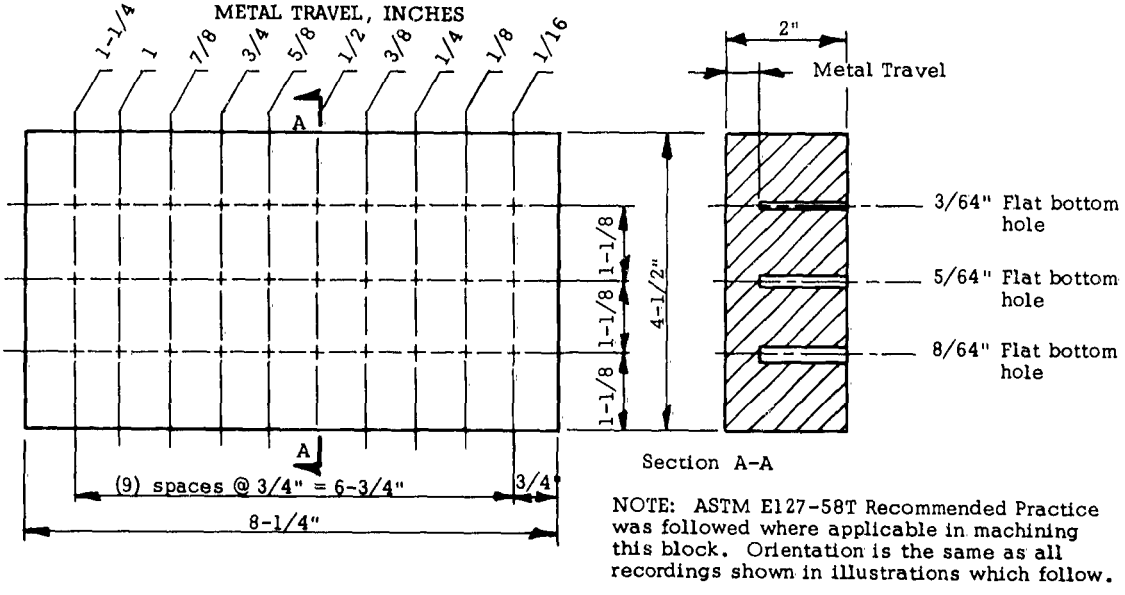

Figure 22. Sketch of Thick Test Plate, 2024-T4 Aluminum.

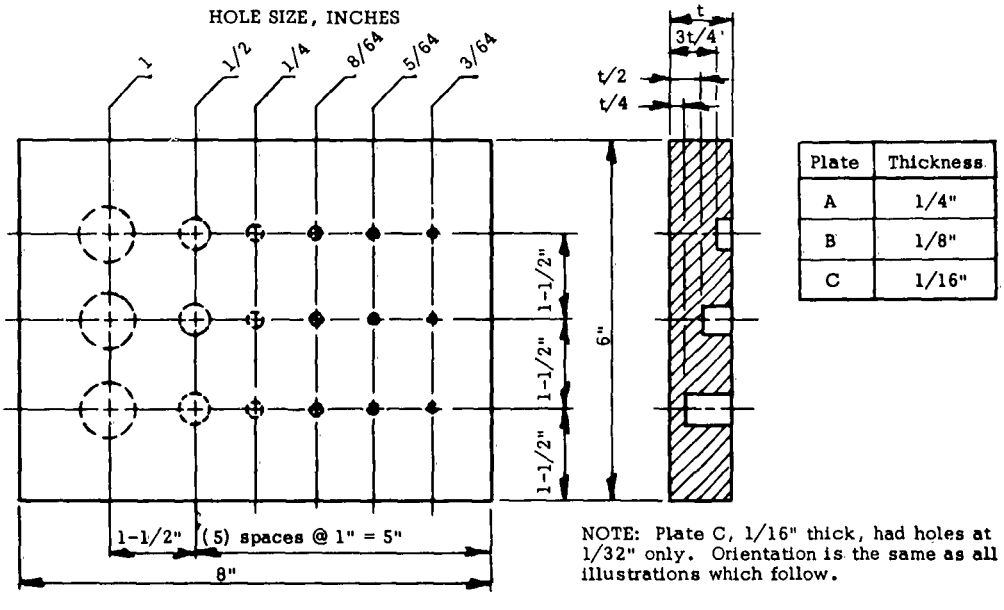

Plate	Thickness
A	1/4"
B	1/8"
C	1/16"

Figure 23. Sketch of Thin Test Plates, 2024-T4 Aluminum.

TEST PROCEDURES

A. EVALUATION OF COLLIMATORS FOR PLAN VIEW RECORDING

Test 1. Thick Plate

For these tests the 1-1/2 inch Test Plate was used. Facsimile paper recordings were made at 2.25, 5.0 and 10 mc using first, each of the collimators, and then without collimation. Both IF and Video presentation were used with each combination of test frequency and collimator diameter.

Water travel was adjusted so that the collimator was 1/16 of an inch or less above the Test Plate. The test equipment configuration is shown in Figure 24.

The recorder sensitivity and instrument gain levels were adjusted so that the 3/64 of an inch diameter flat bottom hole at the theoretical flaw depth was recorded as near actual size as possible. The theoretical flaw depth was determined by the test frequency and collimator diameter. Table 16 lists the depth-collimator combinations used. Typical A-Scan signals used to obtain recordings are shown in Figure 24.

Recordings made at 5.0 mc are shown in Figures 26 through 31.

Test 2. Thin Plate

Three (3) test panels with laminar type defects (flat bottom hole) ranging from 3/64 of an inch diameter to 1 inch diameter were recorded. Configuration of the panels used is shown in Figure 23. The test frequencies used were 2.25, 5.0 and 10.0 mc. A 1/4 of an inch diameter collimator was used for all tests. Two recording techniques were used, (1) gating for signals reflected directly from the reference defects, and (2) gating for presence (or absence) of signals from a stainless steel reflector approximately 1/2 of an inch below the test plate. Figure 25 illustrates this technique. The collimator was 1/16 of an inch above the test plate for all recordings. All recordings illustrated were made using the IF presentation. Typical A-Scan signals observed are also shown in Figure 25.

The recordings of thin plates shown in Figures 32 through 35 were made at 5.0 mc.

B. COMPARISON OF FOCUSED TRANSDUCERS FOR RECORDING

Test 1. Thick Plate

Recordings of the 1-1/2 inch Test Plate were made using the focused transducers listed in Table 15. Test frequencies were 2.25, 5.0 and 10.0 mc.

Water distance was adjusted so that the "usable energy" patterns were within the test plate. Gain and sensitivity levels were adjusted for optimum presentation of the 3/64, 5/64, and 8/64 of an inch diameter flat bottom holes within the "usable energy" pattern.

TABLE 16

COLLIMATOR DIAMETERS* USED FOR TEST RECORDINGS			
METAL DISTANCE TO FLAW, INCHES	ORIFICE DIAMETER INCHES		
	2.25 mc	5.0 mc	10.0 mc
1/16	1/8	1/8	1/16
1/8	1/4	1/4	1/8
1/4	3/8	1/4	1/8
3/8	3/8	1/4	1/8
1/2	1/2	3/8	1/4
5/8	1/2	3/8	1/4
3/4	1/2	3/8	1/4
7/8	---	3/8	1/4
1	---	3/8	1/4
1-1/4	---	1/2	3/8

*Exact diameter of first Fresnel zone is listed in WADD TR 59-466, pg. 25, for metal distances up to 5-3/4 inches.

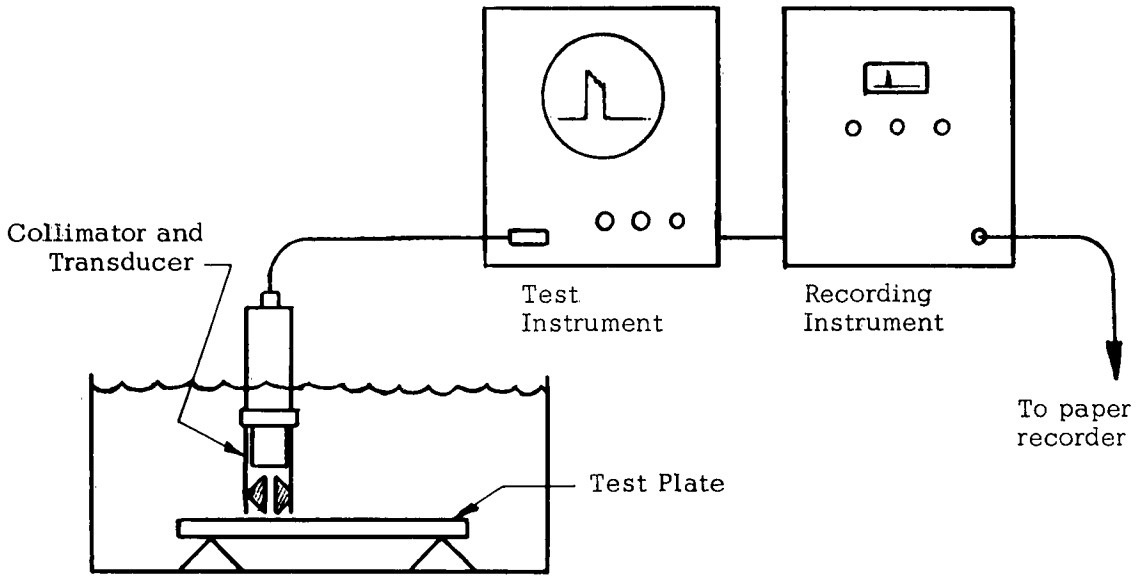

A. Test Equipment Configuration

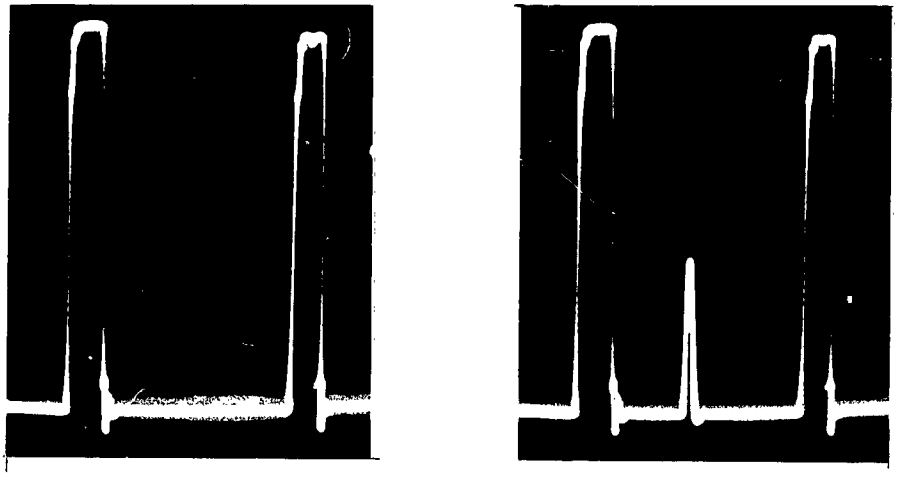

B. No Defect

C. Defect in Plate

Figure 24. Test Configuration and Reflected Signals for Direct Recording Technique.

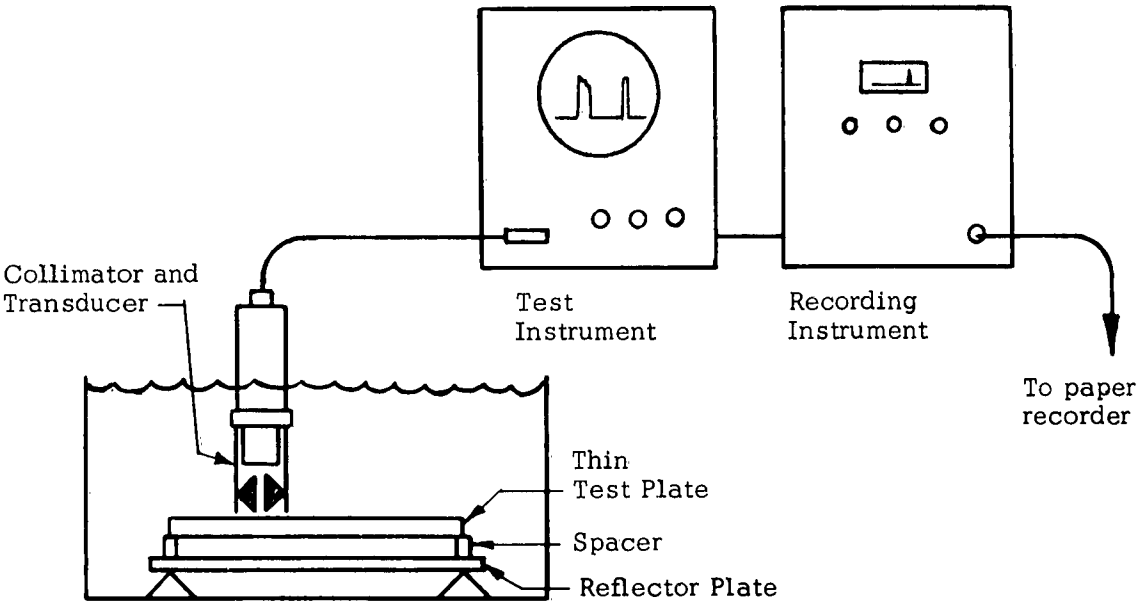

A. Test Equipment Configuration

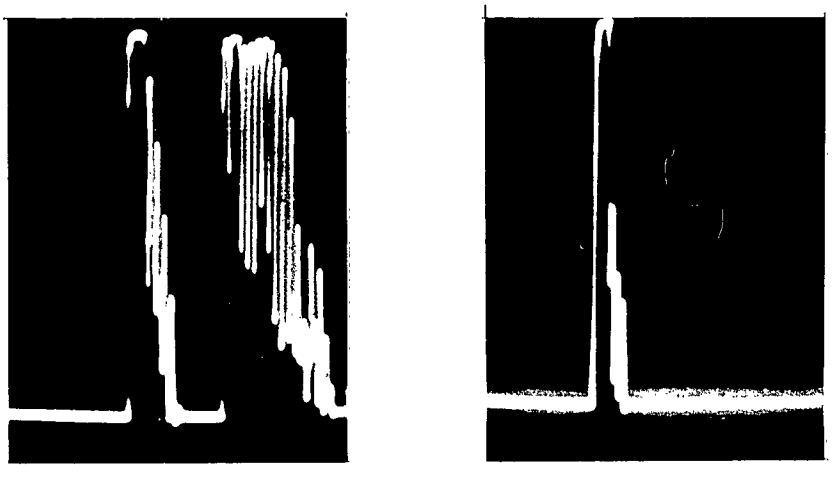

B. No Defect

C. Defect in Plate

Figure 25. Test Configuration and Reflected Signals for Reflector Recording Technique.

Typical recordings are shown in Figures 37 through 39.

Test 2. Thin Plate

The thin Test Plates as listed in Paragraph B, Materials and Test Samples, were used. Focused transducers used were 3/4 of an inch diameter, lithium sulphate. Test frequencies were 2.25, 5.0 and 10.0 mc.

Recordings were made using the following techniques:

1. Focus on plate, gate for decrease in multiples
2. Focus on plate, gate for loss of signal from stainless steel reflector approximately 1/2 of an inch below test plate
3. Focus on reflector, gate for loss of signal from reflector.

Typical recordings are shown in Figures 40 through 43.

RESULTS AND DISCUSSION

A. EVALUATION OF COLLIMATORS

In WADC Technical Report 59-466 it was reported that increased flaw response was obtained where the beam size was collimated to the dimensions (diameter) of the first Fresnel zone. For a given flaw depth and test frequency the pulse energy incident on the flaw was all of the same phase, i.e., either compression or rarefaction. Thus, maximum reflected energy was obtained. Optimum orifice size was determined from the relationship,

$$D = 2\sqrt{d\,\lambda}$$

where D = orifice diameter, inches

d = flaw depth, inches

and λ = wavelength, inches.

If wavelength λ, and flaw depth, d, were held constant any orifice diameter equal to or smaller than that determined from the equation above would result in all energy incident on the flaw being in phase. Conversely, it seems that if orifice diameter and wavelength (test frequency) were fixed, a range of depths would exist where the energy incident on the flaw would be in phase. Then, a series of collimators of different diameters could be used to inspect a large range of flaw depths. The test results discussed below indicated that that was the case.

Tests for previous report WADC TR 59-466 used optimum collimator diameters which were calculated for each flaw depth observed. Flaw depth ranges where

collimation was beneficial (increased signal height 20% or more) are listed in Table 17. The 5-3/4 inch depth listed in the table as the limit at 10.0 mc was actually the maximum depth tested.

TABLE 17

MAXIMUM FLAW DEPTH FOR BENEFICIAL USE OF COLLIMATORS	
Frequency Mc	Flaw Depth Inches
2.25	1-3/4
5.0	3-1/4
10.0	5-3/4

Test 1. Thick Test Plate

The test results indicated that for each frequency there was a minimum useful collimator diameter. The minimum diameters are listed in Table 18.

TABLE 18

MINIMUM USEFUL COLLIMATOR SIZE FOR RECORDING PURPOSES	
Frequency Mc	Orifice Diameter Inches
2.25	1/4
5.0	1/8
10.0	1/16

If beam collimators are considered as circular piston sources, a great deal of information regarding their radiation characteristics becomes available. For example, the beam divergence becomes about 10° for a circular piston source in the range of 2-1/2 to 3 wavelengths diameter. A decrease in source diameter results in greater beam divergence while an increase in diameter results in less divergence.

It was interesting to note that the minimum useful orifice size for each of the test frequencies corresponded to approximately 2-1/2 wavelengths measured in the material being tested. Apparently, beam divergence greater than 10° limits the usefulness of collimators.

Frequency - 5.0 mc
Transducer - 3/4" diameter
Lithium Sulphate

Collimator - 1/8 inch diameter
Presentation - IF

Figure 26. Facsimile Paper Recording of Thick Test Plate, 5.0 mc., 1/8 inch Collimator.

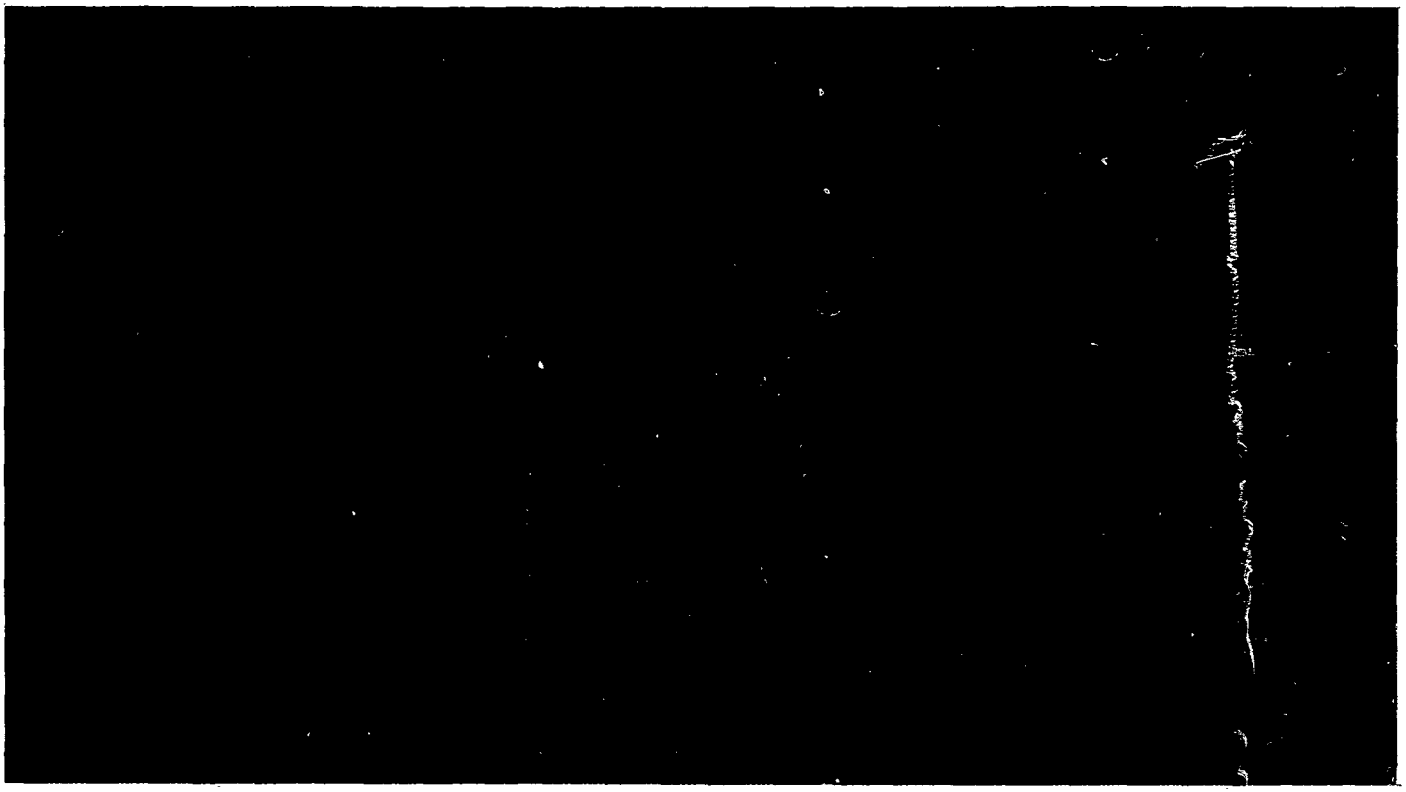

Frequency - 5.0 mc
Transducer - 3/4 inch diameter Lithium Sulphate

Collimator - 1/4 inch diameter
Presentation - IF

Figure 27. Facsimile Paper Recording of Thick Test Plate, 5 mc., 1/4 inch Collimator, IF Presentation.

Frequency - 5.0 mc.
Transducer - 3/4 inch diameter Lithium Sulphate

Collimator - 1/4 inch diameter
Presentation - Video

Figure 28. Facsimile Paper Recording of Thick Test Plate, 5.0 mc., 1/4 inch Collimator, Video Presentation.

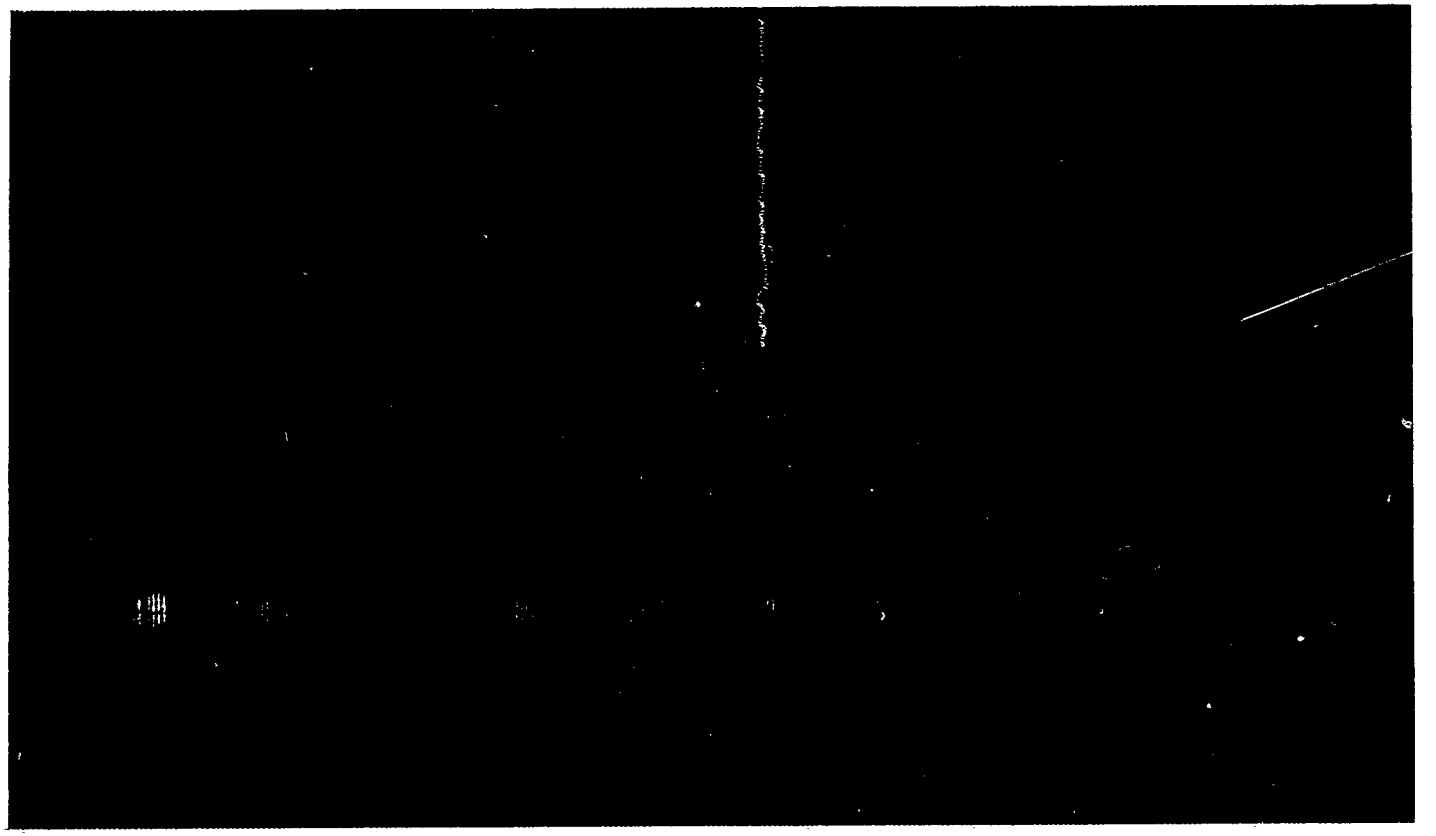

Frequency - 5.0 mc.
Transducer - 3/4 inch diameter
Lithium Sulphate

Collimator - 3/8 inch diameter
Presentation - IF

Figure 29. Facsimile Paper Recording of Thick Test Plate, 5.0 mc., 3/8 inch Collimator.

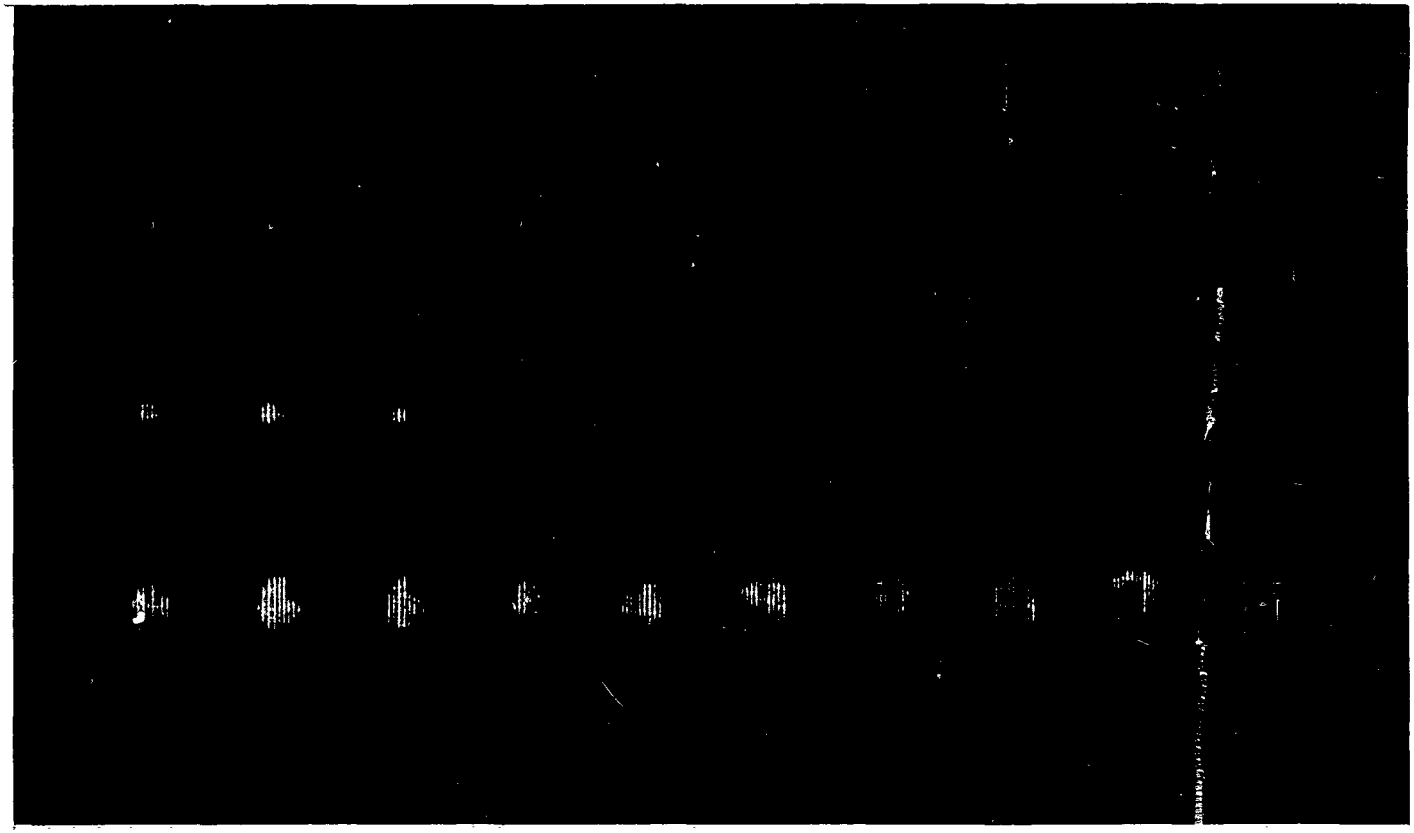

Frequency - 5.0 mc.
Transducer - 3/4 inch diameter Lithium Sulphate

Collimator - 1/2 inch diameter
Presentation - IF

Figure 30. Facsimile Paper Recording of Thick Test Plate, 5.0 mc., 1/2 inch Collimator.

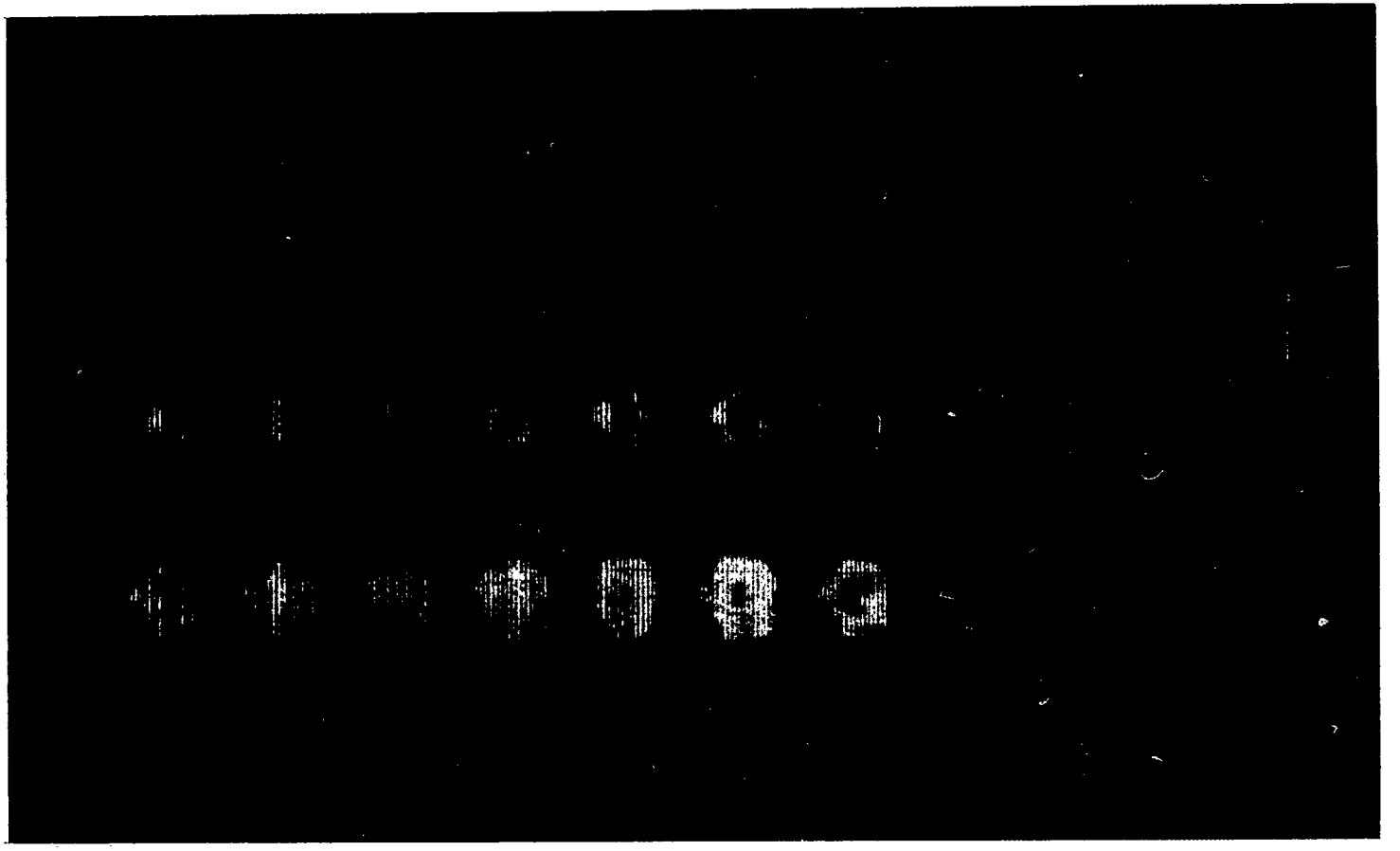

Frequency - 5.0 mc.
Transducer - 3/4 inch diameter Lithium Sulphate

Collimator - None
Presentation - IF

Figure 31. Facsimile Paper Recording of Thick Test Plate, 5.0 mc., No Collimator.

Obviously, the maximum collimator size would equal the transducer diameter. It does not seem that any advantage would be obtained, however, since the results using the 1/2 inch collimator were generally similar to those without collimation. The main differences observed were a reduction in defect magnification and decreased effects of beam intensity pattern when the 1/2 inch collimator was used.

It was observed that without collimation and even when using the larger collimators the beam intensity pattern was recorded, the white areas representing areas of higher intensity. It was found that an increase in gain or a change of recorder sensitivity level generally eliminated the pattern in the recording. However, at high level gain and/or sensitivity settings the flaws indicated on the recordings were greatly magnified. Evaluation of flaws under those conditions was difficult. If the location of all flaws detected were the sole requirement the use of high level gain settings might not be objectionable.

On all the recordings at 2.25 mc the size of the 5/64 and 8/64 of an inch diameter flat bottom holes was found to be magnified when the 3/64 of an inch flat bottom hole was recorded at or near true size. By decreasing the gain and/or sensitivity levels the 5/64 and 8/64 of an inch diameter flat bottom holes could be recorded in approximately true size. Generally, that resulted in completely overlooking, i.e., not recording, the 3/64 of an inch diameter flat bottom hole.

The use of 5.0 mc resulted in better resolution of flaws nearer the surface. Better proportion of recorded hole sizes was also obtained. At 10.0 mc resolution of 5/64 and 8/64 flat bottom holes at 1/16 of an inch metal distance was readily achieved using collimators and with some care the 3/64 flat bottom hole could also be recorded. It should be noted, however, that with the instrument settings used, the 3/64 flat bottom hole at 1/16 of an inch metal distance was not recorded.

Table 19 lists the range of metal distance where best defect definition was observed for each combination of frequency and collimator size. One of the two criteria was used to determine the ranges listed in the table: (1) Where the defects appeared at or near true size throughout the range or, (2) where the 3/64, 5/64, and 8/64 of an inch diameter flat bottom holes were recorded in proportional sizes.

Flat bottom holes outside the ranges listed were also recorded. These indications were, generally, not true size or proportional sizes. Therefore, flat bottom holes of one size could be interpreted as having the same dimension as a different size defect at a different metal distance. Most often, where they were recorded at all, the result was that 8/64 and 5/64 flat bottom holes could be interpreted as 5/64 and 3/64 flat bottom holes respectively.

For actual inspection of parts a reference standard with defects in the range of interest should be used to establish instrument settings. The choice of frequency and collimator size, also, should be of primary interest.

Another factor of interest was that the IF presentation allowed better resolution of defects than Video presentation for each combination of frequency and collimator diameter. Comparison of Figures 27 and 28 demonstrates a typical difference in resolution between IF and Video presentation. Thus, it was seen that instrument settings have considerable effect upon test results. Probably, IF presentation would yield better results for inspection of thin materials (1/4" or less) and near surface defects.

TABLE 19

METAL DEPTH RANGE FOR BEST DEFINITION			
COLLIMATOR DIAMETER INCHES	METAL DEPTH, INCHES		
	2.25 mc	5.0 mc	10.0 mc
1/16	---	---	1/16 - 1/8
1/8	---	1/8-3/8	1/16 - 1/4
1/4	1/8-1/2	1/4-1/2	1/4 - 3/4
3/8	1/4-1/2	1/4-1	3/8 - 1-1/4*
1/2	1/2-1	5/8-1-1/4*	1 - 1-1/4*

*Maximum metal depth tested.

Test 2. Thin Plate

The use of collimators to record laminar type flaws in thin plates (1/4 of an inch or less) seemed quite feasible in the light of investigations using the 1-1/2 inch Thick Test Plate. In those tests it was observed that best near surface resolution was achieved using the small diameter collimators and IF presentation. Consequently, all final recordings of the Thin Plates were made using a 1/4 of an inch diameter collimator (minimum useful diameter at 2.25 mc).

In some preliminary recordings considerable difficulty was encountered when attempting to record defects in the thin plates using a collimator diameter smaller than 2-1/2 to 3 wavelengths. This same limitation was encountered while testing the 1-1/2 inch plate and is discussed in the preceding section.

In some additional preliminary tests, the use of collimators considerably larger than 2-1/2 to 3 wavelengths resulted in a constant factor which was added to the size of the defects. This factor appeared to increase in proportion to collimator diameter. Despite this factor, the defects were recorded in proportional sizes so that interpretation could be easily accomplished.

At 2.25 mc it was not possible to resolve the 3/64 flat bottom hole in any of the plates. None of the defects in the 1/16 inch plate were recorded when gating directly on the signal reflected from the flat bottom holes. The 1/8 and 1/4 inch plates were recorded directly but the recordings showed defects only where the flaw size equaled or was larger than the collimator orifice.

Using 5.0 mc, the defects in the 1/16 inch plate could not be recorded directly. However, the defects in the 1/8 inch plate and 1/4 inch plate were recorded directly. Using 10.0 mc all three plates were recorded successfully gating directly on the reflected signal. Figures 32 through 35 show recordings of the 1/8 inch plate using both direct and reflector techniques.

It was interesting to observe the change in reflected signal which was used to record the flat bottom holes in the Thin Plates. It was found that the amplitude of the multiple reflections decreased where the metal distance decreased. Typical signals from the 1/4 inch plate are shown in Figure 36. Note that the multiple reflections decrease seemingly in proportion to the decrease in metal distance. Apparently, some form of "wave interference" effect occurred in these thin plates which was related to plate thickness, wavelength and pulse length. No attempt was made to further define this phenomenon, however.

The use of this effect was necessitated by the fact that the various defect depths in the Thin Test Plates could not be adequately resolved at all test frequencies. The occurrence of this "wave interference" was found to be reliable and quite useful. The interference effect seemed to be limited to thin plates, however, and it was suspected that the 1/4 inch Plate approached the maximum thickness where "interference" would have been useful.

Good flaw definition was achieved when using the reflector technique. Test holes 3/64 of an inch diameter and larger were recorded in all three test plates at

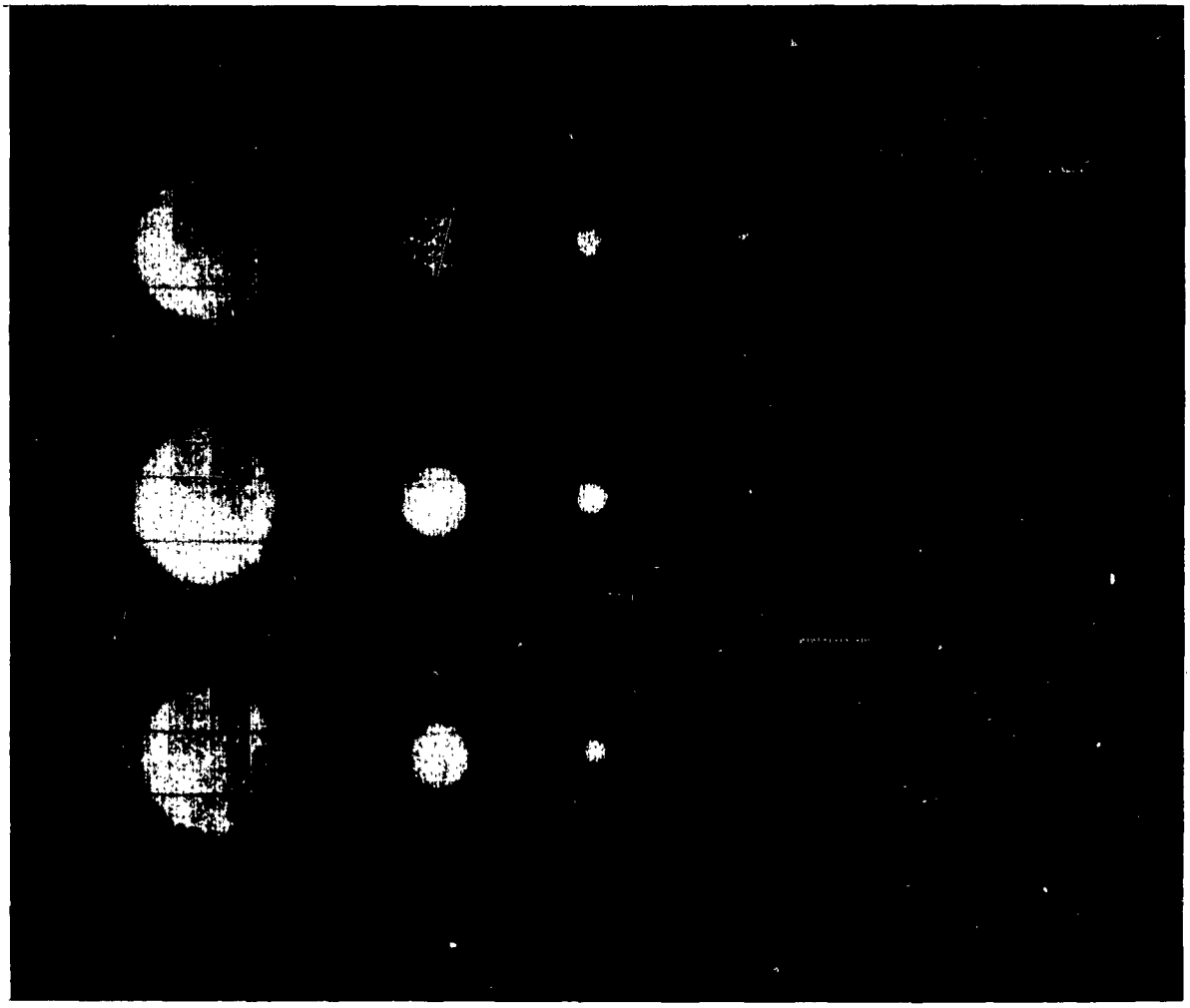

Frequency - 5.0 mc.
Transducer - 3/4 inch diameter
Lithium Sulphate
Plate Thickness - 1/4 inch

Collimator - 1/4 inch diameter
Presentation - IF

Figure 32. Facsimile Paper Recording of 1/4 Inch Plate, 5.0 mc., 1/4 Inch Collimator, Direct Technique.

Frequency - 5.0 mc.
Transducer - 3/4 inch diameter
Lithium Sulphate

Plate Thickness - 1/4 inch

Collimator - 1/4 inch diameter
Presentation - IF

Figure 33. Facsimile Paper Recording of 1/4 Inch Plate, 5.0 mc., 1/4 Inch Collimator, Reflector Technique.

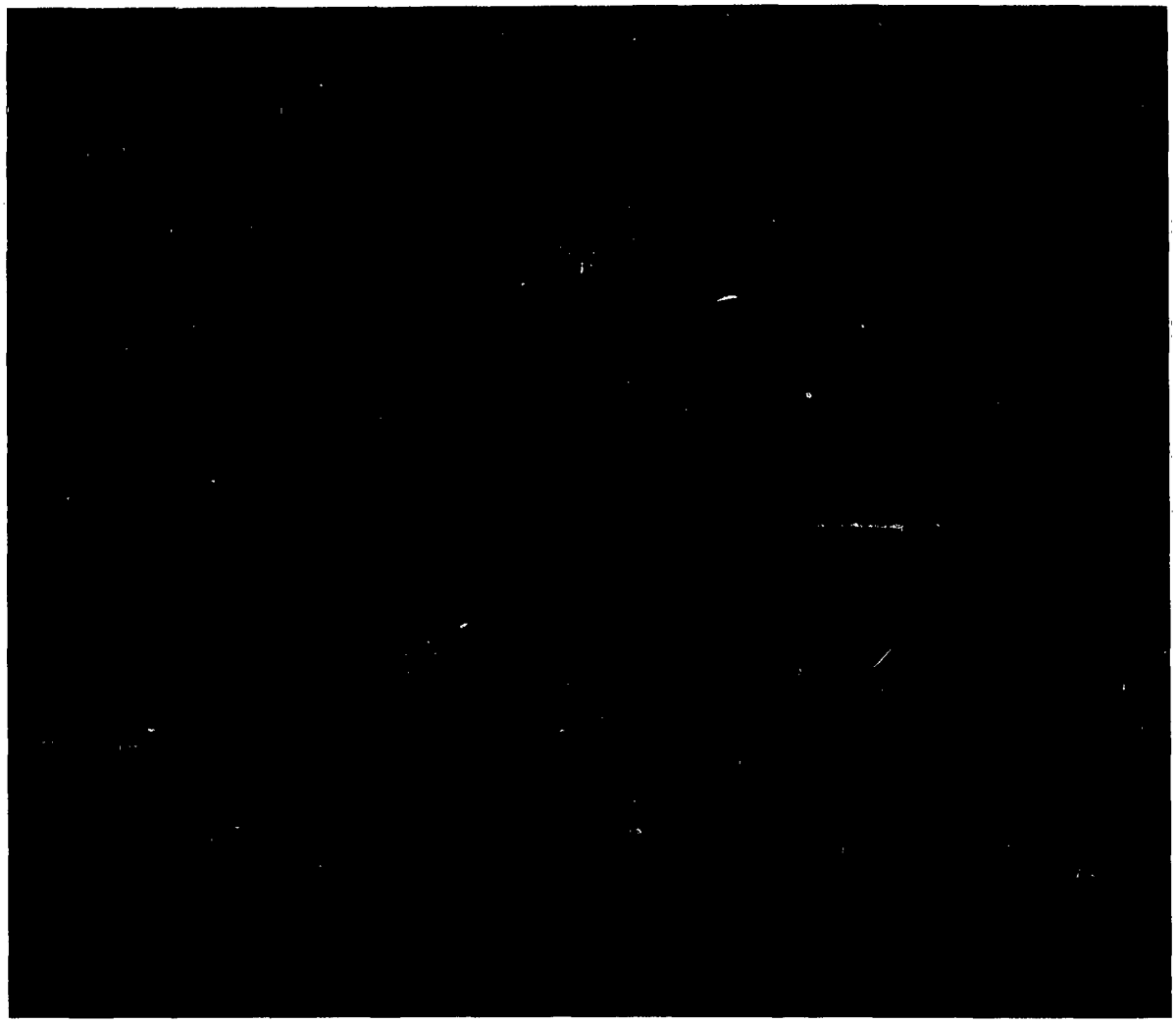

Frequency - 10.0 mc.
Transducer - 3/4 inch diameter
Lithium Sulphate

Plate Thickness - 1/8 inch

Collimator - 1/4 inch diameter
Presentation - IF

Figure 34. Facsimile Paper Recording of 1/8 Inch Plate, 10.0 mc., 1/4 Inch Collimator, Direct Technique.

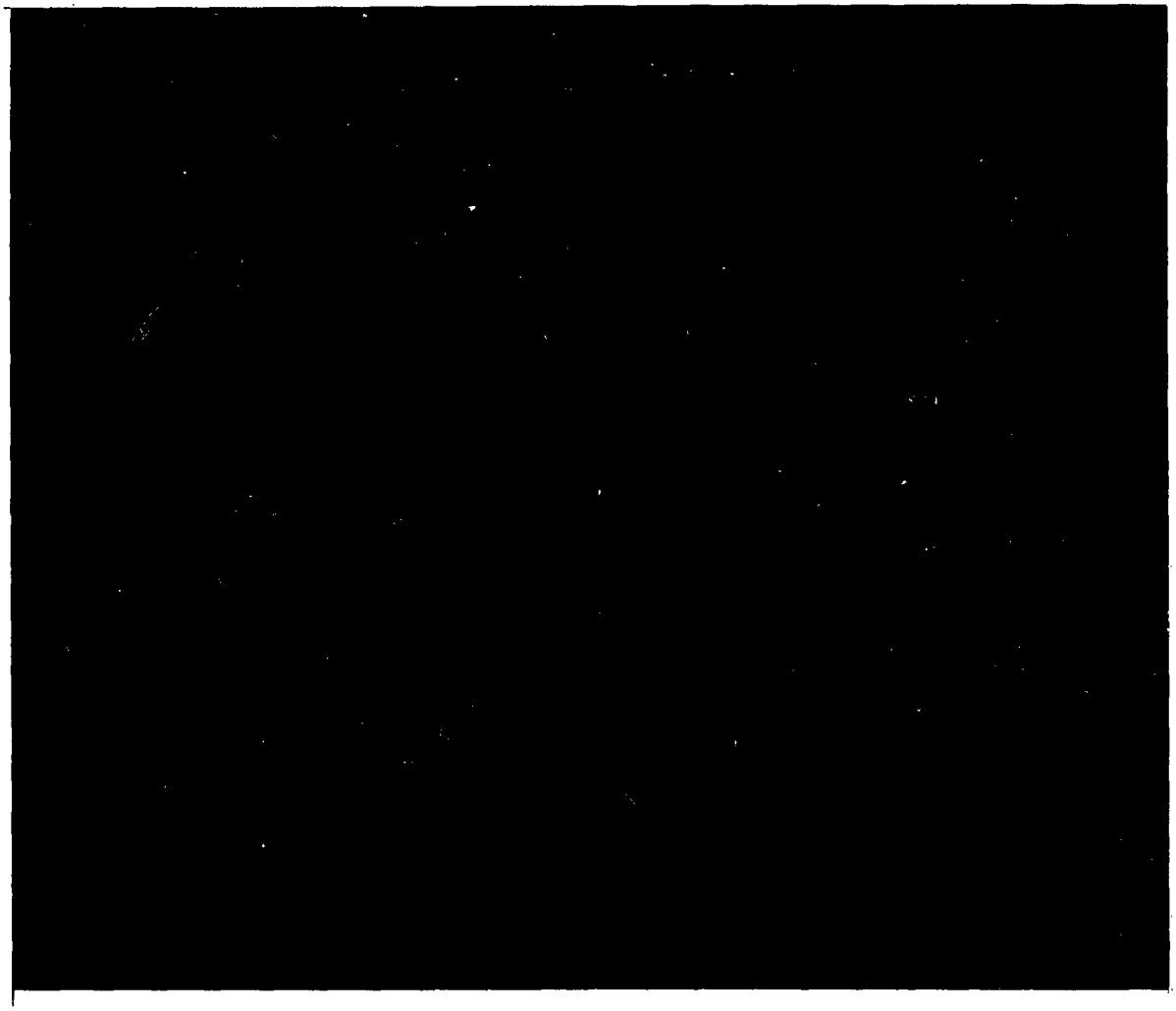

Frequency - 10.0 mc.
Transducer - 3/4 inch diameter
Lithium Sulphate

Plate Thickness - 1/8 inch

Collimator - 1/4 inch diameter
Presentation - IF

Figure 35. Facsimile Paper Recording of 1/8 Inch Plate, 10.0 mc., 1/4 Inch Collimator, Reflector Technique.

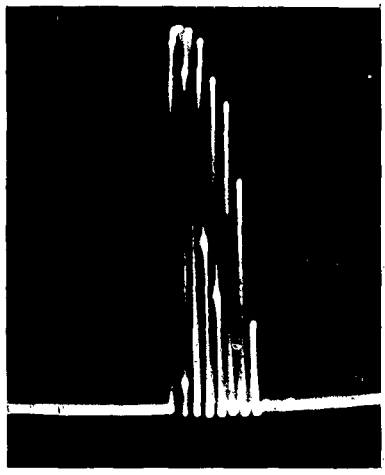

A. No Defect

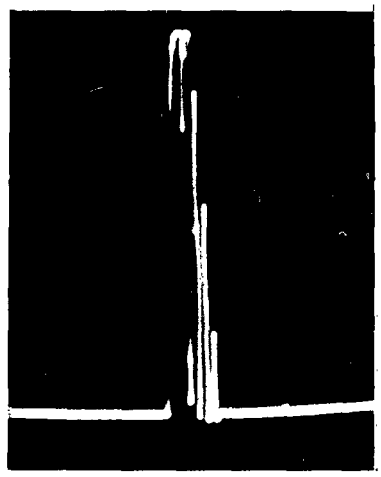

B. Defect at 3/16" Metal Distance

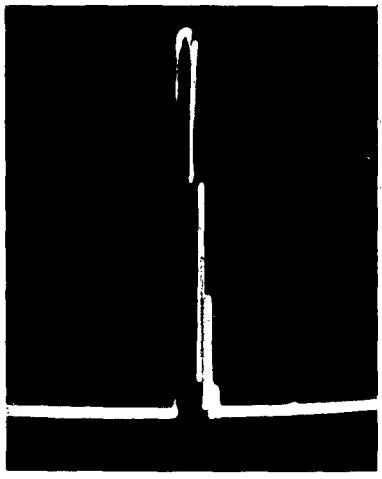

C. Defect at 1/8" Metal Distance

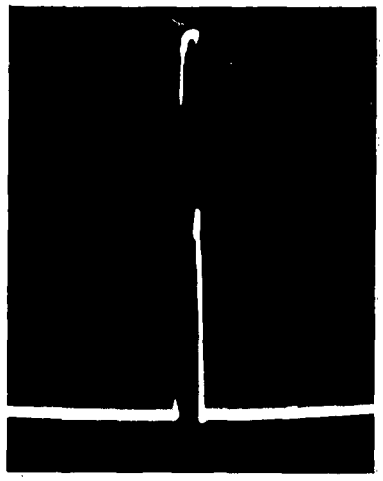

D. Defect at 1/16" Metal Distance

Figure 36. Change of Reflected Signal for Various Defect Locations, 1/4" Plate at 10.0 mc.

10.0 mc. At 5.0 mc the 5/64 of an inch diameter flat bottom holes were detected and satisfactorily recorded for each of the three plates. The 3/64 of an inch diameter defects were not reliably recorded.

With the instrument settings used only minimal magnification of defects occurred. When checked, it proved to be a constant factor added to the true size. Thus, flaw evaluation using the reflector recording technique can be as precise as direct inspection for thin plates. In fact, plates thinner than those tested could be easily recorded.

It was found that some caution was required while using the reflector technique. The surface of the reflector had to be smooth and clean to avoid false indications. Also, the test plates occasionally trapped small air bubbles at the back surface which appeared as defective areas on the recordings.

B. COMPARISON WITH FOCUSED TRANSDUCERS

Test 1. Thick Plate

In the recordings obtained with focused transducers several general observations may be made. First, the use of 2.25 mc resulted in greatest magnification of 5/64 and 8/64 of an inch flat bottom holes when the corresponding 3/64 of an inch flat bottom hole was recorded at or near true size. Best resolution was achieved using 10.0 mc. Better resolution was achieved at all frequencies when IF presentation was used. Better resolution of defects near the front surface was obtained when focus was on the surface, i.e., when water travel was adjusted to obtain a maximum front surface reflection. The range of metal distance which could be accurately recorded was generally decreased when focus was on the surface, however. Figures 37 through 39 show some typical recordings obtained using focused transducers.

The widest range of flaw depths was recorded consistently at 10.0 mc. When the 10.0 mc focused transducer was used each recording (with one exception) displayed the 8/64 of an inch flat bottom hole at a consistent size and with minimal magnification through the entire range of metal distances in the Thick Test Plate. The 5/64 flat bottom holes and the 3/64 flat bottom holes were satisfactorily recorded over narrower ranges of metal depths at the same time. However, those ranges were greater than recorded using either 5.0 or 2.25 mc.

It was expected that gain settings would be generally lower using focused transducers than when using collimators due to energy concentration in the focal zone. This was readily borne out in these tests. Apparently the "useful" energy pattern generated by focused transducers resembles the zone achieved with collimators. The most significant difference being the higher energy level in the "useful" zone of the focused transducers.

The magnification of defects was apparently determined by the flaw size-wavelength ratio. For instance, the flat bottom holes used were all small compared to one wavelength at 2.25 mc. while at 10.0 mc these same flat bottom holes were two or more wavelengths in diameter. The choice of frequencies where flaw dimensions were larger than 2 or 3 wavelengths resulted in better definition over a wider range of metal distance.

Frequency - 2.25 mc
Transducer - 3/4 inch diameter
focused Lithium Sulphate

Focal Point - for optimum
Presentation - IF

Figure 37. Facsimile Paper Recording of Thick Plate, 2.25 mc, Focused Transducer.

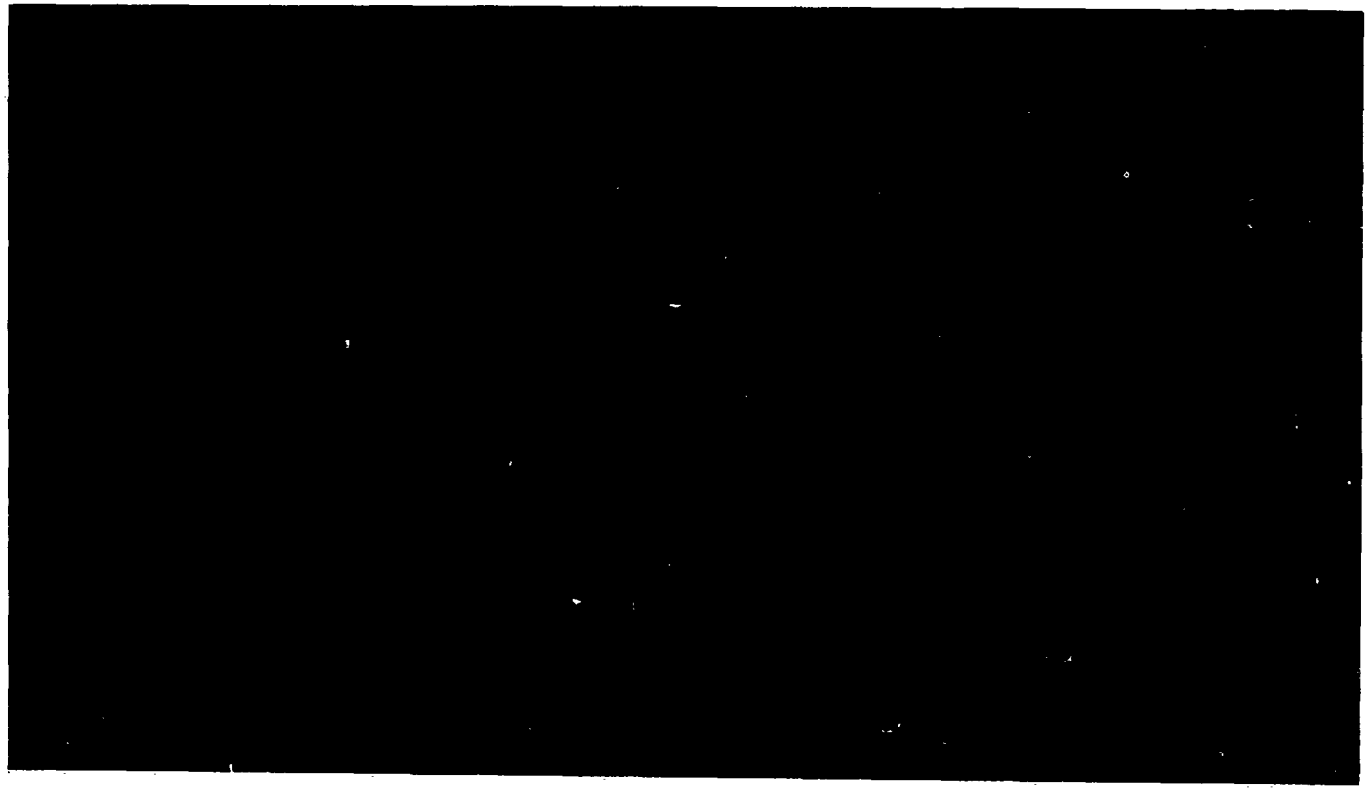

Frequency - 5.0 mc
Transducer - 3/4 inch diameter focused Lithium Sulphate

Focal Point - for optimum
Presentation - IF

Figure 38. Facsimile Paper Recording of Thick Plate, 5.0 mc., Focused Transducer.

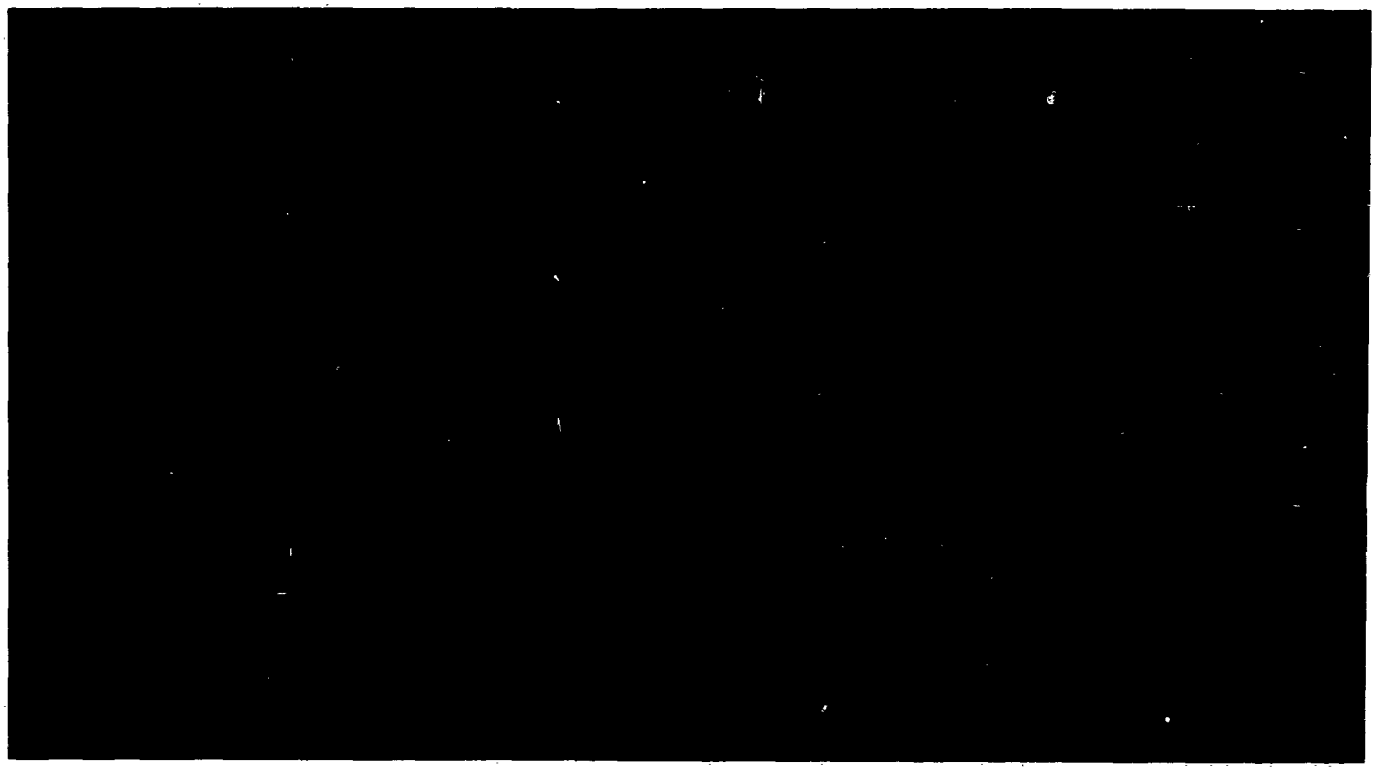

Frequency - 10.0 mc
Transducer - 3/4 inch diameter focused Lithium Sulphate
Focal Point - on surface
Presentation - IF

Figure 39. Facsimile Paper Recording of Thick Plate, 10.0 mc., Focused Transducer.

It seems, then, that higher frequencies could be used where it is desirable to accurately record flaws which are detected. The lower frequencies could be used to "overlook" the smaller or insignificant flaws and record only the more significant areas.

Test 2. Thin Plate

In using focused transducers with a reflector technique, another variable is added, viz., the focal point can be varied in position. For this discussion the focal point will be considered to be located at the distance from the transducer which gives maximum reflected signals as water travel is varied. Two positions of the focal point were used: (1) At the surface of the plate, and (2) at the surface of the reflector.

Contrary to what was expected, better results were generally obtained when the focal point was at the reflector. The exception to this, if it can be called that, was at 10.0 mc. At that frequency there was little difference in the recordings and all test holes were detected in each of the plates.

In addition, better resolution was obtained at 5.0 mc than at 2.25 mc. Apparently, there was a frequency-flaw size relationship similar to that pointed out for the thick plates even though the variation in metal distance was small. Figures 40 through 43 show typical recordings.

When recording directly, the signal change which was gated was a decrease in multiple reflections. This decrease was observed at all frequencies using focused transducers as well as collimated transducers and was discussed earlier in Paragraph A2, Results and Discussions. An illustration of this effect is shown in Figure 36.

CONCLUSIONS

A. BEAM COLLIMATORS

The use of beam collimators for C-Scan recording was investigated at 2.25, 5.0 and 10.0 mc. Collimator diameters were 1/16, 1/8, 1/4, 3/8 and 1/2 of an inch. It was found that defects within a range of metal depths were well defined when using each collimator at a given frequency. Table 19 lists the ranges where best definition was obtained.

A minimum useful collimator size was found to exist. This minimum size was determined to be about 2-1/2 wavelengths diameter measured in the material at the test frequency. Best near surface resolution was obtained using the smaller collimators at each frequency.

Best defect definition was obtained over correspondingly wider ranges using 10.0 mc than at 5.0 or 2.25 mc. This considers that all test collimators were used. The range of best definition for any particular collimator was greatest at 10.0 mc.

The use of collimators to record defects in the Thin Test Plates (1/4 of an inch or less) yielded results similar to those obtained from the Thick Test Plate (1-1/2

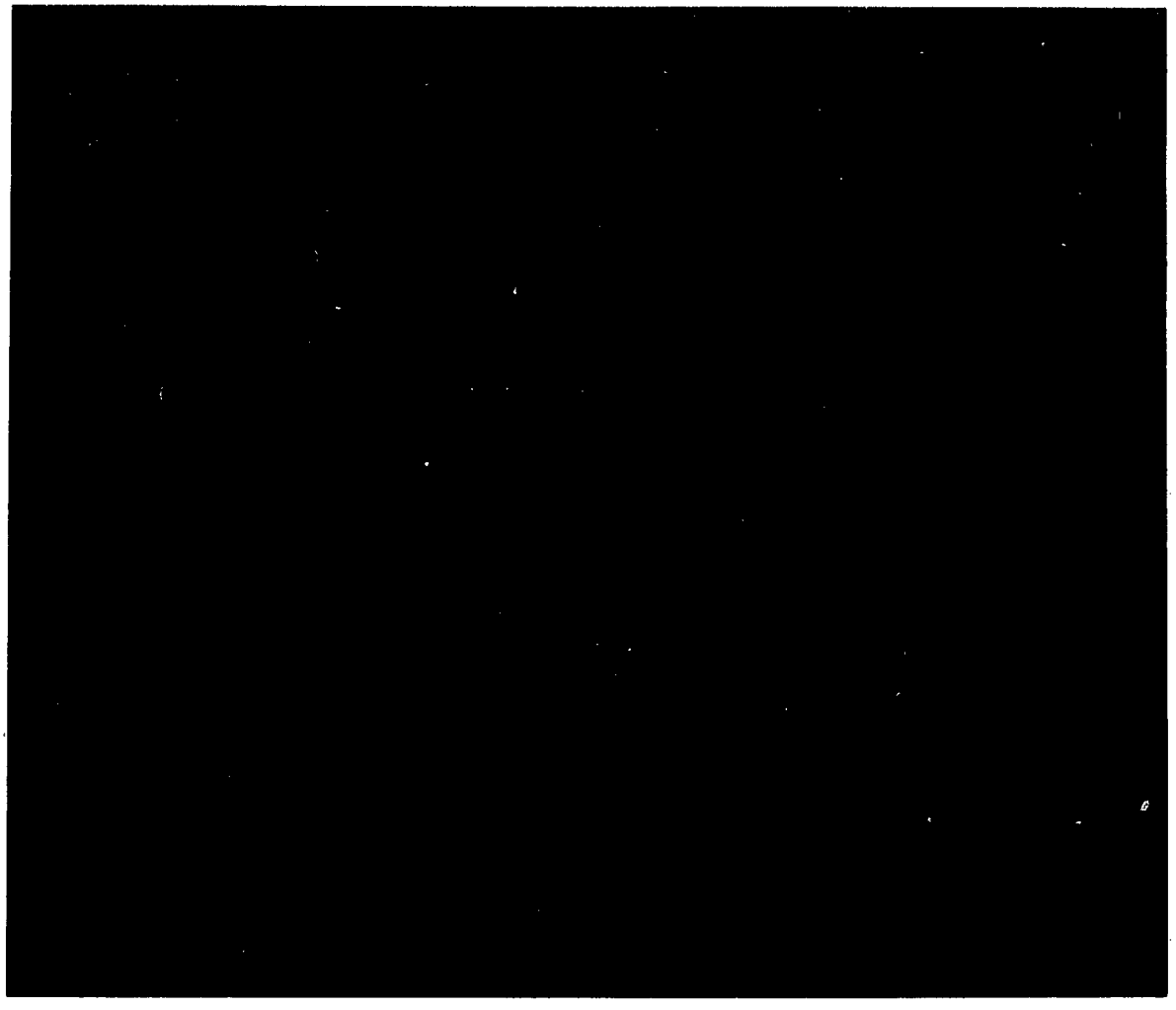

Frequency - 2.25 mc.
Transducer - 3/4 inch diameter focused Lithium Sulphate
Focal Point - on reflector
Presentation - IF

Plate Thickness - 1/4 inch.

Figure 40. Facsimile Paper Recording of 1/4 Inch Plate, Reflector Technique, 2.25 mc.

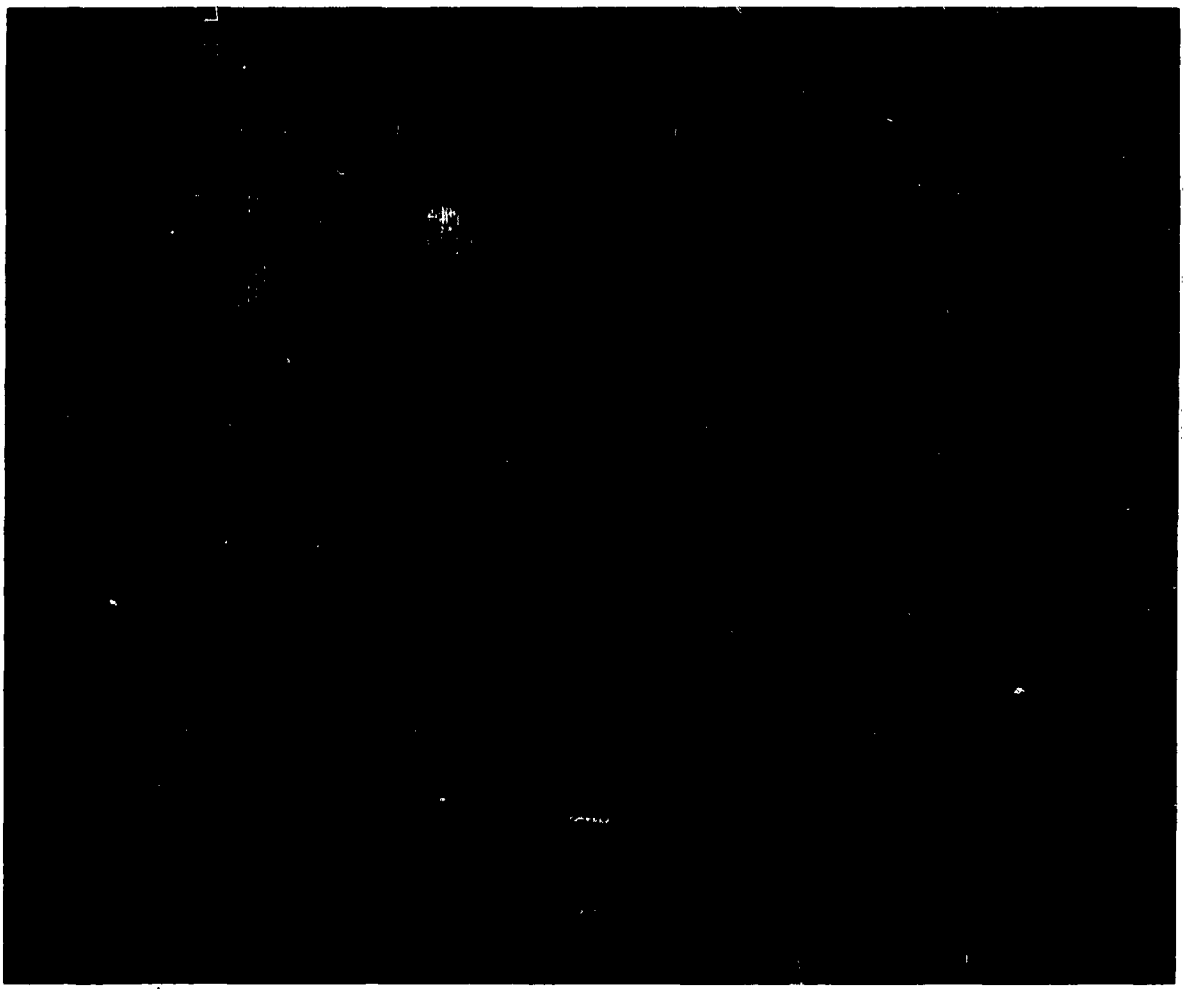

Frequency - 5.0 mc.
Transducer - 3/4 inch diameter focused Lithium Sulphate
Focal Point - on surface
Presentation - IF

Plate Thickness - 1/4 inch

Figure 41. Facsimile Paper Recording of 1/4 Inch Plate, Direct Technique, 5.0 mc.

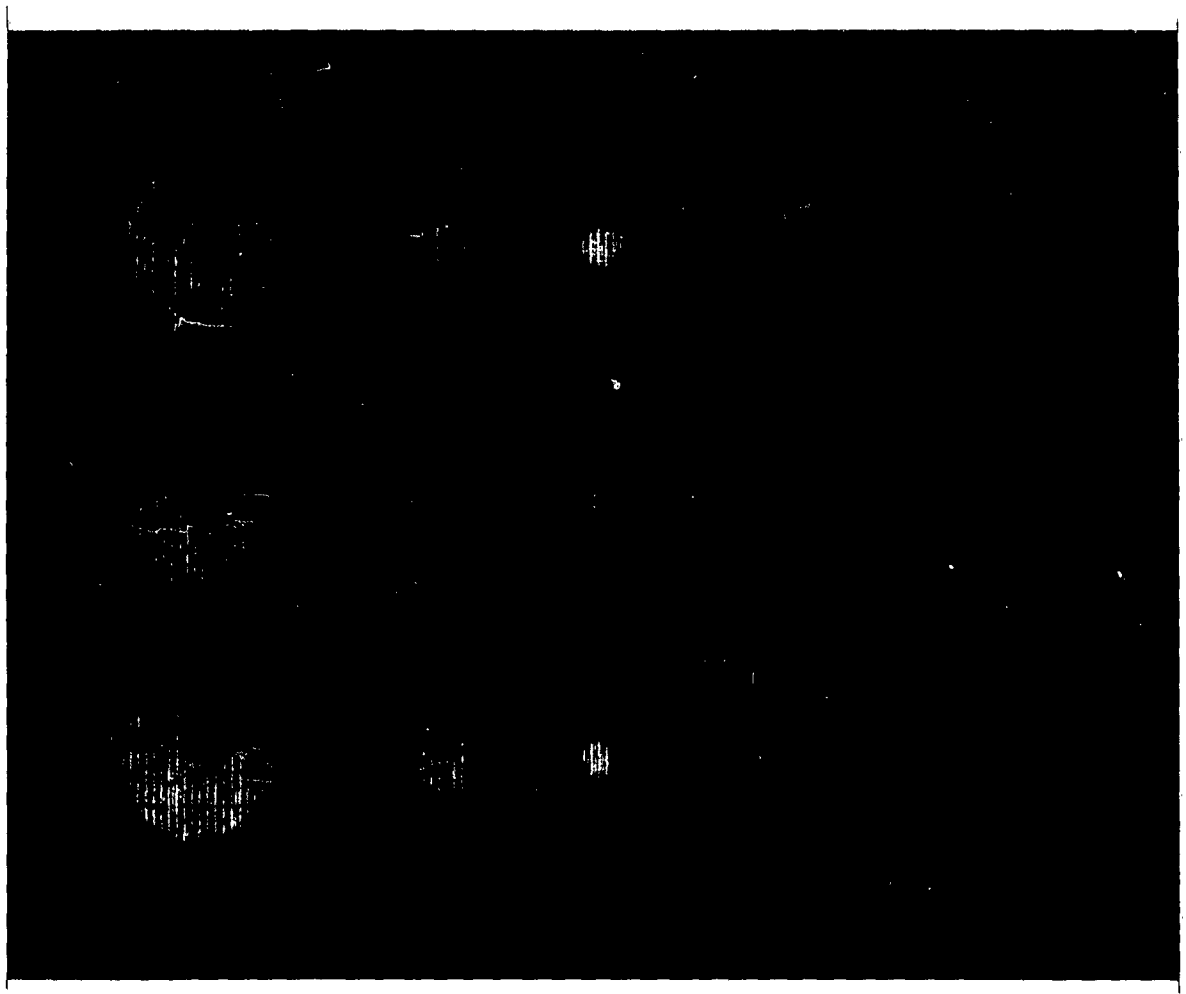

Frequency - 10.0 mc
Transducer - 3/4 inch diameter focused Lithium Sulphate
Focal Point - on surface
Presentation - IF

Plate Thickness - 1/4 inch

Figure 42. Facsimile Paper Recording of 1/4 Inch Plate, Direct Technique, 10.0 mc.

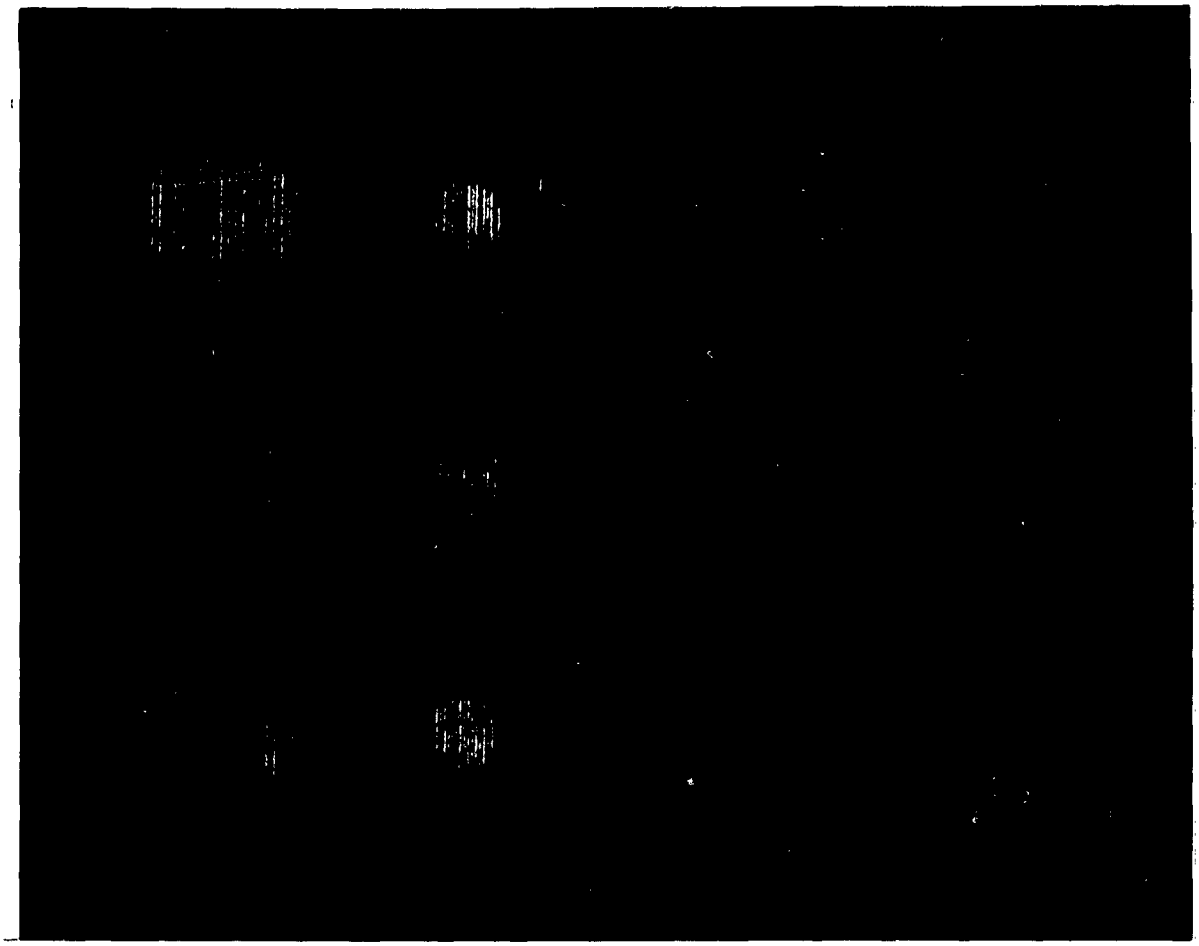

Frequency - 5.0 mc
Transducer - 3/4 inch diameter focused Lithium Sulphate
Focal Point - on reflector
Presentation - IF

Plate Thickness - 1/4 inch

Figure 43. Facsimile Paper Recording of 1/4 Inch Plate, Reflector Technique, 5.0 mc.

inch). Best definition was obtained using 10.0 mc. However, at all test frequencies the signal gated to obtain recordings directly from the plates was a decrease in multiple reflections. Apparently, the decrease was due to a "wave interference" effect.

Use of a reflector technique to record the Thin Plates resulted in better overall definition at each frequency than recording directly. All the defects 3/64 of an inch diameter and larger in each of the Thin Plates was recorded using 10.0 mc. At 5.0 mc all defects 5/64 of an inch diameter and larger were recorded. The collimator used was 1/4 of an inch diameter.

B. FOCUSED TRANSDUCERS

The results obtained using focused transducers were similar to those observed using collimators. Best resolution was obtained in the Thick (1-1/2 inch) Test Plate using 10.0 mc. Defect definition was also better over a wider range at 10.0 mc than at 5.0 or 2.25 mc.

In the Thin Plates all defects 3/64 of an inch diameter and larger were detected and recorded using 10.0 mc focused transducers. Correspondingly, larger minimum defects were resolved using 5.0 and 2.25 mc. The signal gated for recordings was a decrease in multiple reflections as in the tests with collimators.

When the reflector technique was used with focused transducers better definition was obtained when the focal point was at the reflector surface, i.e., water travel was adjusted so that the reflected signal from the reflector was at a maximum.

C. GENERAL

It appears, then, that collimators are quite useful for C-Scan recordings. Good results can be obtained within the limitations described. One seemingly attractive advantage would be the low cost where flat transducers are already available.

Focused transducers would have some advantage where greater energy concentration is required. Such a condition would occur where the material being tested had high acoustic impedance and/or attenuation. Within the limits of the tests for this report, however, no definite advantage or disadvantage was observed for the use of collimated transducers as compared to focused transducers.

RECOMMENDATIONS

With the advent of many sandwich materials and particularly brazed and cemented honeycomb structures in missile construction a need for adequate inspection techniques has appeared. The results in this report indicate a possibility of establishing criteria for ultrasonic inspection of these structures. Although some structures such as brazed honeycomb are presently being inspected and recorded ultrasonically there is no source of information regarding inspection techniques or parameters affecting these techniques. Neither are any real standard reference panels or recommendations for construction of reference standards available.

It is recommended that a program be established to (1) define some of the acoustic parameters affecting ultrasonic inspection of these structures; (2) recommend inspection techniques which could be used; and, (3) recommend techniques for construction of reference standards.

SECTION V

EVALUATION OF SHEAR AND SURFACE (RAYLEIGH) WAVE CHARACTERISTICS

The results of tests performed for WADC Technical Report 59-466 indicated some inconsistencies when compared with shear and surface (Rayleigh) wave theory and investigations reported in other publications. The inconsistencies observed were in tests using thin plates. Those tests were conducted using commercially available, fixed angle transducers.

This report presents the results of tests which attempt to clarify some of the previous apparent inconsistencies. Some additional tests were performed to evaluate the distinguishing characteristics of shear and surface (Rayleigh) waves. Velocity, attenuation, refraction and reflection characteristics of these waves were investigated.

TEST EQUIPMENT

The following equipment was used to conduct the shear and surface (Rayleigh) wave studies for this report:

1. Curtiss-Wright Immerscope, Model 424A
2. Branson Instruments Sonoray
3. Immersion Tank and Manual Carriage
4. Immersion Refractometer, Automation Industries, Inc., Ultrasonics Division design. See Figure 44.
5. Adjustable Angle Contact Adapters, Automation Industries, Inc. design. See Figure 45.
6. Ultrasonic Transducers as listed in Table 20.
7. Automation Industries, Inc. Search Tube Manipulator, Model 314.
8. Special Shear-Surface Wave Separator, Automation Industries, Inc. design. See Figure 46.

MATERIAL AND TEST SAMPLES

The following materials were used as test samples:

1. Aluminum sheet and flat rolled bar, 2024-T4, thickness as listed in Table 21.

Figure 44. Immersion Refractometer.

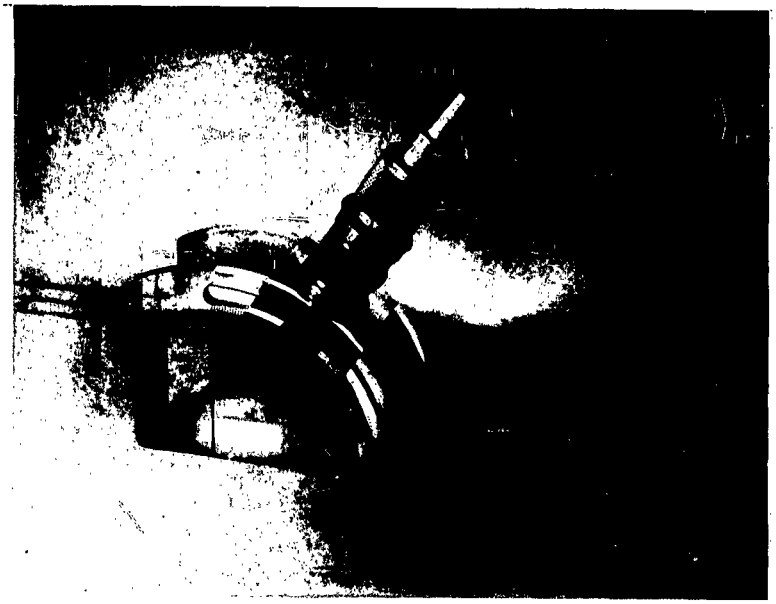

Figure 45. Adjustable Angle Contact Adapter

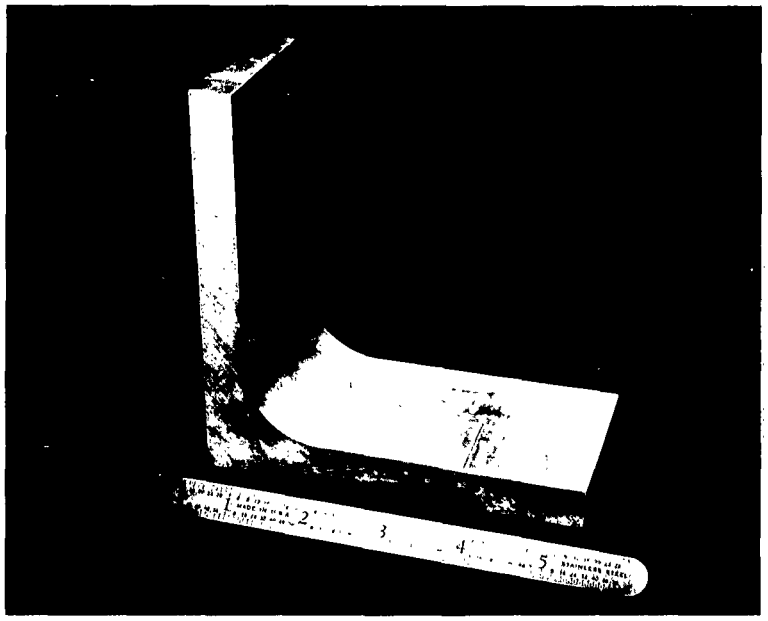

Figure 46. Shear-Surface Wave Separator.

TABLE 20

TRANSDUCERS FOR SHEAR AND SURFACE WAVES			
MANUFACTURER	TYPE	FREQUENCY Megacycles	SIZE Inches
Automation Industries	Lithium Sulphate Immersion	2.25	3/4 dia.
Automation Industries	Lithium Sulphate Immersion	5.0	3/4 dia.
Automation Industries	Lithium Sulphate Immersion	10.0	3/4 dia.
Branson Instruments	Type Z, flat Contact	2.25	1/2 dia.
Branson Instruments	Type Z, flat Contact	5.0	1/2 dia.
Sperry Products	Quartz, 45° Shear Contact	2.25	1/2 x 1 crystal
Sperry Products	Quartz, 45° Shear Contact	5.0	1/2 x 1 crystal
Sperry Products	Quartz, Surface Wave Contact	2.25	1/2 x 1 crystal
Sperry Products	Quartz, Surface Wave Contact	5.0	1/2 x 1 crystal

TABLE 21

THICKNESS OF TEST PLATES	
Test Plate	Thickness, In.
1	0.062
2	0.125
3	0.315
4	0.50
5	1.50

Dimensions of the test plate varied from 4 inches minimum width and 24 inches minimum length. All test plates had ends milled square in the direction of wave propagation.

TEST PROCEDURES

Due to the variety of tests performed reference sketches are provided to define the terms used. Figure 47 shows the test variables for the immersed tests and Figure 48 defines the variables for the contact tests.

A. IMMERSED METHOD

Test 1. Signal Amplitude versus Incident Angle

For these tests the signal amplitude reflected from the square milled end of each of the five test plates was recorded as a function of the incident angle. The indications recorded were at those angles where a steady change in signal amplitude could be observed as the metal distance was varied. The transducer was positioned so that the intersection of the center of the incident beam with the surface of the test plate was 3 inches from the end of the plate. Water distance was held constant at 2 inches. Test frequencies were 2.25 and 5.0 mc. The transducers were flat, 3/4 of an inch diameter lithium sulphate. Gain was held constant for all tests on each plate. Results of these tests using the 0.062 and 0.125 inch plates are shown in Figures 49 and 50.

Test 2. Signal Amplitude versus Metal Distance

All five test plates listed in Table 21 were used. The signal amplitude was observed and recorded as metal distance from the end of the plate was varied. Data was recorded using each incident angle at which a distinct maximum signal from the end of the plate was observed in the tests described in Paragraph A1. Test frequencies were 2.25 and 5.0 mc. Transducers used were flat, 3/4 inch diameter lithium sulphate. Results are shown in Figures 51 and 52.

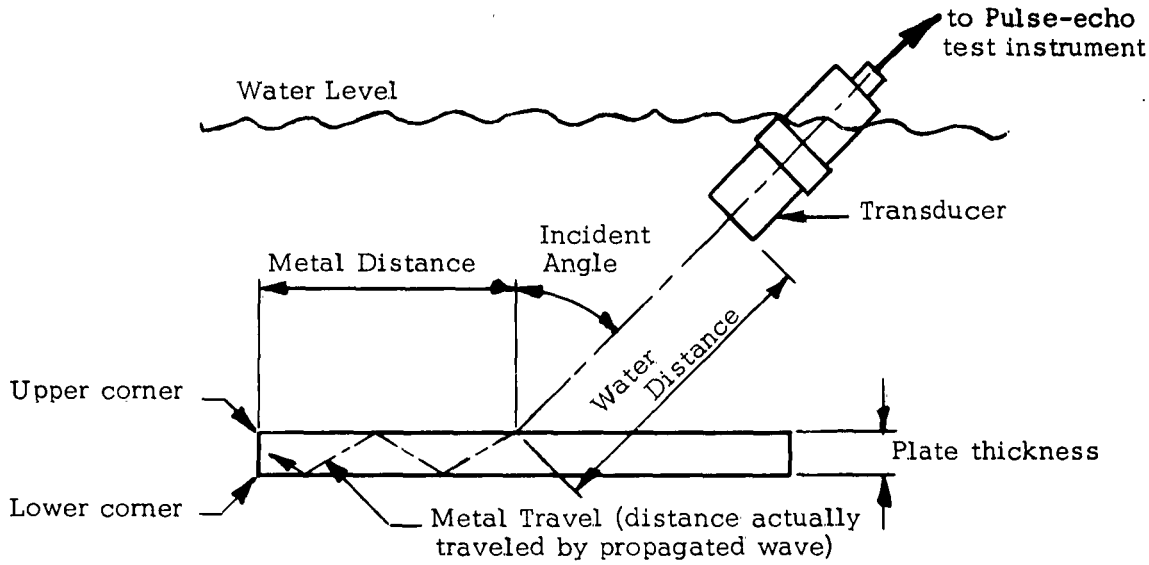

Figure 47. Definition of Terms for Immersed Testing.

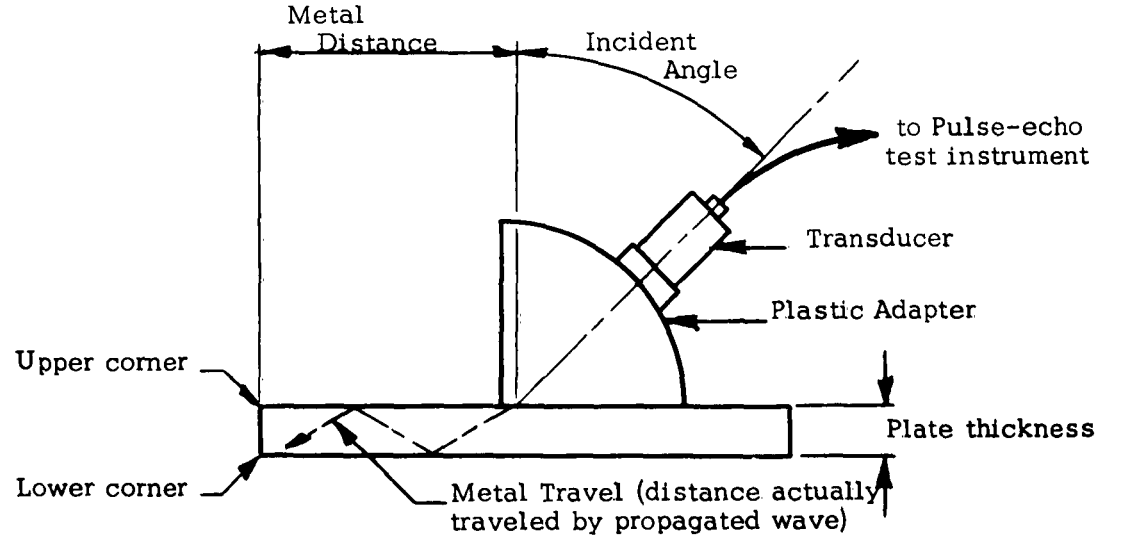

Figure 48. Definition of Terms for Contact Testing.

Test 3. Speed of Wave Propagation

The speed of wave propagation along the plate was measured at each incident angle used in Test 2 above. In order to do this a 35° (included angle) groove was machined in each of the test plates. The position of the groove was normal to the direction of wave propagation (i.e., parallel to end of plate) at a distance of 3.00 inches from the end of the plate. The reflected signal from the test plate then indicated first, the groove, and second, the end of the plate. The Two Transducer, Water Comparison technique was then used to determine the speeds. This technique is described in Appendix III. The results of these measurements are listed in Table 22.

Test 4. Signal Amplitude versus Metal Travel - Shear Waves

All five test plates were used in these tests. The incident angle was adjusted so that a 45° shear wave was propagated in the panels. The transducer was then positioned so that the lower corner at the milled end of the plate was detected directly through the plate and the maximum signal amplitude noted. The scanning carriage was then moved away from the edge of the panel until a position was reached where a maximum reflection was obtained from the top corner. The metal travel was further increased while alternately observing the signals reflected from the upper and lower corners of the plate until the signal height was 1/4 of an inch or less.

Test frequencies were 2.25 and 5.0 mc. Transducers were flat 3/4 of an inch diameter, lithium sulphate. Water distance was 2 inches. Gain was held constant at each test frequency. Figures 53 shows the results of these tests at 2.25 mc.

In addition to the foregoing tests the 1-1/2 inch panel was tested at 5.0 mc using 30°, 60° and 75° shear waves. The same procedure was used for determining signal amplitude. Water distance was held constant at 2 inches for all tests. Figure 54 shows the results of these observations.

Test 5. Refractometer Test

The immersion refractometer was constructed so that the incident angle could be varied from 0° to approximately 80° while the refracted beam remained normal to the back surface. The refractometer was used to determine the variation in reflected signal from the back surface that occurred as the incident angle was varied from 0° through 45°. Test frequencies were 2.25, 5.0 and 10.0 mc. All transducers were flat 3/4 of an inch diameter, lithium sulphate. Results of varying the incident angle are shown in Figure 55.

The velocity of the generated waves was measured using the Two Transducer, Water Comparison method. The results of these measurements are listed in Table 23.

B. CONTACT METHOD

Test 1. Signal Amplitude versus Incident Angle

In this series of tests the signal amplitude was measured as a function of the incident angle. Test frequencies were 2.25, and 5.0 mc. The transducers were 1/2 of an inch diameter, Type Z. All five test plates were observed for these tests. The incident angle was varied from 0° to 75° angle using the Variable Angle Adapter. Signal amplitude data was recorded at each angle where a distinct signal was observed. Figure 56 shows the results obtained using 2.25 mc.

Test 2. Signal Amplitude versus Metal Distance - Surface Waves

The fixed angle surface wave transducers as listed in Table 20 were used. Test frequencies were 2.25 and 5.0 mc. The signal amplitude reflected from the end of each test plate was observed as the metal travel was varied. Gain was held constant for all tests at each frequency. Test results are shown in Figures 57 and 58.

Test 3. Shear-Surface Wave Separator

A special test block, shown in Figure 46, was used for this test. Configuration was such that a shear wave propagated at 90° from the normal (parallel to the surface) could be observed separately from a surface wave. The ability of surface waves to follow contours was utilized in the design.

Using the Variable Angle Adapter the incident angle was varied from 50° through 75° in 1° increments. Signal amplitude was recorded for both surface and shear wave indications. The test frequency was 2.25 mc using a 1/2 of an inch diameter Type Z transducer. The results of this test are shown in Figure 59.

The velocity represented by the position of both indications was determined using the Two Transducer, Water Comparison technique. A scribe line approximately 0.003 of an inch deep was machined in the block as a reference point for velocity measurements. Location of the scribe line was such that metal distance traveled by the surface wave was twice the distance traveled by the shear wave. The results of these measurements is noted in Table 24.

RESULTS AND DISCUSSION

A. IMMERSED METHOD

Test 1. Signal Amplitude versus Incident Angle

In these tests the signal response was similar for all test plates which were 0.315 of an inch thick or greater. A signal was observed which reached a maximum value at the critical incident angles for longitudinal and shear waves. These maxima occurred using both 2.25 and 5.0 mc. The velocity measurements discussed in Section A3 indicated that both longitudinal and shear waves had been observed. See table 22.

The tests showed that 90° longitudinal or 90° shear waves may be generated quite readily. The amplitude of these signals was such that inspection of flat plates or welds for cracks, lack of fusion or various inclusions seems to be a good area of application.

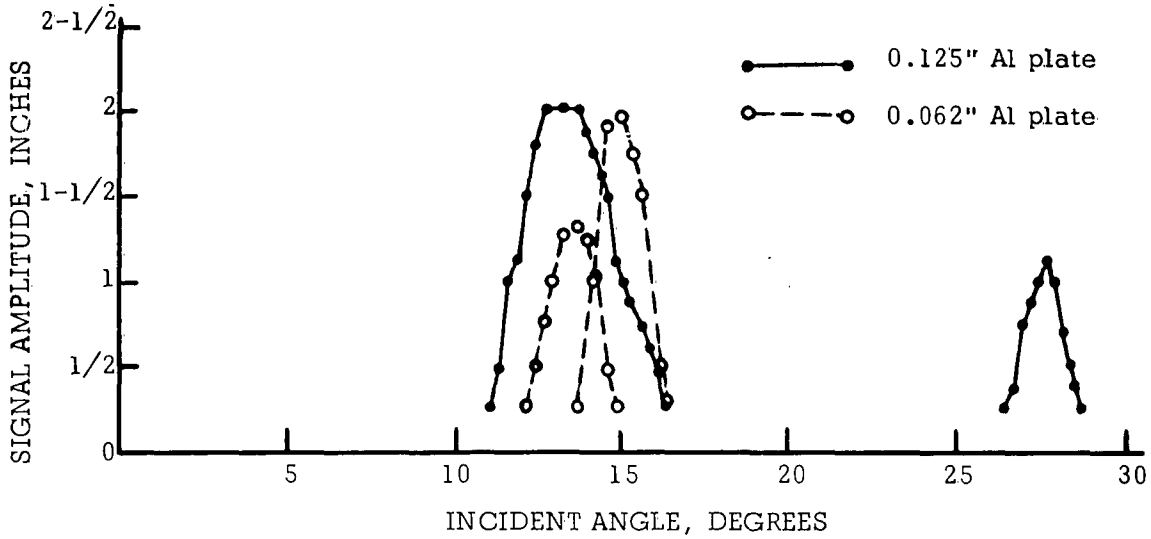

Figure 49. Signal Amplitude vs. Incident Angle - 2.25 mc, Immersed Test.

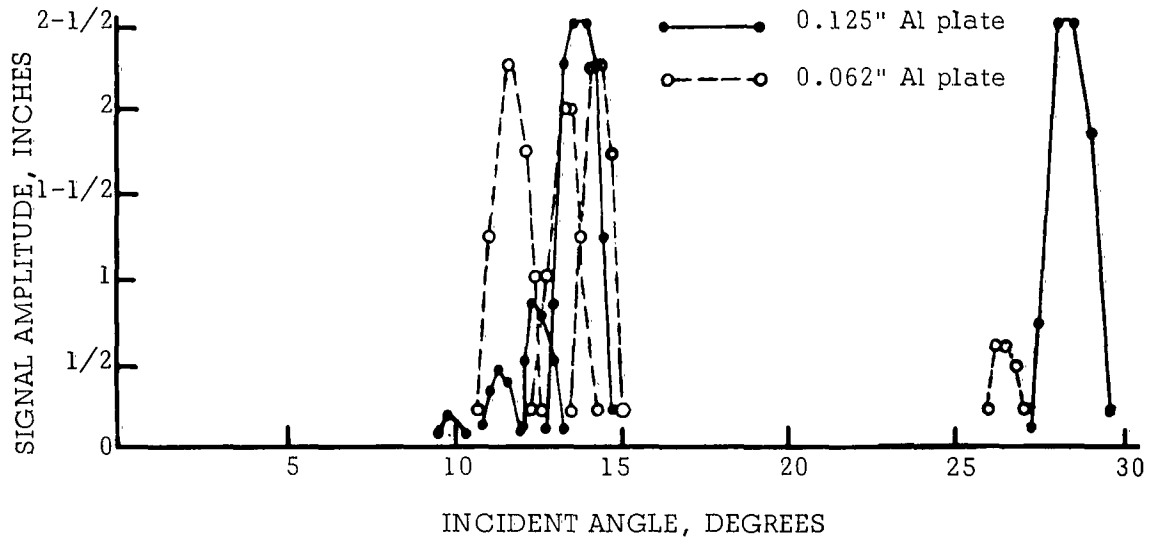

Figure 50. Signal Amplitude vs. Incident Angle - 5.0 mc, Immersed Test.

It was interesting to note the signals in addition to the 90° longitudinal and 90° shear waves observed in the 0.125 and 0.062 of an inch thick plates when tested using 5.0 mc signals. The velocity along the plate for these additional signals increased as the incident angle increased. The characteristic velocities were not those of either longitudinal or shear waves. The incident angles were much smaller than would have been required for generation of surface (Rayleigh) waves. Apparently, the indications were due to a different vibrational phenomena such as Lamb waves. Some preliminary checks indicated that this was indeed the case. A great deal more investigation is needed in this area to provide sufficient data concerning the nature of these waves and possible applications thereof.

Test 2. Signal Amplitude versus Metal Travel

Data was obtained using the five test plates in order to study the attenuation of shear waves as compared to other waves in plates. Figures 51 and 52 show Signal Amplitude versus Metal Distance at several incident angles for longitudinal and shear waves. The curves for the 0.500 inch plate were typical of results for all plates thicker than 0.125 of an inch. Generally, the apparent attenuation of shear waves in each plate for both 2.25 and 5.0 mc was lower than for the longitudinal waves. One reason for this could be the lower impedance of the shear waves. The shear wave impedance was about 1.22×10^4 lbs/in^2-sec while impedance of longitudinal waves was 2.50×10^4 lbs/in^2-sec. The transmission coefficients were calculated using these acoustical impedance values. For longitudinal waves the transmission coefficient, $T_L = 0.29$ while for shear waves the tansmission coefficient, $T_S = 0.50$. Thus, it appears that considerably more shear wave energy was propagated into the part. Apparently, the higher energy level of the shear waves enabled greater metal distances to be observed.

Figure 51 also shows a family of Signal Amplitude versus Metal Travel curves obtained when using 5 mc to test the 0.125 inch plate. As the incident angle was increased, the metal distance at which a reflected signal could be observed also increased. An attempt was made to determine the nature of wave propagation observed by first assuming longitudinal wave propagation, then shear wave propagation reflecting back and forth between the surfaces of the plate. The resultant velocity of these waves along the plate was calculated for each angle. The results did not agree with the measurements in Test 3 for any angle (except 13° and 28°), thus, further indicating the existence of a compound wave motion.

Test 3. Velocity of Wave Propagation

Table 22 shows the velocities measured at each angle in each of the plates. The velocities measured for the longitudinal and shear waves were virtually the same at 2.25 and 5.0 mc. However, the velocities of other waves were apparently dependent upon the incident angle. The existence of these waves seemed to be dependent upon plate thickness and frequency at any given angle. Some comparison with published data indicated the possible existence of Lamb waves.

Test 4. Signal Amplitude versus Metal Travel - Shear Waves

Since many commercially available shear transducers generate shear waves at 45° in the metal being inspected, the effect of plate thickness on total metal travel at this angle was of interest.

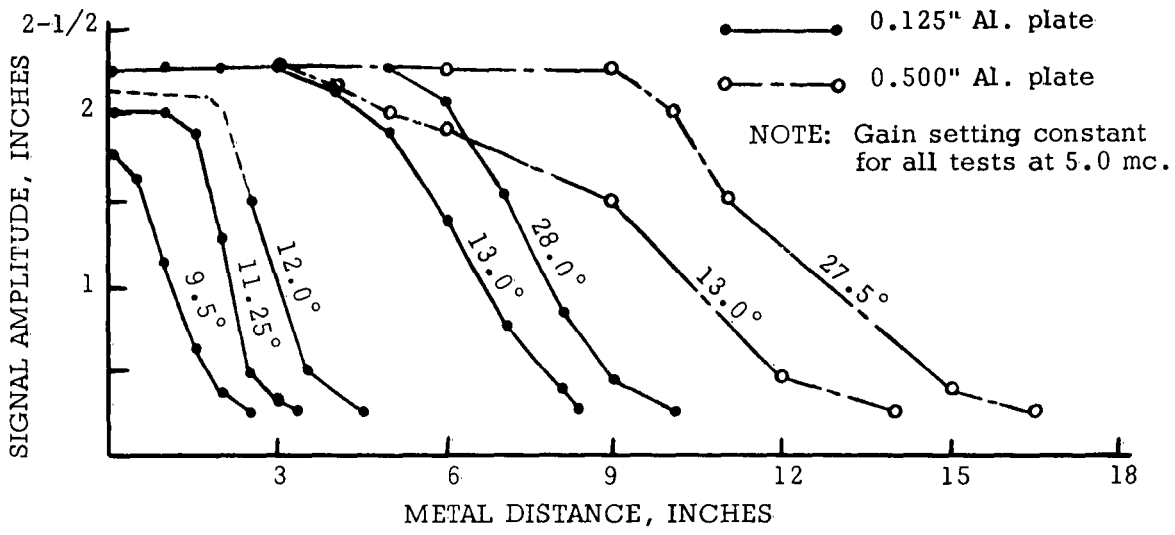

Figure 51. Signal Amplitude vs. Metal Distance at Various Incident Angles - 5.0 mc Immersed Tests.

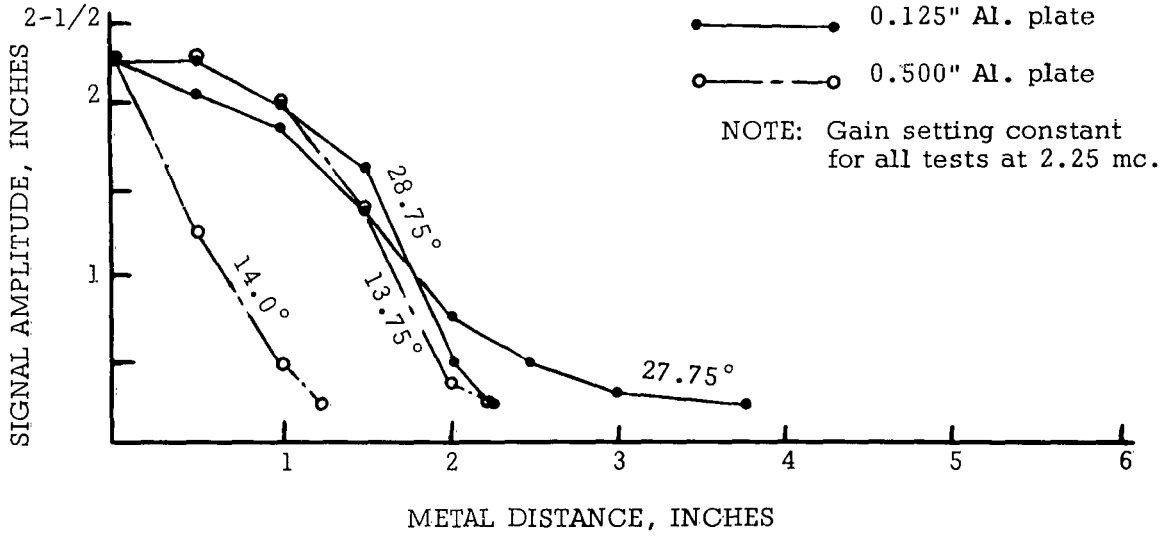

Figure 52. Signal Amplitude vs. Metal Distance at Critical Incident Angles - 2.25 mc Immersed Tests.

TABLE 22

WAVE VELOCITIES IN TEST PLATES				
	2.25 mc		5.0 mc	
Plate Thickness Inches	Incident Angle Degrees	Velocity in/sec x 10^5	Incident Angle Degrees	Velocity in/sec x 10^5
1.50	14.0	2.49	13.0	2.45
	28.7	1.27	27	1.24
0.500	14.0	2.54	13.0	2.51
	28.7	1.26	27.5	1.25
0.315	14.0	2.50	13.5	2.41
	28.0	1.28	27.5	1.23
0.125	13.7	1.93	9.5	0.67
	27.7	1.28	11.2	0.81
			12.0	1.11
			13.5	2.54
			28.7	1.25
0.62	13.2	1.68	11.1	0.90
	14.0	1.83	11.9	0.94
	15.0	1.82	12.7	1.20
	29.5	1.67	13.2	1.67
			13.9	1.71
			26.5	1.16

Figure 53 shows the results of these tests at 2.25 mc. Generally, a decrease in total metal travel was observed as plate thickness decreased. The number of observed reflections within the plates increased somewhat for the thinner plates using 5.0 mc, but the number of reflections remained approximately the same for all plates when 2.25 mc was used. Thus, energy loss at the interface due to transmission out of the part or mode conversion at the reflecting points is apparently a direct and large loss factor.

It was speculated that perhaps the angle of propagation of the shear waves was also a factor since it would affect both transmission and mode conversion. The test results shown in Figure 54 tended to confirm this. The total metal distance observed in the 1.50 inch thick plate for each of the angles of propagation, i.e., 30°, 45°, 60°, and 75° remained approximately the same. However, the number of reflections decreased as the angle increased. Two possible solutions appear: (1) less energy entered the plate at the greater incident angles, or (2) losses due to mode conversion and transmission (out of the part) increased as the angle of propagation increased. In the Refractometer tests it was observed that energy entering the part and being reflected was fairly constant for the range of angles used in this test. Then, if the foregoing assumptions are correct, greater losses occur due to mode conversion and transmission out of the part.

Additional tests are required to definitely establish the nature of this phenomena and to determine whether similar results occur when testing the thinner plates.

Test 5. Refractometer Test

In examining the results of the Refractometer Tests one fact should be kept in mind, viz., the gain setting was adjusted at each frequency so that none of the indications reached saturation (100% of display amplitude). However, the gain was held constant for each test frequency.

Figure 55 shows the results of this test. It is interesting to observe the apparent attenuation of shear waves in relation to the longitudinal waves at each frequency. The apparent attenuation of shear waves at 2.25 mc was very low compared to longitudinal waves. At 5.0 mc the apparent attenuation of shear waves was nearly equal to that for longitudinal waves while at 10.0 mc the attenuation of shear waves is greater than for longitudinal waves.

In general, it has been found that attenuation is inversely proportional to wavelength, i.e., attenuation increases as wavelength decreases. The wavelength of shear waves is approximately half that of longitudinal waves at any given frequency. Thus, it appears that additional factors must be involved.

Probably the most important of these is specific acoustical impedance. For shear waves the specific acoustical impedance, Z, is approximately 1/2 of the impedance for longitudinal waves due to the lower velocity of shear waves. The energy loss due to impedance mismatch is then lower for shear waves than for longitudinal waves. This energy loss is the same for all frequencies, however.

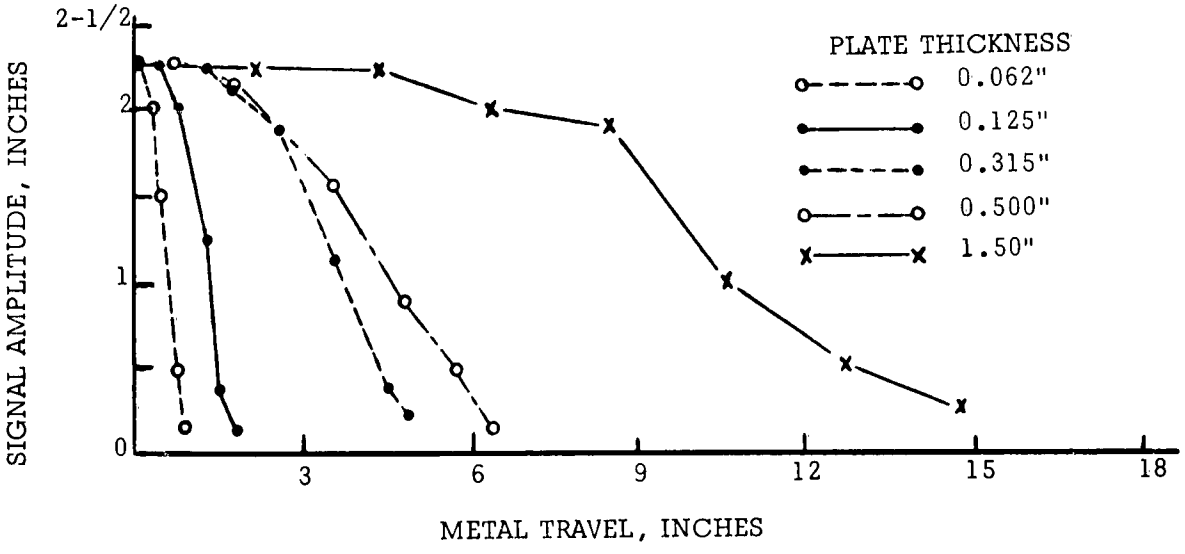

Figure 53. Signal Amplitude vs. Metal Travel, 45° Shear Waves, 2.25 mc, Immersed Tests.

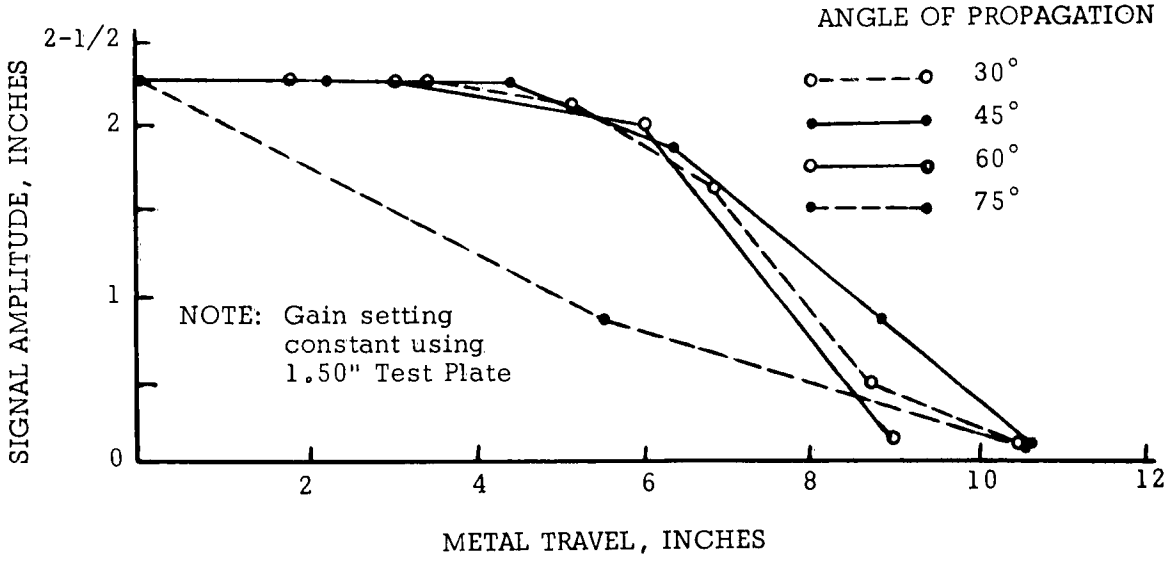

Figure 54. Signal Amplitude vs. Metal Travel, Various Angle Shear Waves, 5.0 mc Immersed Tests.

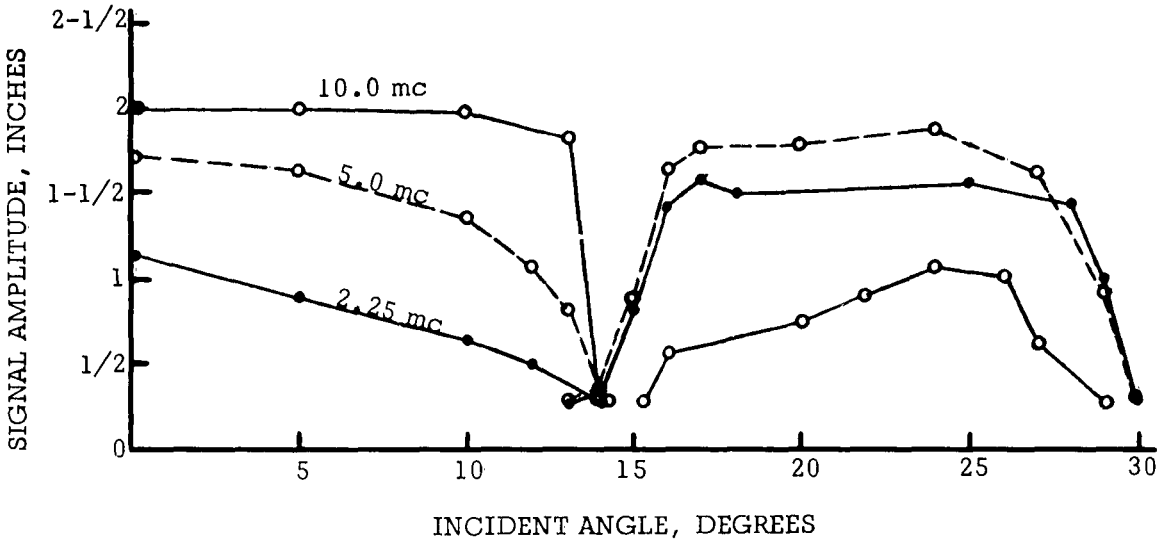

Figure 55. Signal Amplitude vs. Incident Angle Using Immersion Refractometer.

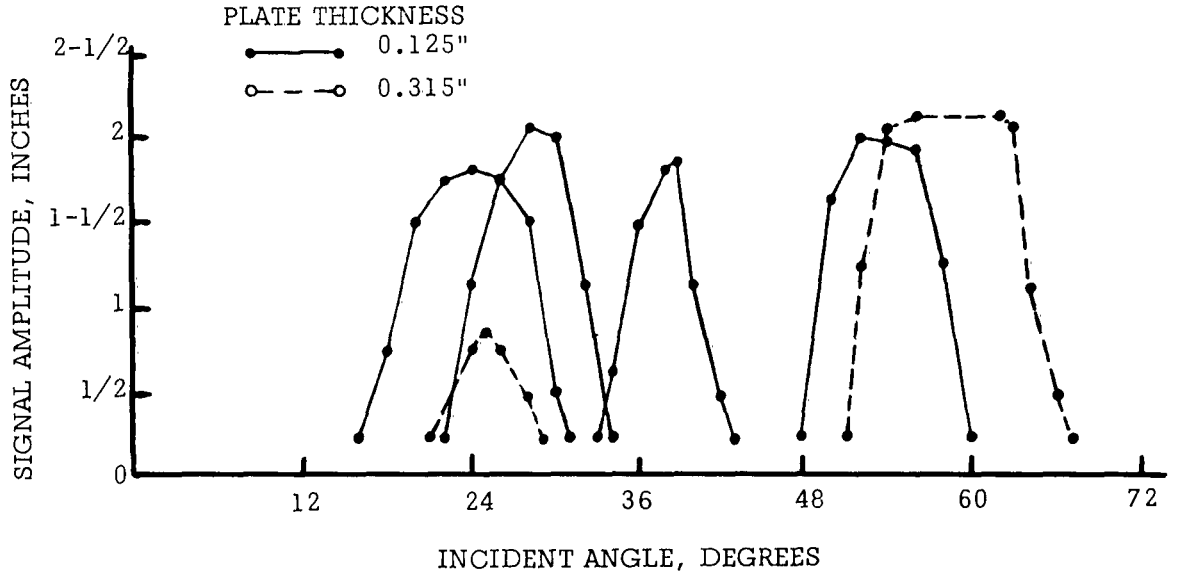

Figure 56. Signal Amplitude vs. Incident Angle, 2.25 mc Contact Tests.

Now, if a typical attenuation versus wavelength curve is considered in conjunction with the difference in impedance values, it can be shown that the test results obtained should have been expected. Using the typical curve in Figure 60, consider each frequency separately.

First, at 2.25 mc the longitudinal wave encounters some finite value of attenuation. Then, the 2.25 mc shear wave, due to its shorter wavelength, encounters greater attenuation. Recall, however, that the energy propagated in the metal was greater for the shear wave. It appears that the increase in propagated energy using the shear waves was greater than the higher attenuation loss in the refractometer. At 5.0 mc the increase in shear energy appeared to be approximately equal to the attenuation of the shear wave. At 10.0 mc the attenuation of the shear waves is much greater than the energy increase. It should be emphasized that these tests were limited in scope. Further investigation is needed to establish definite values for impedance and attenuation losses using shear waves.

The velocities of the longitudinal and shear waves in the Refractometer were determined using the Two Transducer, Water Comparison method. See Table 23 below.

TABLE 23

VELOCITY OF WAVES PROPAGATED IN IMMERSION REFRACTOMETER	
Type of Wave	Velocity
Longitudinal Wave	2.48×10^5 in/sec
Shear (Transverse Wave)	1.21×10^5 in/sec

Observations over the complete range of incident angles did not disclose any measurable variation in velocity.

B. CONTACT METHOD

Test 1. Signal Amplitude versus Incident Angle

Figure 56 shows the results of varying the incident angle while observing the reflected signal height for 2.25 mc test frequency. These figures do not include results using the 0.500 and 1.50 inch plates since the signals obtained were typified by the 0.315 inch plate. In the thicker plates (0.315 of an inch or greater) reflected signal maxima were observed only at the critical incident angles for longitudinal and shear waves while testing at 2.25 mc. At 5.0 mc these two maxima were observed in all the test plates. Additional maxima were observed in the 0.125 and 0.062 inch plates at other than critical angles. The distinguishing characteristic of these maxima was a steady increase in signal amplitude as the metal distance was decreased.

When using 2.25 mc to test the 0.125 inch plate the two maxima obtained appeared as quite broad signals. The 90° shear wave could not be observed.

No data was recorded for the 0.062 inch plate at 2.25 mc. This was not due to lack of signals but because of the profusion of them. It was not possible to distinguish any particular signal as being distinct from any others.

Test 2. Signal Amplitude versus Distance - Surface (Rayleigh) Waves

Since the characteristic phenomena of surface waves was not observed during any of the immersion tests some investigation was deemed necessary using contact method. Examining the results shown in Figures 57 and 58 indicates that apparent attenuation of surface waves was lower using 2.25 mc than when using 5.0 mc where the plate thickness was 0.315 of an inch or greater. At 5.0 mc the apparent attenuation decreased when the thin plates, 0.125 and 0.062 of an inch thick, were tested. This decrease in attenuation seemed to be associated with reinforcements of the propagated wave by the back surface. On the thinner plates it was possible to damp the wave, i.e., decrease the signal amplitude, by touching the back surface of the plate. The effect was the same as observed when touching the front surface of a thick plate to decrease the amplitude of a surface wave.

Test 3. Shear-Surface Wave Separator

This test determined velocities and comparative amplitudes of shear and surface waves using the Variable Angle Adapter. Figure 59 indicates that the shear wave signal was detected several degrees beyond the critical angle. This effect was probably due to beam spread. The transducer was 1/2 of an inch diameter, and test frequency was 2.25 mc. In plastic the 1/2 inch diameter is approximately 11 wavelengths. This factor alone will contribute 5-6° of beam spread.

The surface wave was observed as a separate indication, and, through part of the range of incident angles, simultaneously with the indication of the shear waves. No variation in the velocity of either the shear or surface waves was observed throughout the test range. Velocities observed are tabulated in Table 24.

TABLE 24

VELOCITY OF SOUND IN SHEAR-SURFACE WAVE SEPARATOR	
Type of Wave	Velocity, in/sec x 10^5
Shear (transverse)	1.20
Surface (Rayleigh)	1.11
Longitudinal (reference)	2.44

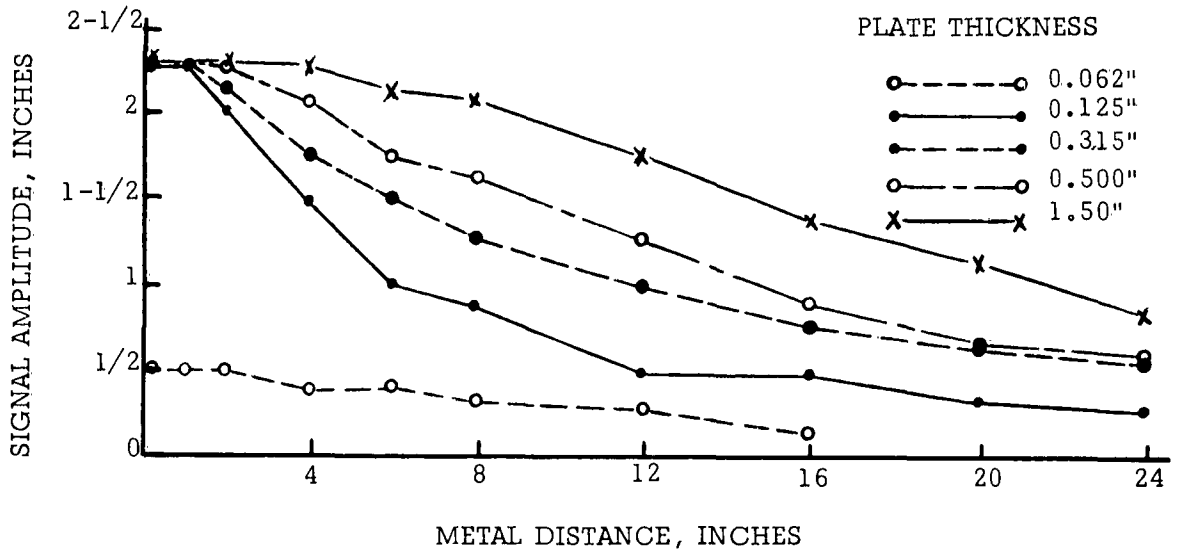

Figure 57. Signal Amplitude vs. Metal Distance, Surface (Rayleigh) Waves, 2.25 mc Contact Tests.

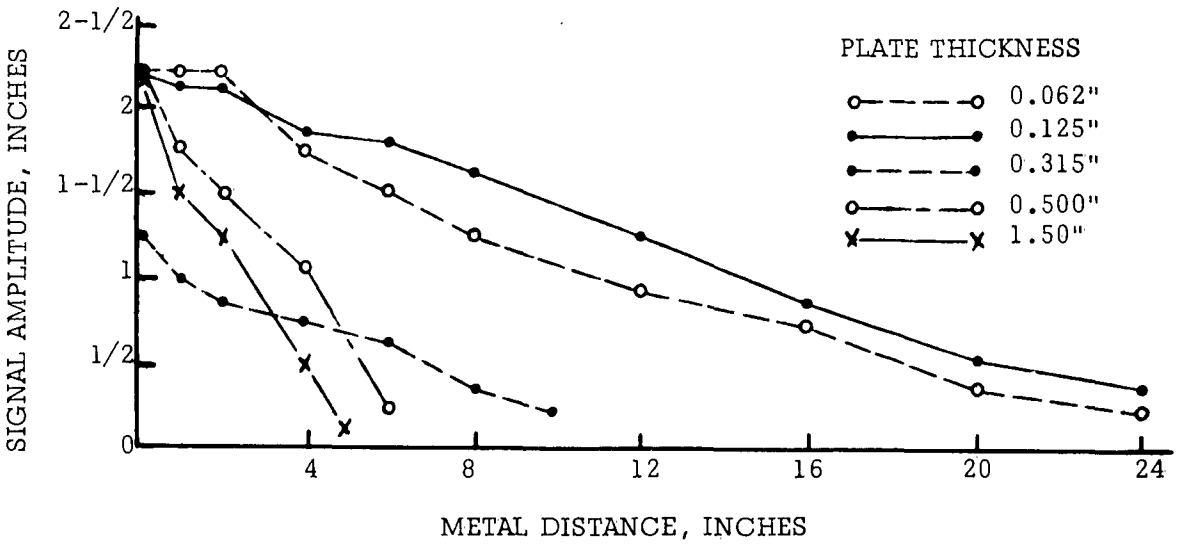

Figure 58. Signal Amplitude vs. Metal Distance, Surface (Rayleigh) Waves, 5.0 mc Contact Tests.

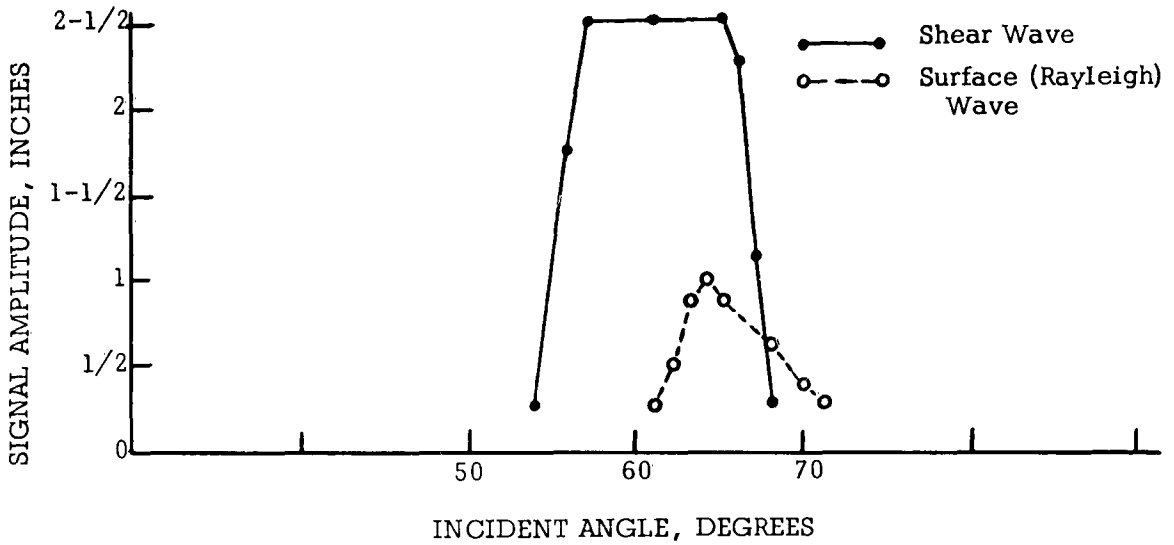

Figure 59. Signal Amplitude vs. Incident Angle Using Shear-Surface Wave Separator, 2.25 mc Contact Test.

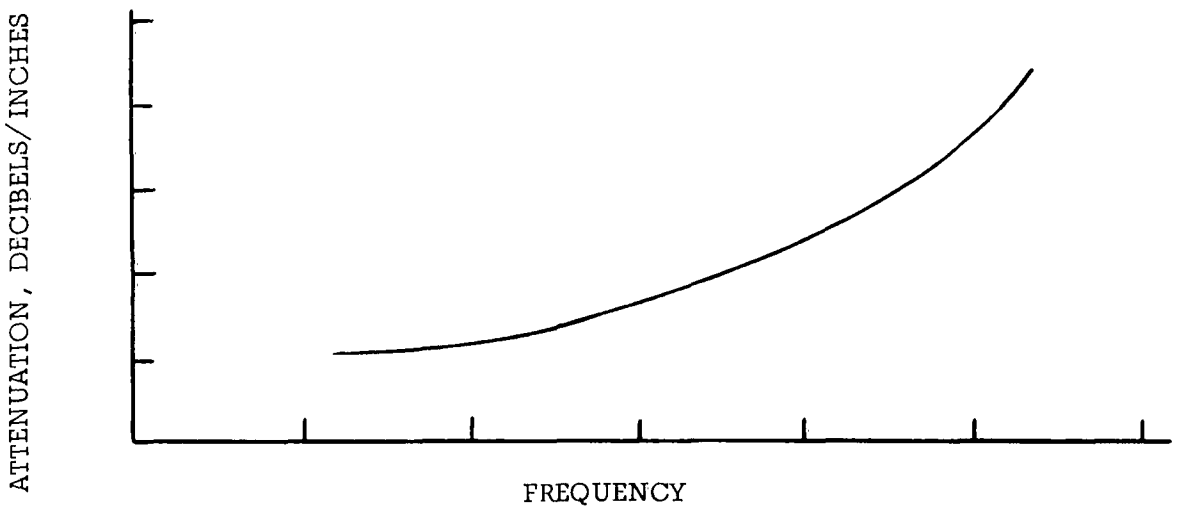

Figure 60. Typical Attenuation vs. Frequency Plot.

The signal amplitude of the surface waves observed was considerably less than that of the shear waves. However, metal travel for the surface waves was twice that for shear waves. Similar results were observed in preliminary tests at 5.0 mc also.

CONCLUSIONS

A. IMMERSED METHOD

It was shown that at the respective critical incident angles longitudinal and shear waves can be readily generated in plates over a wide range of thickness. Sufficient energy was transmitted into the plates to be useful for flaw detection where the surfaces are flat.

Reflected signals at incident angles other than those for critical shear and longitudinal waves were observed in the 0.125 and 0.062 of an inch thick plates. Several of these signals were detected using 5.0 mc. Similar signals were observed at different incident angles while testing at 2.25 mc. Velocity measurements and subsequent calculations indicated that these signals were caused by wave propagation of a compound nature, not being wholly longitudinal or shear waves. In addition, the generation of these waves seemed to be dependent upon frequency, plate thickness and incident angle. The characteristics observed indicate that Lamb waves were generated. The limited published data available did not allow complete correlation. Further, the greater part of previously published data was collected using two transducer, transmit-receive techniques.

Shear wave tests indicated that total metal travel decreases as plate thickness decreases. The greatest losses were apparently due to transmission and mode conversion of each reflection at the interface since the number of reflections for each plate thickness was generally the same. The use of larger incident angles, thus reducing the number of reflections, appears to be desirable where large metal travel distances are required.

It was found that the amplitude of reflected shear waves remained relatively constant over a wide range of angles 30°–75° in aluminum). It appears, then, that a considerable range of angles is available for inspection purposes with sufficient energy available for normal inspection. Where the incident angle can be varied, the choice of angle will depend upon the nature of the defects and experience with the particular application.

It was also observed that the amplitude of reflected shear wave signals was greater than the amplitude of longitudinal wave signals at the lower test frequencies. This was apparently due to the lower specific acoustical impedance for shear waves, (1.22×10^4 lbs/in^2-sec.), as compared to the higher value for longitudinal waves, (2.50×10^4 lbs/in^2-sec.). The attenuation encountered in this range of frequencies, 2.25 to 5.0 mc, was low and apparently not as significant as the difference due to acoustic impedance. However, at 10.0 mc the reflected shear wave signal was less than for longitudinal waves. Thus, the apparent attenuation for shear waves as compared to longitudinal waves seemed to reach a significant value in aluminum around

10.0 mc. It was expected that attenuation of shear waves in comparison to longitudinal waves at the same frequency would have increased rapidly if the frequency had been increased. Other results, using the Immersion Refractometer indicated that longitudinal and shear wave velocities remain constant regardless of incident angle.

No indications of surface (Rayleigh) waves were observed using immersed testing. As an interesting sidelight, a 2.25 mc fixed angle surface wave contact transducer was placed about 3 inches from the edge of a 1/2 inch thick aluminum plate and a reflected signal obtained from the edge of the plate. The instrument gain was adjusted so that the surface wave reflection was about 2 inches high. By immersing the edge of the plate in water the signal was made to disappear. In fact, immersion of less than 1/8 of an inch in water caused the reflected signal to disappear. Apparently, the water provided an extended medium which carried the transmitted signal away from the plate. Thus, it seems there is no need to consider surface (Rayleigh) wave propagation when using immersed testing.

B. CONTACT METHOD

In using the 5.0 mc fixed angle surface wave transducer a decrease in apparent attenuation was observed as plate thickness decreased. It appeared that this was due to some type of reinforcement of the waves by the back surface.

Additional signals at other than critical angles were observed in the thin plates, 0.062 and 0.125 of an inch thickness. Apparently, these were of a compound nature and were the same or similar to the "Lamb" waves observed using the immersion method. It seems, then, that use of these waves could be made by either contact or immersed method. The investigations completed for this report were accomplished using a single transducer, pulse-echo method thus indicating the probable usefulness of this technique for flaw detection. Previous investigations have applied two transducer, transmit-receive techniques.

The Shear-Surface Wave Separator was used to determine the effective range of incident angles required to generate shear and surface waves. It was found that the ranges overlapped to some extent. Apparently the overlapping range of angles at which shear waves and surface waves were simultaneously generated was partially due to beam spreading using the small crystal. This overlap would probably be decreased by using transducers in which the size of the crystal was 15-20 wavelengths or more. The amplitude of the reflected surface waves was considerably less than for the shear waves. Similar results were found to occur when testing flat plates. Using 10.0 mc, no indications of surface waves were observed. These limited observations indicate that surface waves, as such, have a limited usefulness at higher frequencies due to the low energy level and difficulty of generating the waves at frequencies higher than 5.0 mc.

RECOMMENDATIONS

The results of this investigation indicate the possibilities of satisfactory results using shear waves, throughout a wide range of angles. It is recommended that further

investigations be performed to determine what limitations could be expected in using shear waves for flaw detection. Quantitative values of attenuation should be obtained and evaluation of various types of standard reference blocks for use with shear waves should be made.

It is also recommended that further investigation be conducted to better establish performance criteria for Lamb waves and to evaluate the use of this type of acoustic wave energy for flaw detection.

APPENDIX I

CALIBRATION OF MASTER CONTROL TEST BLOCKS

Figures 61 through 63 show the Distance-Signal Amplitude curves obtained from the control blocks used in Sections I and II. The test frequency was 5.0 mc. The curves obtained at 2.25 mc were identical to those shown in Appendix III of WADC Technical Report 59-466.

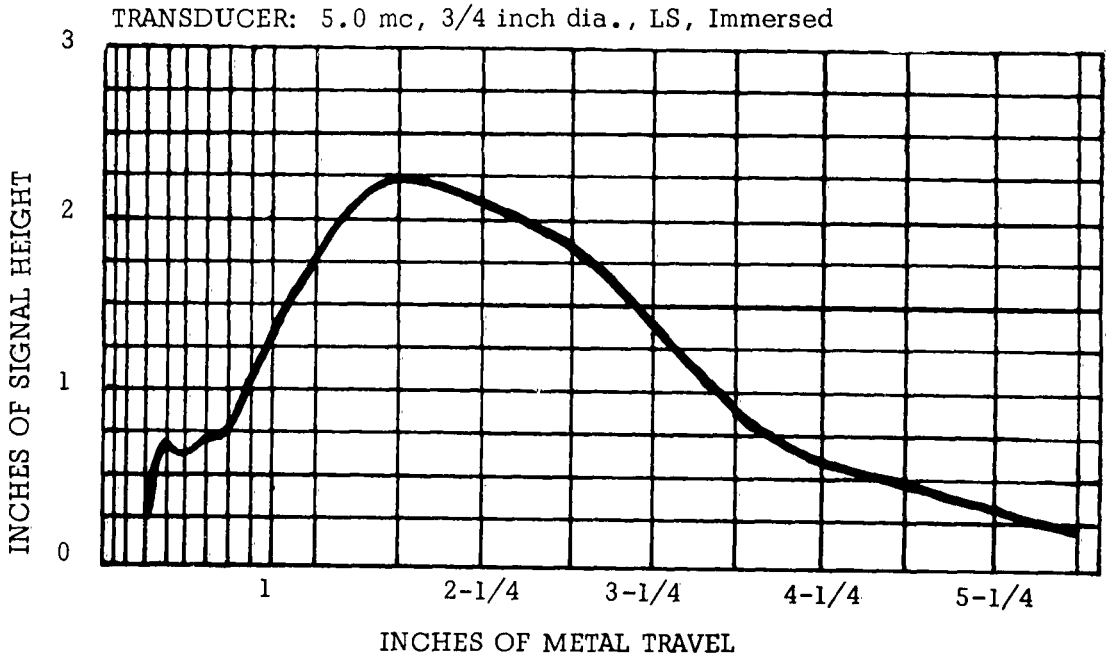

Figure 61. Calibration Curve for Group I Master Control Set - 4130N Steel.

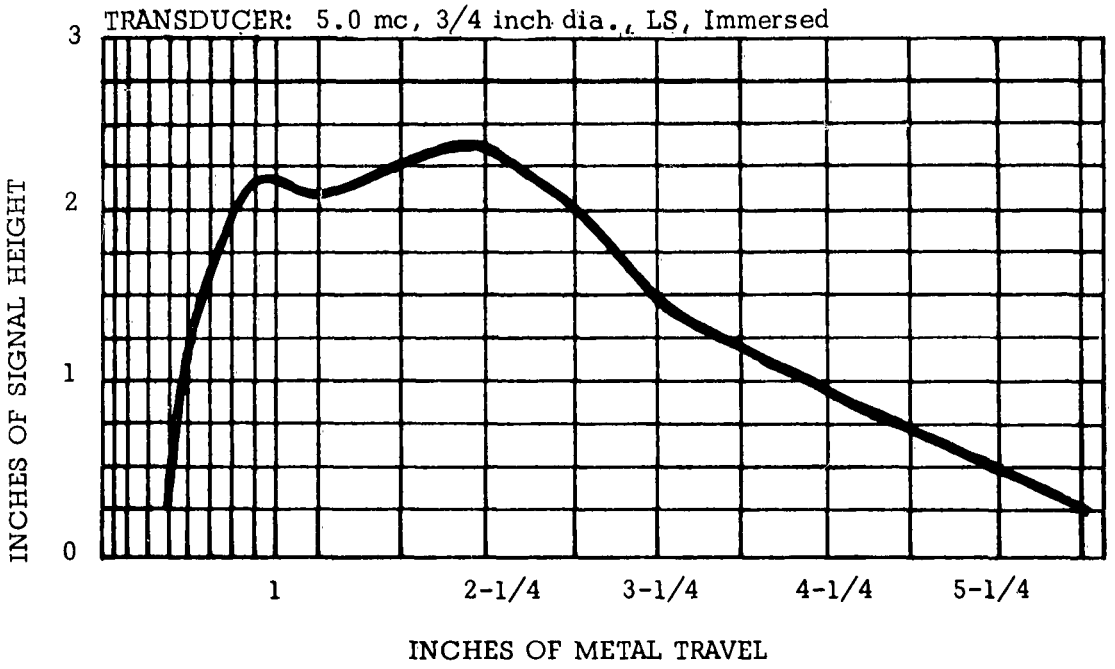

Figure 62. Calibration Curve for Group II. Master Control Set - Ti-100A Titanium.

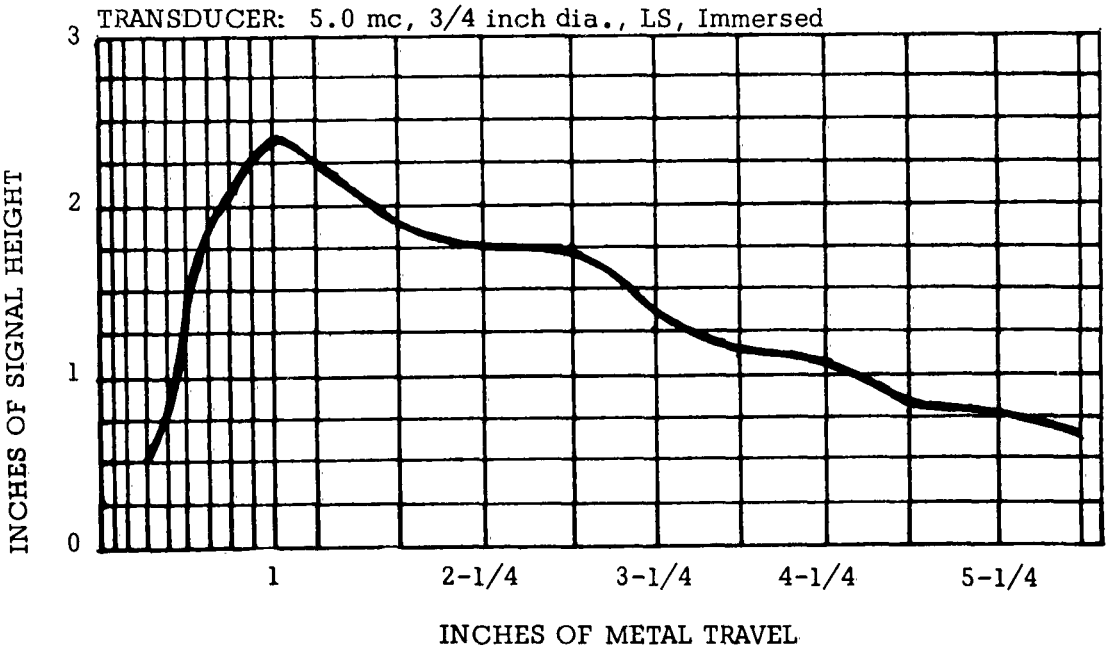

Figure 63. Calibration Curve for Group III. Master Control Set - 7075-T6 Aluminum.

APPENDIX II

METALLURGICAL DATA

Materials listed in Table 2, which were evaluated in the heat treated conditions, were heat treated in accordance with applicable Government specifications or if non-existent, the latest available manufacturer's recommended procedures. The heat treatment of each material was as follows:

INCONEL X - ANNEALED

Heat Treatment:	1625° ±25°F for 24 hours Air cooled Aged at 1300° ±25° for 20 hours Air cooled

VASCOJET 1000 - ANNEALED

Heat treatment:	Preheated at 1450°F for 30 minutes Heated to 1850° ±25°F for 1-3/4 hours Air cooled Triple tempered at 1000°F for 2 hours

B120VCA - ANNEALED

Heat treatment:	Aged at 900°F for 48 hours

Photomicrographs of materials tested for this report but not included in this section are shown in WADC Technical Report 59-466.

TABLE 25

MECHANICAL PROPERTIES					
MATERIAL AND CONDITION	YIELD STRENGTH psi	ULTIMATE STRENGTH psi	ELONGATION PERCENT	RA PERCENT	HARDNESS
Aluminum					
7075-T6 Forging #1	64,480	74,480	9.7		Rb 90-92
7075-T6 Forging #2	64,820	76,620	9.7		Rb 89-92
7075-T6 Rolled Bar #1	73,080	80,900	16.2		Rb 88-90
7075-T6 Rolled Bar #2	85,730	93,330	10.0		Rb 91-93
4130 Steel					
Normalized	53,550	89,550	27.1	63.7	Rc 8-11
Vascojet 1000 Forging					
Annealed	49,580	92,720	25.7	55.9	Rc 16-18
Heat Treated	253,780	313,050	6.2	9.6	Rc 54-55
Vascojet 1000 Bar					
Annealed	48,620	92,730	31.0	68.5	Rc 9-12
Heat Treated	235,870	309,650	6.6	18.7	Rc 53-55
17-4 PH Stainless					
Annealed	157,000	158,050	12.0	69.3	Rc 34-36
Inconel X Bar					
Annealed	120,980	170,430	24.7	37.7	Rc 38-41
Heat Treated	121,600	176,350	21.3	32.6	Rc 40-42
Inconel X Forging					
Annealed	83,500	149,000	27.0	39.3	Rc 29-31
Heat Treated	108,850	173,270	19.8	19.9	Rc 35-36
120 Titanium Forging					
Annealed	135,430	141,680	8.7	19.7	Rc 42-45
Heat Treated	156,400	200,000	2.1	2.4	Rc 49-50
120 Titanium Bar					
Annealed	125,430	129,700	19.7	40.6	Rc 34-36
Heat Treated	145,000	192,300	3.7	8.3	Rc 46-48
Molybdenum Bar	83,380	86,970	17.3	25.8	

NOTE: Hardness values are the high and low reading from each set of blocks
All other values are average of three tests.

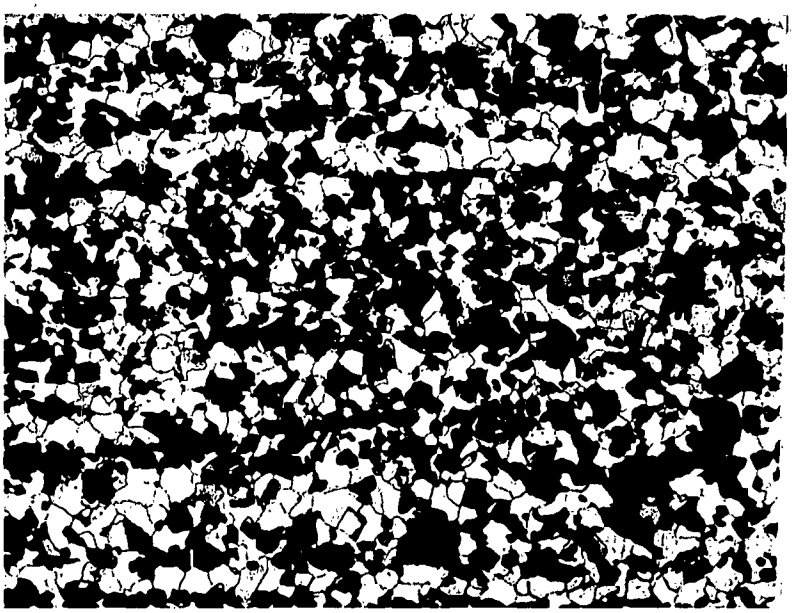

Figure 64. Photomicrograph, 4130 Steel (Normalized), Longitudinal Section, 150X.

Figure 65. Photomicrograph, C.P. Molybdenum, Longitudinal Section, 250X.

A. Rolled Bar

B. Forged Bar

Figure 66. Photomicrographs, Vascojet 1000, Longitudinal Sections, 250X.

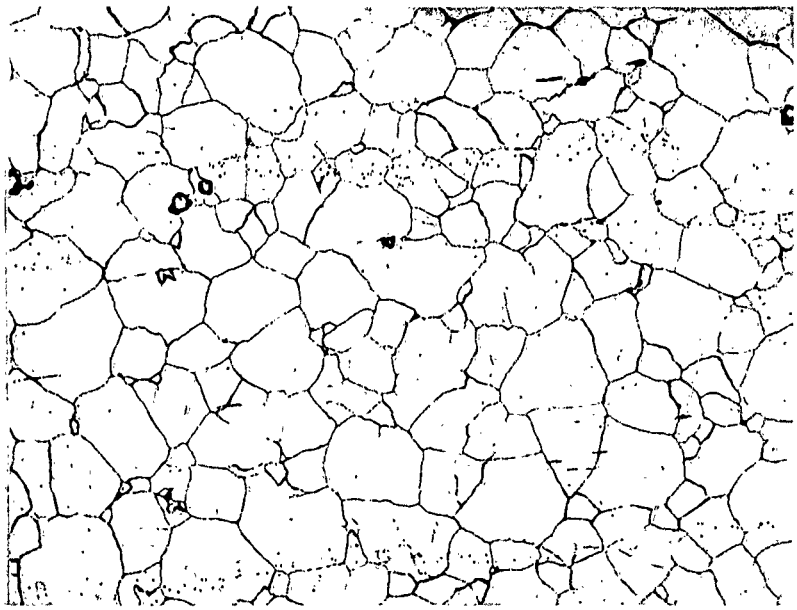

A. Rolled Bar

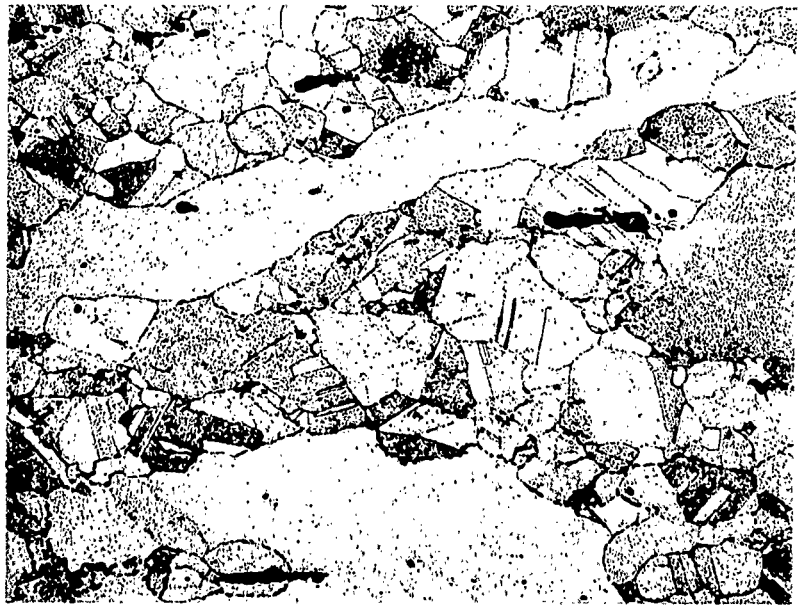

B. Forged Bar

Figure 67. Photomicrographs, Inconel X, Longitudinal Sections, 250X.

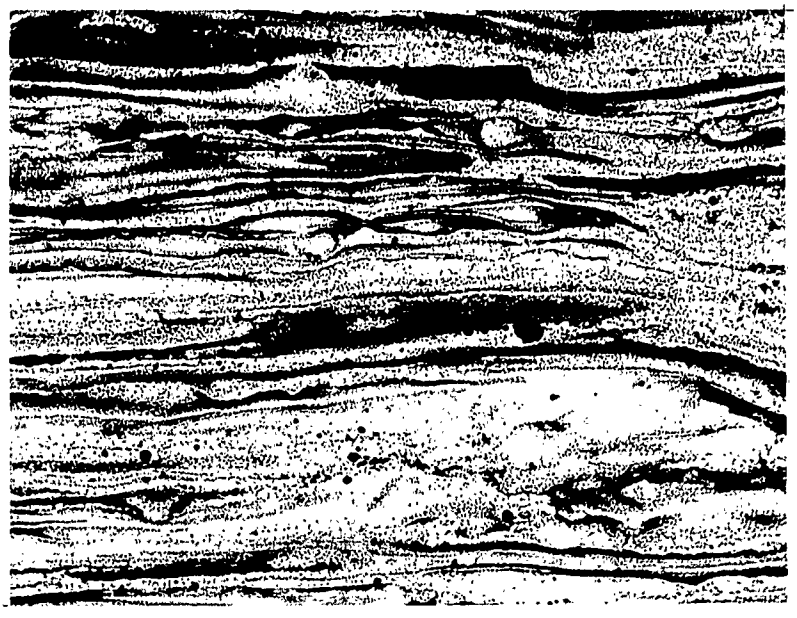

Figure 68. Photomicrograph , ZK-60 Magnesium, Longitudinal Section, 150X.

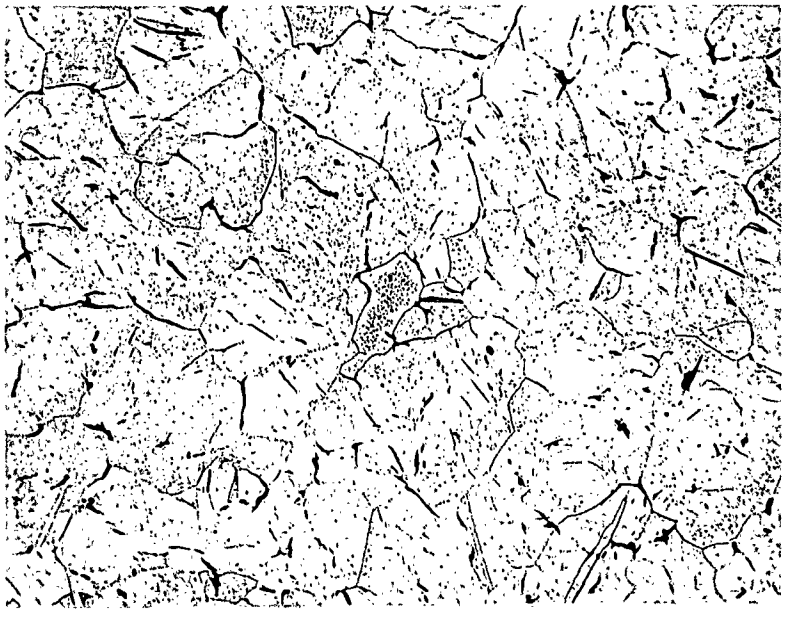

Figure 69. Photomicrograph , Ti-100A Titanium, Rolled Bar, Longitudinal Section, 250X.

A. Rolled Bar

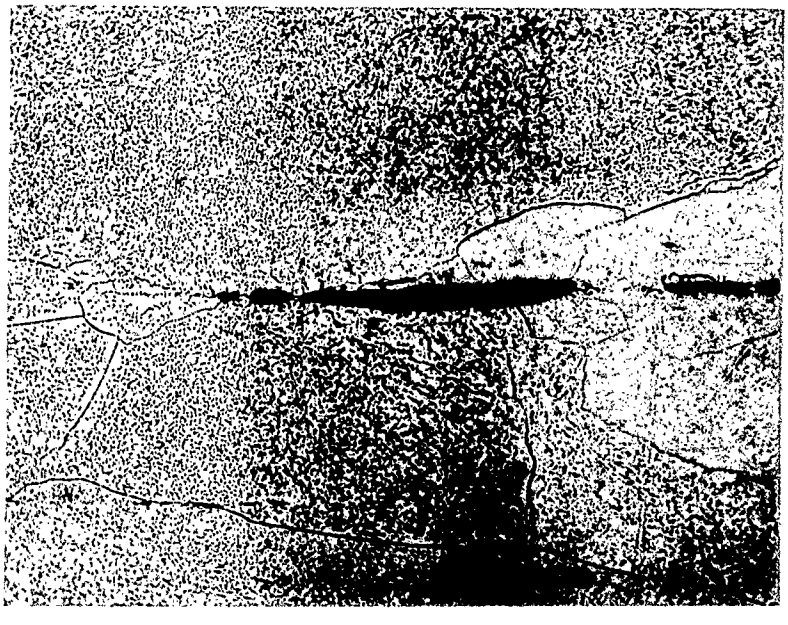

B. Forged Bar

Figure 70. Photomicrographs, B120 VCA Titanium, Longitudinal Sections, 250X.

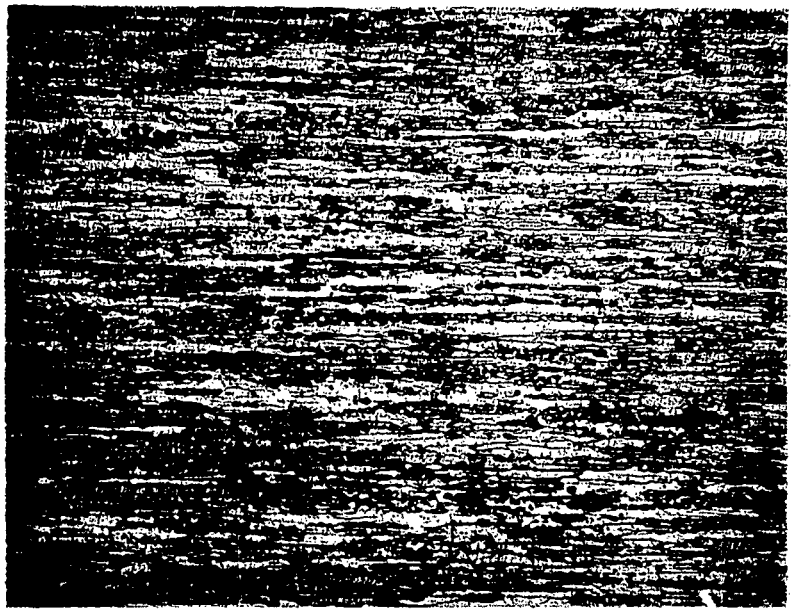

A. Forging #1

B. Forging #2

Figure 71. Photomicrographs, 7075-T6 Aluminum, Longitudinal Sections, 150X.

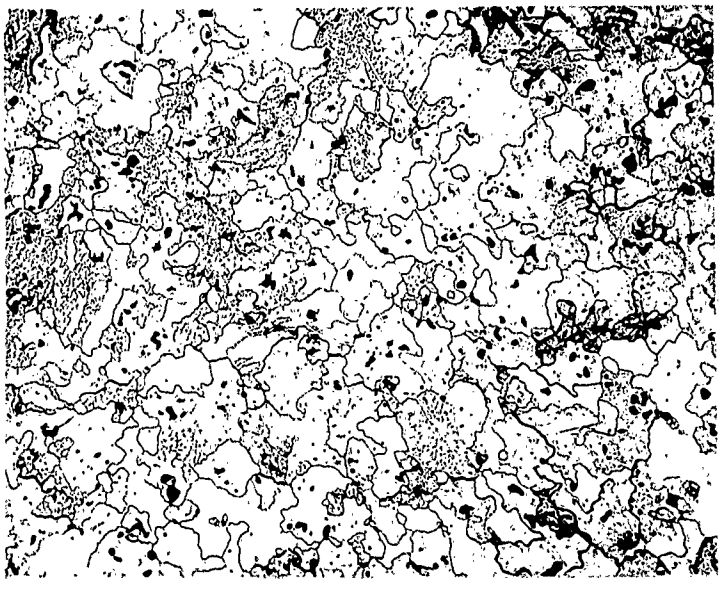

A. Tranverse Section

B. Longitudinal Section

Figure 72. Photomicrographs, 7075-T6 Aluminum, Rolled Bar #1, 150X.

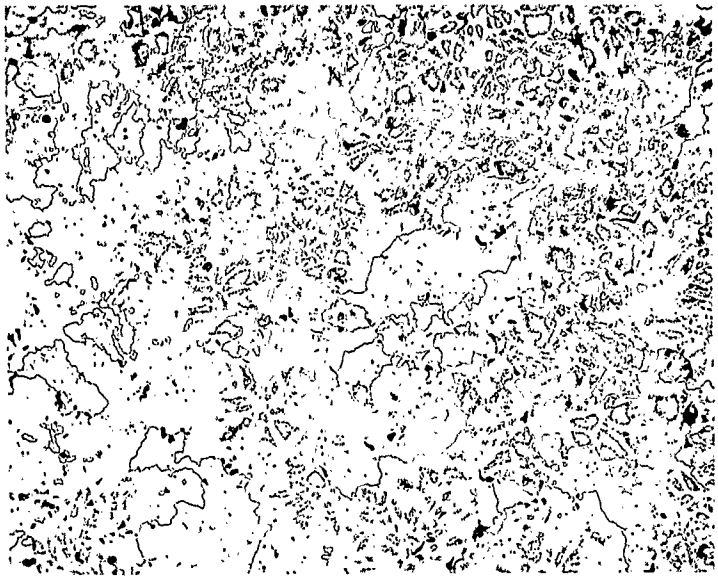

A. Transverse Section

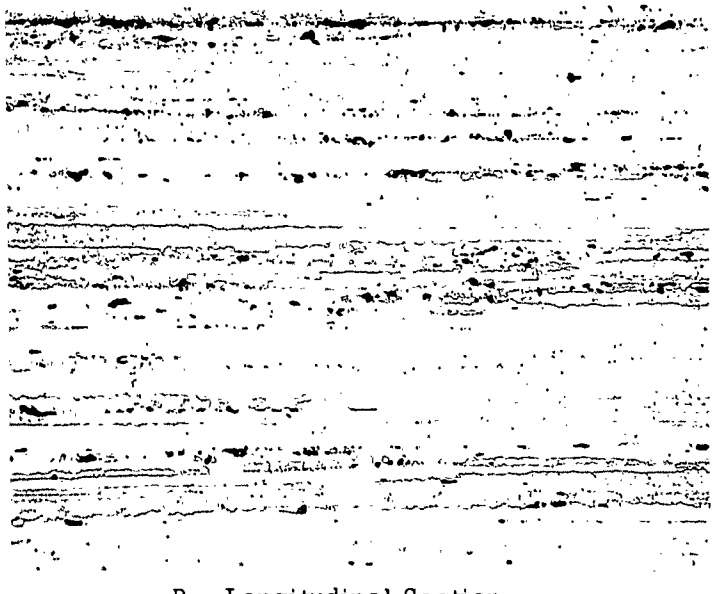

B. Longitudinal Section

Figure 73. Photomicrographs, 7075-T6 Aluminum, Rolled Bar #2, 150X.

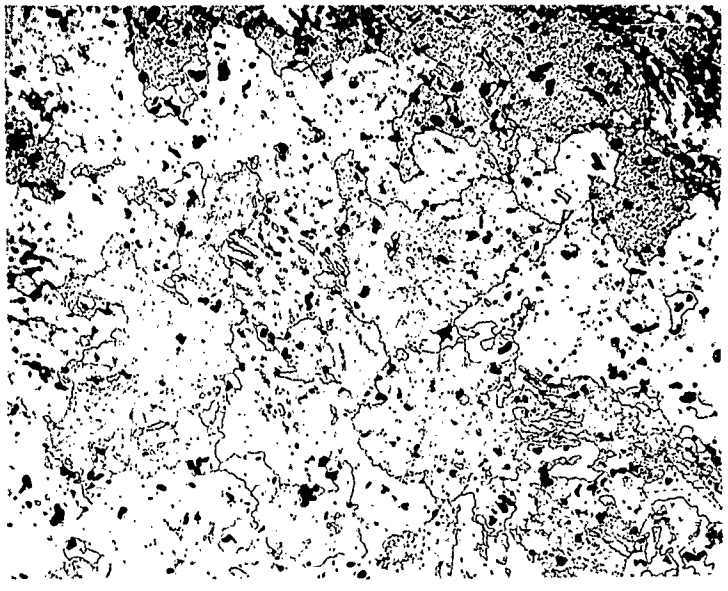

A. Transverse Section

B. Longitudinal Section

Figure 74. Photomicrographs, 7075-T6 Aluminum, Rolled Bar Control Set, 150X, Specimen #1.

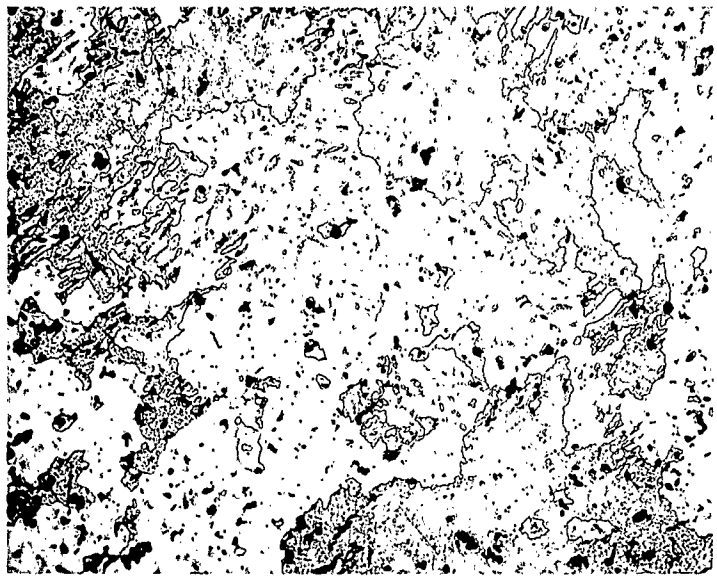

A. Transverse Section

B. Longitudinal Section

Figure 75. Photomicrographs, 7075-T6 Aluminum, Rolled Bar Control Set, 150X, Specimen #2.

APPENDIX III

MEASUREMENT OF ACOUSTICAL PROPERTIES

The methods and techniques used to measure acoustic impedance and attenuation for this report are discussed in the following paragraphs.

By using these methods, measurements of acoustical properties can be related to one another or to theoretical values. Thus, predictions of test results can be made and test efforts more effectively directed.

A brief analysis of impedance and attenuation factors is also included. This analysis presents methods for expressing acoustical energy losses in terms of decibels.

ANALYSIS OF IMPEDANCE AND ATTENUATION

The acoustic impedance of a material determines the amount of sonic energy transmitted and reflected at interfaces between the material and some other given medium. Attenuation, in the broad sense, describes the energy losses within the material. Attenuation will be discussed first.

A more limited definition of acoustic attenuation refers to only those losses brought about by energy conversion. Scattering, beam spread, and certain diffraction effects which appear as energy losses are, in more rigorous discussions, considered separately. In an extended homogeneous medium the losses due to scattering and beam spread occur as a linear decay of the instantaneous amplitude. Losses due to diffraction are considerably more complex. However, Seki, Granato, and Truell give as a rough approximation of the diffraction loss from a circular crystal, one decibel per a^2/λ, where "a" is the radius and "λ" the wavelength. This loss approximation is applicable to the exponential portion of the curve, i.e., beyond the region of Fresnel diffraction (a distance from the source of approximately a^2/λ). It appears then that for the purpose of this investigation, the decibel loss within the material can be considered collectively beyond the Fresnel region.

Let the curve in Sketch A be the amplitude response curve for a given homogeneous medium where the following nomenclature applies:

A = Instantaneous amplitude at X
X = Distance
α = Amplitude decay coefficient/unit length.

If A is attenuated by a factor of α in a distance "dx", then the change in amplitude is:

$$dA = -\alpha A\,dx$$

$$\int_1^2 \frac{dA}{A} = -\alpha \int_1^2 dx$$

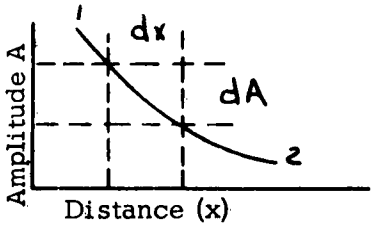

SKETCH A

$$\log_e \frac{A_2}{A_1} = -\alpha (x_2 - x_1)$$

$$\frac{A_2}{A_1} = e^{-\alpha l}$$

where:

$l = X_2 - X_1$ = distance between A_1 and A_2

A_2/A_1 = amplitude ratio between points 1 and 2

e = natural log base

and α = Nepers/unit length.

Since the corresponding intensity "I" is proportional to the square of the amplitude, the intensity ratio is expressed as:

$$\frac{I_2}{I_1} = e^{-2\alpha l}$$

If α is expressed in decibels (one Neper = 8.686 decibels), then:

$$\frac{A_2}{A_1} = e^{-\frac{\alpha l}{8.686}} \quad ; \quad \frac{I_2}{I_1} = e^{-\frac{2\alpha l}{8.686}}$$

The above equations describe the intensity and amplitude relationships for two points within the medium. If energy is transmitted between two or more media then the acoustic impedances of the materials must be considered. The following equations describe the relationships between transmitted and reflected intensities and amplitudes of a beam at normal incidence.

$$R = \frac{I_R}{I_0} = \left(\frac{Z_2 - Z_1}{Z_2 + Z_1}\right)^2 = \left(\frac{r-1}{r+1}\right)^2 = \left(\frac{A_R}{A_0}\right)^2$$

$$T = \frac{I_T}{I_0} = \frac{4Z_2Z_1}{(Z_2 + Z_1)^2} = \frac{4r}{(r+1)^2} = \left(\frac{A_T}{A_0}\right)^2$$

$$R + T = 1$$

where:

R = reflection coefficient

T = transmission coefficient

Z_1, Z_2 = the respective impedances $\rho_1 V_1$ and $\rho_2 V_2$

$r = Z_2/Z_1$

I_R = reflected beam intensity

I_T = transmitted beam intensity

I_o = incident beam intensity

A = amplitude (with the same sub designations as "I")

Taking into account the attenuation losses and impedance effects as described above, an expression can be derived for the amplitude of the n-th back echo in pulse-echo immersion testing.

Consider a sample of "L" thickness immersed in a coupling solution as shown in Sketch B.

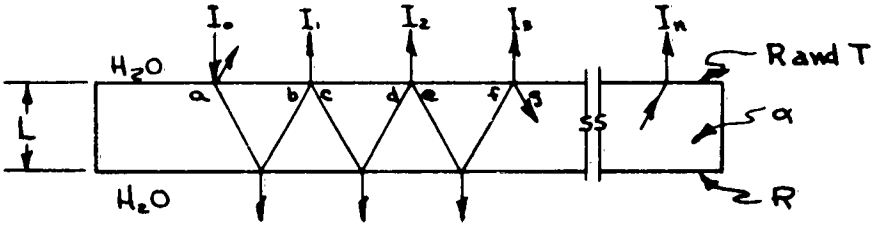

SKETCH B

The intensities at the various points are:

$$I_a = I_o T$$

$$I_b = I_o T R e^{-2\alpha(2L)}$$

$$I_1 = I_o T^2 R e^{-2\alpha(2L)}$$

$$I_c = I_o T R^2 e^{-2\alpha(2L)}$$

$$I_d = I_o T R^3 e^{-2\alpha(4L)}$$

$$I_2 = I_o T^2 R^3 e^{-2\alpha(4L)}$$

$$I_3 = I_o T^2 R^5 e^{-2\alpha(4L)}$$

$$I_n = I_o T^2 R^{(2n-1)} e^{-2\alpha(2nL)}$$

The corresponding amplitude ratio is:

$$\frac{A_n}{A_o} = \left(\frac{I_n}{I_o}\right)^{1/2} = T R^{(n-0.5)} e^{-2n\alpha L}$$

If α is expressed in decibels, then:

$$A_n = A_o T R^{(n-0.5)} e^{-2n\alpha L/8.686} = A_o T R^{(n-0.5)} e^{-0.23 nL\alpha}$$

The above amplitude ratio is sometimes more convenient when expressed in decibels, where the decibel difference between A_n and A_o is:

$$20 \log_{10}\left(\frac{A_n}{A_o}\right)$$

The equation may therefore be written as:

$$20 \log_{10} \frac{A_n}{A_o} = 20 \log_{10} T + 20 \log_{10} R^{(n-0.5)} + 20 \log_{10} e^{-0.23 nL\alpha}$$

$$20 \log_{10} \frac{A_n}{A_o} = -20 \log_{10} \frac{1}{T} - 20 \log_{10} R^{-(n-0.5)} - 20 \log_{10} e^{0.23 nL\alpha}$$

where the terms of the expression represent the various losses, expressed in decibels, contributed by R, T, and α. If these losses are now taken as positive, and we let:

$$T_d = 10 \log_{10} \frac{1}{T}$$

$$R_d = 10 \log_{10} \frac{1}{R}$$

where T_d and R_d are the respective transmission and reflection coefficients expressed in decibels, then:

$$20 \log_{10} \frac{A_n}{A_o} = 2T_d + (2n-1) R_d + 20(0.23 nL\alpha) \log_{10} e$$

$$20 \log_{10} \frac{A_n}{A_o} = 2T_d + (2n-1) R_d + 2 nL\alpha$$

When plotting decibels lost versus round trips through the sample, the function is a straight line on rectangular coordinates with a slope of:

$$2 R_d + 2 L\alpha$$

If the back interface is air (total reflection) then the slope is:

$$R_d + 2L\alpha$$

ATTENTUATION MEASUREMENTS

By using a calibrated attenuator in combination with a single transducer and either a pulse-echo instrument or the Attenuation Comparator several methods were available for making measurements of the ultrasonic attenuation by immersed techniques.

The Attenuation Comparator also operates on the pulse-echo principle, however, it has additional functions built-in. Direct measurements of time delay can be made between indications on the A-Scan trace. An exponential decay curve can be made to fit the decay pattern of multiple reflections from the test sample. The dial settings required to obtain the proper shape of the exponential curve are used to find the attenuation from calibration curves supplied with the instrument.

Three methods for ultrasonic attenuation measurement are listed below. Using conventional pulse-echo test equipment and a calibrated attenuator the first two methods were used. However, all three methods were employed at various times when using the Attenuation Comparator. Thus, results obtained by one method were confirmed using a different method and/or test instrument. The basic test configuration is shown in Figure 76.

A. FRONT SURFACE TO FIRST BACK ECHO METHOD

1. The sample was placed in the buffer tank with one face submerged in distilled water at room temperature. See Figure 16. The sample was then normalized to the path of sound beam.

2. The instrument gain was adjusted so that the amplitude of the first back surface was 1.5 inches in height.

3. Known signal losses were then inserted into the receiver circuit using the attenuator until the height of the front surface echo was decreased to the 1.5 inch reference height selected for the first back surface echo. The attenuator reading was then recorded. The value obtained represented the water/metal impedance loss plus

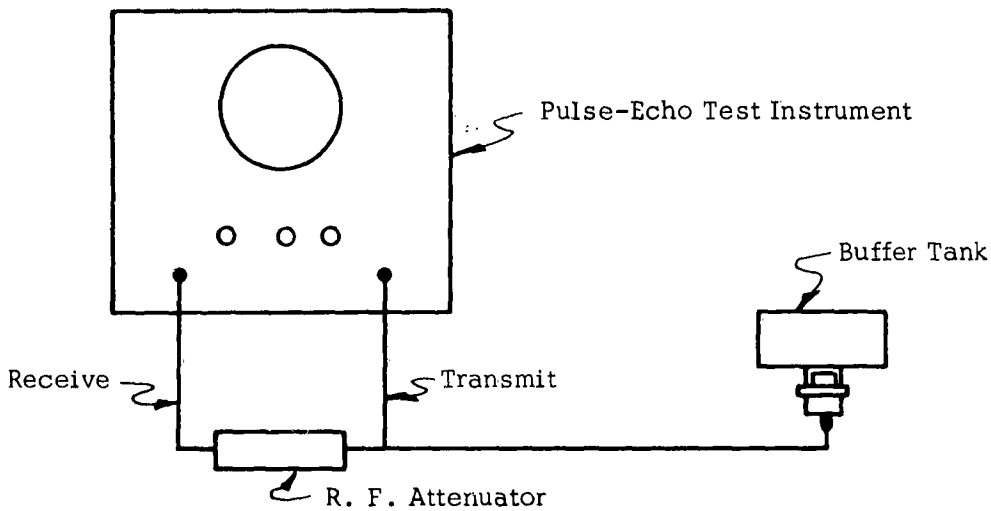

Figure 76. Basic Test Equipment Configuration for Impedance and Attenuation Measurements.

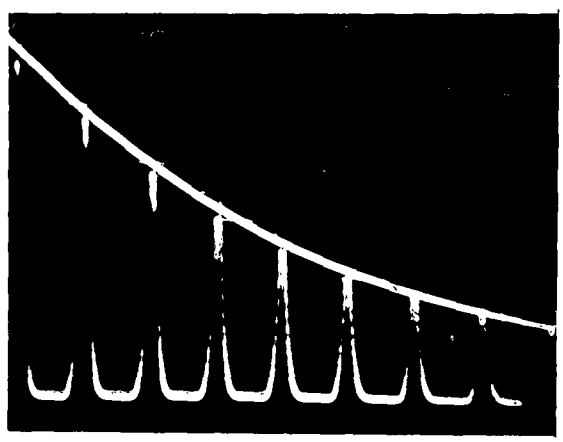

Figure 77. Photograph of Typical Waveform Pattern Obtained Using the Attenuation Comparator.

the attenuation losses for one round trip in the sample. By subtracting the theoretical impedance loss and dividing by the sample length, a value for the attenuation per unit length was obtained. Measurements of impedance losses using the Attenuation Comparator generally indicated good agreement with calculated impedance losses.

B. SUCCESSIVE BACK ECHOES METHOD

1. The sample was placed in the buffer tank and normalized with respect to the sound path. Only one face was submerged.

2. The amplitude of the third or later back echo was adjusted to a height of 1.5 inches on the oscilloscope screen.

3. Known signal losses were then inserted into the receiver circuit until the second back surface echo was decreased to the 1.5 inch reference line. This attenuation reading was recorded and then divided by the number of back echoes. After correcting for the reflection coefficient loss (R_d), the attenuation per round trip and attenuation per unit length were calculated.

   This method was restructed to the shorter test blocks on most materials since an insufficient number of back echoes was obtained for a representative average on the longer blocks.

C. ATTENUATION COMPARATOR METHOD

1. The test sample was placed in the buffer tank with one face submerged and normalized with respect to the sound path. The receiver frequency and transmitted pulse were tuned for maximum amplitude of back surface reflections.

2. Using the exponential waveform of the instrument, the leading edge of the waveform was positioned slightly to the left of the third back surface echo which was set to approximately 3 inches amplitude.

3. The shape of the waveform was then adjusted by means of the "Exponential" and "Range" controls so that it was aligned with the peaks of the train of back echoes.

The "Exponential" and "Range" dial readings were recorded. Figure 77 shows a typical waveform.

4. Steps 1-3 above were repeated with both faces of the specimen submerged.

5. The dial readings were converted to attenuation/microsecond using the Exponential Comparator calibration curve. Then, by taking the difference between the attenuation value with both faces of the specimen submerged and the value obtained with only one face submerged, "R_d" was found. By subtracting "R_d" from the value obtained with only one face submerged, the attenutation per microsecond was found. Then attenuation per unit length was calculated by dividing the sonic velocity of the test specimen into the attenua- per microsecond.

Attenuation measurements using the Attenuation Comparator were limited to test blocks no longer than two inches in most cases. The time delay generator could not accommodate enough of the back echo train on long blocks to effectively use the exponential waveform. Additional attenuation values were obtained by contact testing methods using the exponential waveform on the Attenuation Comparator. The only difference in technique was that the crystal was placed directly on the test samples.

The values obtained by all three methods represent the apparent attenuation in the specimens and include losses due to beam spreading and diffraction effects.

SONIC VELOCITY MEASUREMENTS

A. ATTENUATION COMPARATOR METHOD

It was possible to measure the velocity with an accuracy of approximately 1% by using the Attenuation Comparator instrument and proceeding as follows:

1. A specially machined sample of each material, retaining parallelness of the sample surfaces to ±0.0001 inches per inch, was placed in the small water buffer tank with one face submerged in distilled water at room temperature.

2. The specimen was rotated on the centering platform until the train of back echoes reached a maximum amplitude.

3. By adjusting the centering screws the bottom surface of the sample was normalized with respect to the sound path from the transducer. This was indicated on the oscilloscope when the front surface echo reached a maximum height while

the gain setting was at a minimum. Figure 77 illustrates the type of echo pattern observed with the gain adjusted to a normal operating level.

4. An exponential range was selected where the envelope of the generated waveform was similar to the exponential pattern created by the back echo train.

5. The leading edge of the exponential waveform was matched to the top peaks of successive back echoes and the time delay position recorded for each echo. The gain of the receiver was increased so that each echo had the same amplitude when matched to the leading edge of the exponential waveform.

6. After the round trip time for each echo in Step 5 was obtained, the velocity was found by measuring the sample thickness and using the following formula:

$$V = \frac{2d}{t}$$

where:

t = round trip time in microseconds

d = thickness in inches

V = sonic velocity in inches/microsecond.

B. TWO-TRANSDUCER, WATER COMPARISON METHOD

In order to study velocity characteristics of various wave propagated in plates a two transducer, water comparison method was devised. This method makes use of standard commercial testing equipment without resorting to special or additional equipment. See Figure 78.

A reference groove in the test panel is required to use this method. The groove is machined a known distance away from and parallel to one edge of the plate. The depth of the groove need only be sufficient to reflect an easily observed signal, e.g., 0.005 of an inch.

Say, for instance, a surface (Rayleigh) wave is propagated normal to the groove and the associated parallel edge. The reflected signals observed on the A-Scan trace would be (1) the signal reflected by the groove, and (2) the signal reflected from the edge of the plate.

A second immersed transducer is then coupled to the test instrument using a "T" coupling which enables the use of both transducers simultaneously. Then, manipulate

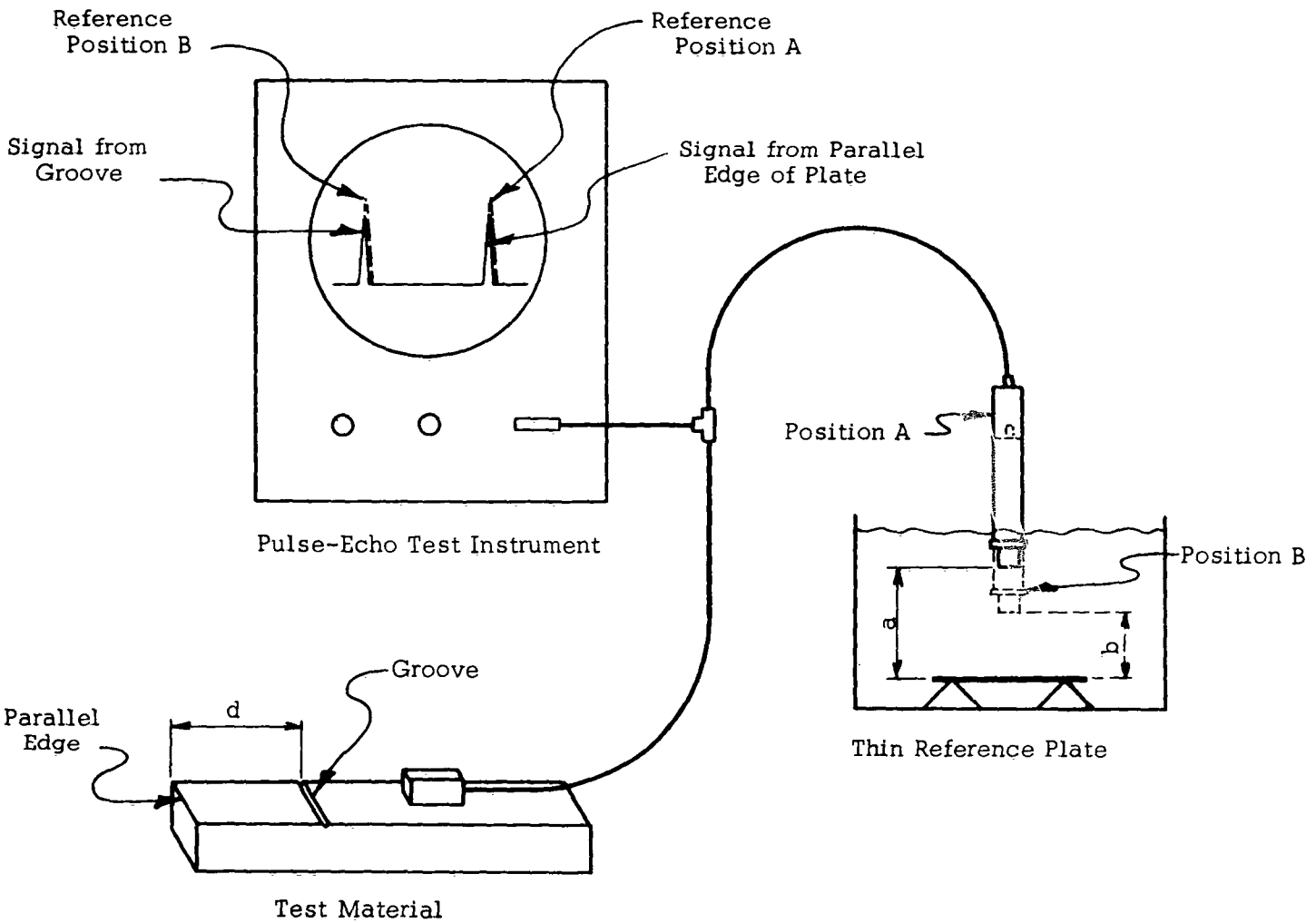

Figure 78. Typical Test Equipment Configuration for Two Transducer, Water Comparison Velocity Measurement.

the second transducer so that a maximum reflected signal is obtained from a very thin plate (less than 0.010" thick). Adjust the water distance to cause this signal to coincide with the signal from the edge of the test plate and measure the water travel from the face of the transducer to the thin plate. After noting this dimension, decrease the water distance until the reference signal coincides with the signal from the groove in the test plate and again measure the water distance. The difference in the two measurements is the water equivalent of the propagated wave in the plate.

With the metal distance from the groove to the edge of the plate known and the velocity of sound in water known, the velocity or speed being observed may be calculated using the following equation:

$$V = \frac{d}{a-b} \times V_w$$

where:

V = unknown velocity, inches/sec (or cm/sec)

V_w = velocity of sound in water, 0.213×10^5 inches/sec (or 1.49×10^5 cm/sec)

d = metal distance from groove to edge of plate, inches (or cm)

and $a-b$ = difference in water travel of Position A to Position B, inches (or cm)

All dimensional units must be consistent.

This same technique, of course, may be applied to any velocity measurement where two separate signals are obtained from the test part and the metal distance between the two reflecting surfaces is known.

APPENDIX IV

ULTRASONIC C-SCAN FACSIMILE RECORDING

Considerable use was made of C-Scan recording techniques in compiling data for this report. However, no basic explanation of the operation of recording systems was presented. It seemed appropriate to include a description of the method at this point.

The Recording System consists of a basic pulse-echo test instrument, a recording instrument, a facsimile paper recorder and mechanical drives and controls. A basic system is shown in Figure 79.

The mechanical apparatus in a normal X-Y scanning system is comprised of a (1) carriage with a transducer mount, and (2) a bridge. The carriage scans with an oscillating motion in the X-direction. After each pass across the part by the carriage and transducer the bridge indexes one step in the Y-direction. The path scanned by the transducer is then as shown below.

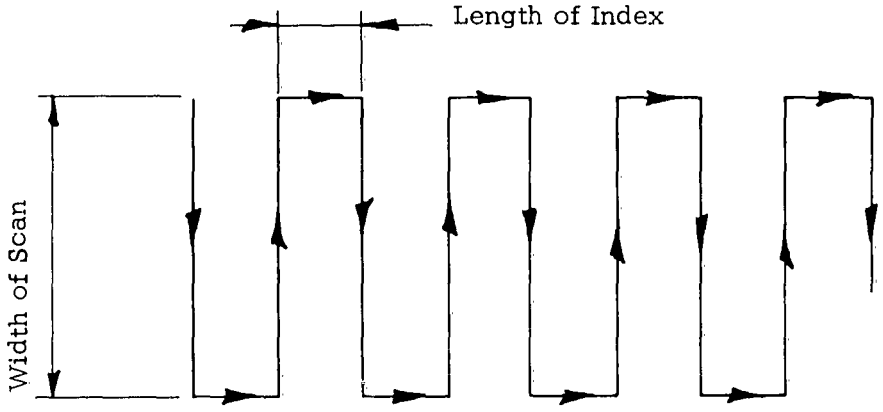

Sketch of Scanning Pattern.

The width of scan is normally controlled with limit switches which are adjustable in position, thus compensating for different dimensions of parts. For full size recordings (1:1 scale), the maximum width of scan is limited by the paper recorder. The usual size is 19 inches wide. Occasionally narrower widths are used on special applications. Parts wider than 19 inches are recorded by making two or more recording runs to include the complete area. The total length being limited by the tank length.

Generally, the length of index is also variable. This variation makes possible the "overlooking" of insignificant or minor discontinuities while still performing

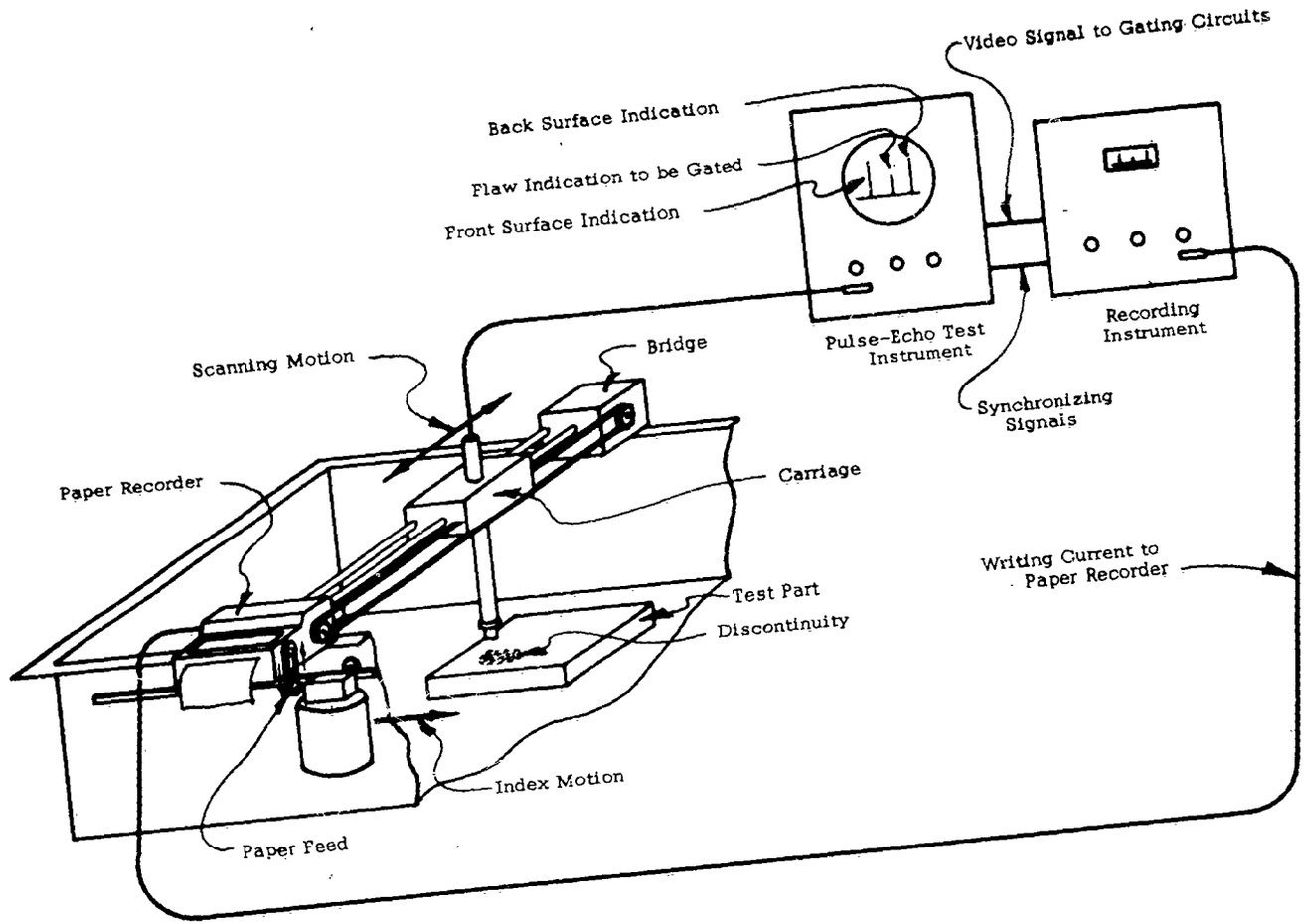

Figure 79. Basic C-Scan Facsimile Recording System

thorough inspection for more critical areas. Also, the time for complete scanning is coincidently reduced. Conversely, very high sensitivity and resolution can be achieved using 15 or 20 mc focused transducers with a short length of index.

The paper feed on the facsimile paper recorder is coupled directly to the indexing motion of the bridge while the recording drum is directly coupled to the scanning motion of the carriage. A helix wire is mounted on the drum so that as the drum oscillates the wire contacts the paper at a point corresponding directly to the position of the carriage.

By observing the scanning pattern it may be seen that if at the instant a reflected signal from a discontinuity was observed a recording device were made to record the signal in a corresponding area on paper, successive scans would outline the area, providing a permanent record of the area. This process is what does occur.

The "writing" action takes place when a current is passed through the paper between the helix wire and a stationary blade directly over the paper. A plating process takes place and appears on the sensitized paper as a darkened area. The "writing" signal is supplied to the paper recorder by a recording instrument which in turn received the original signal from the pulse-echo test instrument. The recording instrument and the pulse-echo instrument are synchronized by signals from the pulse-echo instrument.

Normally, there are several signals which appear on the A-Scan trace. The function of the recording instrument is to select the signal(s) which are to be recorded and supply the "writing" impulse to the paper recorder. The selection of the desired signal(s) is accomplished by a gating circuit which "listens" for some duration of time and allows signals which are received during that time to pass through the "gate" for additional processing. Usually, the gate circuit is triggered (or "opened") by the reflected signal from the front surface of the test part. Circuit design techniques permit a delay before the "opening" of the gate which may be controlled as desired. Recent advances have resulted in a gate that can be made to "open" before the front surface signal. The advantage being that in very thin materials where only a slight change in reflected signal is detected the gate can then operate directly adjacent to the front surface rather than at the usual minimum delay which may represent 1/16 to 1/8 of an inch of material.

The gate duration is also variable so that only particular zones of interest are recorded. For example, the bond line of two brazed or cemented layers might be the only area of interest, or it may be desired to record the entire volume between the front and back surface of several plates which have different thicknesses. These various areas may readily be recorded with proper adjustment of the gate delay and duration (length) controls.

The signals to be recorded pass through the gate to an amplifier section. In this area of the recording instrument further selection of the signals occur. Two controls accomplish this selection, (1) the level setting, and (2) the contrast. The level setting makes possible the selection of signals which have an amplitude greater than some predetermined level. Say, for instance, that it is desired to

record signals from 8/64" flaws while 5/64" or smaller flaws are not to be recorded. The level setting is then adjusted so that a signal with amplitude equivalent to an 8/64" flat bottom hole will cause writing current to flow through the paper recorder. When the adjustment is correctly set reflected signals equivalent to a 5/64" flat bottom hole will not cause writing current to flow. Thus, the level setting establishes the minimum signal amplitude which will be recorded.

The contrast control is used to expand a small change in signal amplitude. If, for example, a thin plate is inspected directly for laminar defects probably only a small change in signal will occur. This small change in signal amplitude must be expanded so that writing current can be made to flow when the signal change does occur. The contrast control enables the expansion of the signal and makes possible the recording of many additional configurations which could not be recorded otherwise.

The final step is for the signal to be converted from the high frequency pulse to a DC pulse which is applied to the facsimile recorder as writing current. Normal settings on the recording instrument will provide writing current to the paper recorder with potentials ranging from 5 to 30 volts. The 5 volt writing signal appears as very faint gray or brown against the white paper background. The 30 volt writing signals appear as black areas on the paper. Gated signals with potentials between 5 and 30 volts appear as various shades of gray or brown becoming darker as the voltage increases. This effect can be reversed by an additional control on the recording instrument which provides for positive or negative presentation of writing current to the paper recorder. By using this control defective areas may be caused to appear as dark areas on a white background or white areas on a dark background.

In order to record defective areas the pulse rate is usually increased from the usual 600 or 800 pulses per second to 1600-2000 pulses per second. Some pulse-echo test instruments have a control incorporated while others must be slightly modified to add this control.

No mention has been made of controls for the carriage and bridge. These controls start and stop the scanning motions. Also, they provide variable index lengths over about a 20:1 range. For example, if the minimum index is 1/32 of an inch the maximum would be about 5/8 of an inch. The scanning rate is normally variable from about 1 to 20 inches per second. On a few specialized recording systems other scanning rates have been used.

Recording systems have been used for recording of information obtained by through-transmission, shear wave, pitch-catch technique and, most frequently, standard longitudinal wave, pulse-echo techniques. Any inspection technique which obtains a varying signal to the pulse-echo instrument may usually be recorded.

It is seen, then, that facsimile C-Scan recording provides a rapidly made, permanent record of ultrasonically detected discontinuities.

APPENDIX V

REFERENCES

1. Books: Hueter, Theodor F., and Bolt, Richard H., Sonics. John Wiley and Sons, New York, N.Y., 1955.

   Babikov, O. I., Ultrasonics and Its Industrial Applications. Consultants Bureau, New York, N.Y., 1960, Translated from Russion.

   Society for Nondestructive Testing, Nondestructive Testing Handbook, Vol. II. The Ronald Press, New York, N.Y., 1959.

   Olson, Harry F., Acoustical Engineering. D. Van Nostrand Company, Inc., Princeton, New Jersey, 1957.

   Mason, Warren P., Piezoelectric Crystals and Their Application to Ultrasonics. D. Van Nostrand Company, Inc., Princeton, New Jersey, 1950.

   McGonnagle, Warren G., Nondestructive Testing, McGraw-Hill Book Company, Inc., New York, N.Y., 1961.

2. Reports: Posakony, Gerald J., and McMaster, Robert C., The Analysis of Focused Ultrasonic Test Techniques. Technical Paper No. 601, Automation Industries, Inc., 1960.

   Cook, E. G. and Van Valkenberg, H., Surface Waves at Ultrasonic Frequencies. American Society for Testing Materials, Bulletin No. 198, May, 1954.

   Worlton, D. C., Lamb Waves at Ultrasonic Frequencies. Hanford Report HW-45649, 1956.

   White, J. K., McClung, R.W., and Allen, J. W., Implications of Ultrasonic Attenuation to Nondestructive Testing. Metallurgy Division, Oak Ridge National Laboratory, ORNL-2651, April 1959.

   Van Valkenberg, H.E., Wilson, R.A., and Olha, W.R., Ultrasonic Inspection Equipment Program, Technical Report TR-065, Contract AF 33(600)-29879, 1956.

3. Journals, Magazine Articles, Manuals: Roderick, R. L. and Truell, R., The Measurement of Ultrasonic Attenuation in Solids by the Pulse Technique and Some Results in Steel. Journal of Applied Physics, Vol. 23, No. 2, 267-279, February, 1952.

   Seki, H., Granato, A., and Truell, R. Diffraction Effects in the Ultrasonic Field of a Piston Source and Their Importance in the Accurate Measurement of Attenuation. Journal of the Acoustical Society of America, Vol. 28, No. 2, 230-238, March 1956.

   Sperry Products, Incorporated, Ultrasonic Attenuation Comparator Operating and Maintenance Instructions, Sperry Products, Publication Number AC 001-1159.

Aeronautical Systems Division, Dir/Materials and Processes, Metals and Ceramics Lab, Wright-Patterson AFB, Ohio.
Rpt Nr ASD-TDR-62-8. DEVELOPMENT OF ULTRASONIC TECHNIQUES FOR DEFECT EVALUATION. Final report, Feb 63, 136p. incl illus., tables, 14 refs.

Unclassified Report

The results of investigations to determine the effects of several metallurgical and acoustical variables on the ultrasonic signal strength using commercially available ultrasonic flaw detection equipment are reported. Applied to various metals used in aerospace structures and components, these

(over)

1. Method of forming and heat treatment of alloys
2. Ultrasonic energy
3. Flaw detection
I. AFSC Project 7381, Task 73812
II. Contract AF 33 (616)-6793
III. Automation Industries, Inc., Torrance, Calif.
IV. J. B. Ramsey, W. M. Rowe
V. Aval fr OTS
VI. In ASTIA collection

Aeronautical Systems Division, Dir/Materials and Processes, Metals and Ceramics Lab, Wright-Patterson AFB, Ohio.
Rpt Nr ASD-TDR-62-8. DEVELOPMENT OF ULTRASONIC TECHNIQUES FOR DEFECT EVALUATION. Final report, Feb 63, 136p. incl illus., tables, 14 refs.

Unclassified Report

The results of investigations to determine the effects of several metallurgical and acoustical variables on the ultrasonic signal strength using commercially available ultrasonic flaw detection equipment are reported. Applied to various metals used in aerospace structures and components, these

(over)

1. Method of forming and heat treatment of alloys
2. Ultrasonic energy
3. Flaw detection
I. AFSC Project 7381, Task 73812
II. Contract AF 33 (616)-6793
III. Automation Industries, Inc., Torrance, Calif.
IV. J. B. Ramsey, W. M. Rowe
V. Aval fr OTS
VI. In ASTIA collection

investigations resulted in the separation and determination of important acoustical properties that were expected to indicate the cause for differencies in the transmission of ultrasonic energy in the various materials. A method was developed for applying correction factors to test blocks of one metal in order to estimate the size of defects in other metals. Beam collimation techniques were studied to determine optimum conditions for detecting defects and displaying them on both cathode ray image and C-Scan (plan view) facsimile paper recordings. Some investigations were also performed to separate and identify shear and surface (Reyleigh) waves.

investigations resulted in the separation and determination of important acoustical properties that were expected to indicate the cause for differencies in the transmission of ultrasonic energy in the various materials. A method was developed for applying correction factors to test blocks of one metal in order to estimate the size of defects in other metals. Beam collimation techniques were studied to determine optimum conditions for detecting defects and displaying them on both cathode ray image and C-Scan (plan view) facsimile paper recordings. Some investigations were also performed to separate and identify shear and surface (Reyleigh) waves.